Ph.D Thesis in Physics

Self-Energies of Single-Particle States in Deformed Nuclei Generated by Dynamical Coupling to the Surface

Donati Paola

The Niels Bohr Institute
Blegdamsvej 17, DK-2100 Copenhagen Ø, Denmark

Supervisor : Lektor Thomas Døssing (Niels Bohr Institute)

Co-Supervisor : Prof. Yoshifumi R. Shimizu (Kyushu University, Fukuoka)

Københavns Universitet
27th july 1998

To my family
Gaetano,Ester,
Rita and Felice.

Per me si va ne la città dolente,
per me si va ne l'etterno dolore,
per me si va tra la perduta gente.
Giustizia mosse il mio alto fattore:
fecemi la divina podestate,
la somma sapienza e 'l primo amore.
Dinanzi a me non fuor cose create
se non etterne, e io etterno duro.
Lasciate ogne speranza, voi ch'intrate".
(Dante Alighieri,"Inferno", Canto III)

Canta, no llora,
porquè cantando
se allegran,
cielito lindo,
los corazones.
(Spanish song)

Contents

List of Figures

List of Tables

Introduction

Mean field theory plays an essential role in the study of many-particle systems. This is because it reduces the dynamic of a many-body system to that of independent particles moving in a self-consistent potential. This is the case of the nuclear many-body system, the nucleus. In fact, in first approximation, one can depict a nucleus as a system of non-interacting nucleons moving in a potential well, the mean field, which is generated by averaging over all interactions.

The Hartree-Fock approximation to the average field is the sum of two terms, a local term (Hartree) and a non-local part (Fock). The Hartree potential represents the average interaction felt by a nucleon due to all other nucleons and it is called direct term. The Fock potential is called exchange contribution and it arises from the fact that the nucleons are fermions and they satisfy Pauli principle, that is their wave-function are antisymmetric respect to an exchange in coordinates. This non-locality introduces in the single-particle potential a dependence on the linear momentum of the nucleon. This momentum-dependence of the average potential can be, for many purpose, accounted for an effective mass, the so called *k-mass* which is considerably smaller than the nucleon bare mass $m(m_k = 0.6m - 0.7m)$. The Hartree-Fock approximation to the average single-particle field describes quite well the properties of the scattering states and of the deeply bound single particle states, but fails to yield the density of single-particle levels near the Fermi energy. Indeed, the latter can be reproduced with a purely local field with an effective mass equal to the bare mass. The fact that the density of levels is intimately related with the properties of the effective mass can be understood by a simple inspection of the expression of the level density in the Fermi gas model

$$\rho(E) = \frac{1}{\sqrt{48}E} \exp 2\sqrt{aE}. \quad (1)$$

The level density parameter a is proportional to the nucleon effective mass. Consequently, an increase in the effective mass leads to an increase in the level density and viceversa. From the above discussion we can argue that we have to face of the following problem of the enhancement of the effective mass: why do we need to use a big effective mass $m^* \sim m$ around the Fermi energy and a small mass far from that region?

This limitation of the Hartree-Fock approximation in describing the nucleon levels close to the Fermi energy can be explained by the fact that this is a static approximation where one neglects important correlations between nucleons. In particular,the fluctuations of the mean field surface can renormalize the motion of the single particle in an important way. The RPA approximation provides an accurate description of these collective nuclear vibrations and of the corresponding particle-vibration coupling strengths.

The particle-vibration coupling leads, among other things, to an energy dependence of the average nuclear field, because the phonon describing the surface modes propagate in the nuclear medium with a finite velocity. Also, here, this nonlocality can be accounted for in terms of an effective mass, the so called ω-*mass* which is considerably larger than the bare mass. In fact, the effect of the energy dependence appears to approximately cancel that of the non-locality near the Fermi surface , and it becomes negligible for single-particle levels far from Fermi energy. Because the total effective mass entering the single-particle Schrödinger equation is $m^* = \frac{m_k m_\omega}{m}$ and $m^* \approx m$ around the Fermi energy, time dependent mean field theory can account for the observed density of levels.

However, there are basic differences between the results of the empirical independent particle model (bare nucleon mass and Woods-Saxon potential), and the Hartree-Fock results renormalized by the particle-vibration coupling and associated with the effective mass. While the single-particle levels of the empirical model do not depend on the intrinsic excitation energy of the nucleus (temperature T), the ω-*mass*

and thus m^* is expected to depend on T.

In fact, in the case of spherical nuclei, the dependence of the ω-*mass* on temperature can be parametrized as [14]

$$m_\omega(T) = m_\omega(0)e^{-\frac{T}{T_0}} + m(1 - e^{-\frac{T}{T_0}}), \tag{2}$$

with $T_0 \approx 2$ MeV. This means that, already at T$\approx$ 2 MeV, the increase of the ω-*mass* over the bare mass value, is reduced by a factor of 1/e.

The extension of the calculations which have led to the above results, to the case of deformed strongly rotating nuclei is essential to be able to extract spectroscopic information from particle and gamma decay processes associated with the cooling of the compound nucleus. In fact, at finite temperature one has to deal with an ensemble of nuclei, most of which have a deformed shape, even if spherical in the ground state. An accurate knowledge of the effective nucleon mass in this situation is essential to be able to extract spectroscopic information from the study of the compound nucleus cooling process, and to be able to understand how rotational frequency and temperature affects the nuclear structure.

In the present thesis, we have developed, by making use of the Matsubara formalism and the Nuclear Field Theory formalism, the theoretical framework to calculate the properties characterizing the motion of quasiparticle in hot, strongly rotating deformed nuclei (Chapters 1-2). Special attention has been paid to the renormalization of the effective mass associated with the coupling of the single-particle motion to quantal fluctuations of the nuclear surface (Chapters 3-4) .

Because of the violation of rotational and gauge symmetries associated with mean field solutions which do not conserve neither angular momentum (Nilsson states) nor particle number (BCS solutions), spurious states, the so called Nambu-Goldstone modes (see Chapter 5), appear in the vibrational spectrum as solutions with zero energy and have to be eliminated. The technical developmentd needed to do this in actual calculations is discussed in Chapters(6-7).

Applications of the formalism to the case of nuclei close to the yrast line have been carried out. In particular, we have studied the effect on the ω-*mass* of the coupling

to β-, γ- and octupole vibrations of nucleons moving in single-particle levels close to the Fermi energy as a function of rotation and deformation. We have also analyzed the specific effect that the particle-vibration coupling produces on signature paired states (Chapter 8). The conclusion are presented in Chapter (9).

Chapter 1

Hartree-Fock-Bogoliubov Equation in a Rotating Frame

1.1 Introduction

The Hartree-Fock-Bogoliubov approximation (HFB)[2, 3, 4] is a self-consistent mean field method in which nuclear deformations and pairing correlations are treated simultaneously and on equal footing.

The basic idea of the HFB method is to represent the ground state of a nucleus as a *vacuum* of *quasiparticles*, which are defined as the excitations of the system. The main goal is to find the so called Bogoliubov transformation [11] from bare particles to quasiparticles, such that the Hamiltonian can be approximated by an independent quasiparticle Hamiltonian neglecting, as a first approximation, the interactions among quasiparticles. The starting point is the many-body Hamiltonian written as the sum of a kinetic energy term and an effective nucleon-nucleon interaction that can be expressed, in second quantization, in terms of the bare particle creation and annihilation operators $\widehat{c}_i^\dagger, \widehat{c}_j$

$$\widehat{H} = \sum_{i,j} \langle i|\widehat{T}|j\rangle \widehat{c}_i^\dagger \widehat{c}_j + \frac{1}{4} \sum_{i,j,k,l} \langle ij|\widehat{V}|kl\rangle \widehat{c}_i^\dagger \widehat{c}_j^\dagger \widehat{c}_l \widehat{c}_k. \tag{1.1}$$

The final aim of the HFB is to write $\widehat{H}$ as

$$\widehat{H} = E_0 + \widehat{H}_{\rm qp} + \widehat{H}_{\rm qp-int}, \tag{1.2}$$

where E_0 is the energy of the quasiparticle vacuum, $\widehat{H}_{\rm qp}$ describes the independent quasiparticle motion, and $\widehat{H}_{\rm qp-int}$ represents the (weak) interaction among quasiparticles. In the HFB this last term is neglected, so that $\widehat{H}$ is approximated by an independent quasiparticle Hamiltonian $\widehat{H} \approx E_0 + \widehat{H}_{\rm qp}$. The interactions between quasiparticles may be included by applying time-dependent HFB(TDHFB) or the quasiparticle random phase approximation (QPRPA) (see Chapter 2).

When a deformed nucleus experiences a fast rotation, Coriolis and centrifugal forces act on the individual nucleons in the rotating frame and an extra term $-\omega_{\rm rot}\widehat{J}_x$ must be added to the intrinsic Hamiltonian for independent quasiparticle motion. The quantity $\widehat{J}_x$ represents the spin projection on the axis of rotation x, while z corresponds to the symmetry axis. The Coriolis interaction violates time reversal invariance.

Conservation of the particle number is approximately achieved by adding the term $\lambda\widehat{N}$ with an appropriate choice of the chemical potential λ, $\widehat{N}$ being the particle number operator. As a consequence, the Hamiltonian describing a system of independent quasiparticle moving in a mean field rotating with angular velocity $\omega_{\rm rot}$ about the x-axis can be written as

$$\widehat{H'} = \widehat{H} - \lambda\widehat{N} - \omega_{\rm rot}\widehat{J}_x. \tag{1.3}$$

The rotational frequency and the chemical potential are determined through the conditions

$$\begin{aligned} \langle\widehat{J}_x\rangle &= J + \frac{1}{2}, \\ \langle\widehat{N}\rangle &= N, \end{aligned} \tag{1.4}$$

where J is the total angular momentum, where the condition on the average value of the $\widehat{J}_x$ component of the angular momentum is equivalent to the WKB-approximation of the centrifugal potential.

Axially symmetric deformed nuclei are invariant under space inversion P and rotation R by an angle π around the x-axis perpendicular to the symmetry axis. These are the only symmetries left in these nuclei and the resulting states can be

labelled by the eigenvalues of the two operators P and R, namely parity $\pi = \pm 1$ and signature $\alpha = \pm 1/2$.

1.2 Signature Quantum Number

Reflexion symmetry implies that the system is invariant with respect to rotations by π about an axis perpendicular to the symmetry axis. This operation can be carried out through the operator $\widehat{R}_x(\pi)$ defined as

$$\widehat{R}_x(\pi) = e^{-i\pi\widehat{J}_x}. \tag{1.5}$$

The square of this operator is equivalent to a rotation of the system through the angle 2π, and thus it should not influence the wave function of a system composed of an even number of fermions. On the contrary, systems with an odd number of fermions transform under $\widehat{\mathcal{R}}^2_x(\pi)$ like spinors, and consequently the corresponding total wave function changes sign. One can thus write

$$\widehat{\mathcal{R}}^2_x(\pi) = (-1)^A, \tag{1.6}$$

where A indicates the total number of fermions. Denoting by r the eigenvalues of $\widehat{R}_x(\pi)$ and introducing the notation

$$r = e^{-i\pi\alpha}, \tag{1.7}$$

one finds for systems with an even number of nucleons (integer total spin I)

$$\begin{aligned} r = +1 \quad (\alpha = 0), \quad I = 0, 2, 4 \cdots, \\ r = -1 \quad (\alpha = 1), \quad I = 1, 3, 5 \cdots, \end{aligned} \tag{1.8}$$

while for systems with odd particle number we have (half-integer total spin I)

$$\begin{aligned} r = -i \quad (\alpha = +\tfrac{1}{2}), \quad I = \tfrac{1}{2}, \tfrac{5}{2}, \tfrac{9}{2} \cdots, \\ r = +i \quad (\alpha = -\tfrac{1}{2}), \quad I = \tfrac{3}{2}, \tfrac{7}{2}, \tfrac{11}{2} \cdots. \end{aligned} \tag{1.9}$$

The eigenvalues r associated with the rotation operator $\widehat{R}_x(\pi)$ can be used to classify the single-particle states. However, due to its additive nature, it is more

convenient define α as *signature* quantum number. In what follows we shall use $\alpha = 0, 1$ for even nuclei and $\alpha = \pm 1/2$ for odd nuclei.

1.3 Quasiparticle Transformation in a Rotating Frame

Let us start with the mean field Hamiltonian in a rotating frame

$$\widehat{H'} = \widehat{h}_{\rm def} - \Delta(\widehat{P}^\dagger + \widehat{P}) - \lambda\widehat{N} - \omega_{\rm rot}\widehat{J}_x, \tag{1.10}$$

where $\widehat{h}_{\rm def}$ describes single-particle motions in a deformed potential and $\widehat{P}^\dagger$ is the pair creation operator defined by $\widehat{P}^\dagger = \sum \widehat{c}_i^\dagger \widehat{c}_{\bar{i}}^\dagger$ with i labelling the single-particle states and $\bar{i}$ the state time reversed of i. In the standard basis where m_i is the projection of the angular momentum j_i on the symmetry axis z, the operator $\widehat{J}_x$ is not block diagonal with respect to the quantum number m_i. This property, coming from the breaking of the time reversal invariance, can be avoided introducing an appropriate basis for the diagonalization of the HFB equations. For this purpose, we restrict the members of the standard basis to states that satisfy the condition $m_i > 0$ so that the dimension of the equations will be reduced by half. [16]. Moreover, the chosen basis is symmetrized with respect to a rotation of π around the rotational axis x, namely we introduce the signature α as good quantum number to label the quasiparticle states.

This new basis can be defined in terms of the original nucleon creation and annihilation operators $\widehat{c}_k^\dagger, \widehat{c}_k$,as

$$\begin{pmatrix} \widehat{d}_K \\ \widehat{d}_{\bar{K}} \end{pmatrix} = \frac{1}{\sqrt{2}} \begin{pmatrix} 1 & (-1)^{m-\frac{1}{2}} \\ (-1)^{m+\frac{1}{2}} & 1 \end{pmatrix} \begin{pmatrix} \widehat{c}_k \\ \widehat{c}_{\bar{k}} \end{pmatrix}. \tag{1.11}$$

The notation $\bar{k}$ indicates the time-reversal state to k while ($\bar{K}$,K) represents, as we will see below (1.13), a signature pair. We can now introduce the appropriate Bogoliubov transformation that diagonalizes the HFB Hamiltonian (1.10)

$$\begin{aligned} \widehat{a}_\mu &= \sum_i{}' \left(U_{\mu_i} \widehat{d}_i + V_{\mu_i} \widehat{d}_{\bar{i}}^\dagger \right) \\ \widehat{a}_{\bar{\mu}} &= \sum_i{}' \left(\bar{U}_{\mu_i} \widehat{d}_{\bar{i}} + \bar{V}_{\mu_i} \widehat{d}_i^\dagger \right), \end{aligned} \tag{1.12}$$

where U, V, $\bar{U}$ and $\bar{V}$ are real coefficients. The notation $\sum_i'$ is used to specify that we are summing over the states of the new basis (1.11).

The quasiparticle operators $(\widehat{a}_\mu, \widehat{a}_{\bar{\mu}})$ satisfy the property

$$e^{-i\pi\widehat{J}_x}\begin{pmatrix} a_\mu \\ a_{\bar{\mu}} \end{pmatrix} e^{i\pi\widehat{J}_x} = \pm i \begin{pmatrix} a_\mu \\ a_{\bar{\mu}} \end{pmatrix} \tag{1.13}$$

This implies that the quasiparticle state μ has signature $\alpha = 1/2(r = -i)$, while $\bar{\mu}$ is the state with signature $\alpha = -1/2(r = +i)$.

Using the quasiparticle transformation (1.12), the Hamiltonian (1.10) can be brought into the diagonal form

$$\widehat{H} = E_0 + \sum_\mu E_\mu \widehat{a}^\dagger_\mu \widehat{a}_\mu + \sum_{\bar{\mu}} E_{\bar{\mu}} \widehat{a}^\dagger_{\bar{\mu}} \widehat{a}_{\bar{\mu}}. \tag{1.14}$$

The quasiparticle energies E_μ and $E_{\bar{\mu}}$ are eigenvalues and the coefficients U, V, $\bar{U}$, $\bar{V}$ eigenvectors of the matrix

$$\mathcal{M} = \begin{pmatrix} (\boldsymbol{\varepsilon} - \lambda \boldsymbol{I} - \omega_{\rm rot}\boldsymbol{j_x}) & \boldsymbol{\Delta} \\ \boldsymbol{\Delta} & -(\boldsymbol{\varepsilon} - \lambda \boldsymbol{I} + \omega_{\rm rot}\boldsymbol{j_x}) \end{pmatrix}, \tag{1.15}$$

that is

$$\mathcal{M}\begin{pmatrix} \boldsymbol{U_\mu} \\ \boldsymbol{V_\mu} \end{pmatrix} = E_\mu \begin{pmatrix} \boldsymbol{U_\mu} \\ \boldsymbol{V_\mu} \end{pmatrix}, \qquad \mathcal{M}\begin{pmatrix} \boldsymbol{\bar{V}_{\bar{\mu}}} \\ \boldsymbol{\bar{U}_{\bar{\mu}}} \end{pmatrix} = -E_{\bar{\mu}} \begin{pmatrix} \boldsymbol{\bar{V}_{\bar{\mu}}} \\ \boldsymbol{\bar{U}_{\bar{\mu}}} \end{pmatrix}. \tag{1.16}$$

1.4 Cranked Nilsson Model

One of the most popular mean field potential for deformed nuclei is the Nilsson or modified harmonic oscillator potential [27]. Its generalization to the study of the single-particle structure in a rotating frame is called Cranked Nilsson Model [19, 17].

The deformed Hamiltonian $\widehat{h}_{\rm def}$ to be used in the HFB equation (1.10) can be written as

$$\widehat{h}_{\rm def} = \sum_{n=1}^{A} \left\{ \frac{\boldsymbol{p^2}}{2M} + \frac{1}{2}M\left(\omega_x^2 x^2 + \omega_y^2 y^2 + \omega_z^2 z^2\right) + v_{ls}\boldsymbol{l}\cdot\boldsymbol{s} + v_{ll}\left(\boldsymbol{l^2} - \langle \boldsymbol{l^2}\rangle_N\right) \right\}_n . \tag{1.17}$$

The frequencies ω_x, ω_y and ω_z are expressed in terms of the quadrupole deformation parameters ε and γ, with signs chosen according to the Lund convention [17]

$$\omega_j \equiv \omega_0(\varepsilon,\gamma)\left[1-\frac{2}{3}\varepsilon\cos\left(\gamma+\frac{2\pi\nu_j}{3}\right)\right], \qquad j\in\{x,y,z\} \tag{1.18}$$

where $\nu_x = 1, \nu_y = -1$ and $\nu_z = 0$. The calculations will be carried out in the stretched coordinate system, $x' = x\sqrt{M\omega_x/\hbar}$, etc. [17]. The introduction of the stretched coordinates has the advantage of transforming away coupling terms arising from the $\boldsymbol{l}\cdot\boldsymbol{s}$ and $\boldsymbol{l}^2$ factors between oscillator shell N and $N\pm 2$ [27].

It is important to take into account the $N_{\rm osc}$ dependence of the strength v_{ll} of the $\boldsymbol{l}^2$-terms in the Nilsson potential because the unperturbed strength distribution of the quadrupole operator can deviate appreciably from $2\hbar\omega_0$. We therefore adopt the values of the parameter v_{ll} and v_{ls} given by Bengston and Ragnarsson [10].

We use different values of the oscillator frequency ω_0 for neutrons and protons in the Nilsson potential in order to ensure equal root-mean-square radii [9]

$$\omega_0 \rightarrow \begin{cases} \left(\dfrac{2N}{A}\right)^{\frac{1}{3}}\omega_0 & \text{for neutrons} \\ \left(\dfrac{2Z}{A}\right)^{\frac{1}{3}}\omega_0 & \text{for protons,} \end{cases} \tag{1.19}$$

where $\hbar\omega_0 = 41A^{-\frac{1}{3}}$ MeV.

The pairing gaps (Δ_n, Δ_p) and the chemical potentials (λ_n, λ_p), that appear in (1.10), are calculated at each rotational frequency to satisfy the conditions

$$\begin{aligned} G_\tau\langle\omega_{\rm rot}|\widehat{P}_\tau|\omega_{\rm rot}\rangle &= \Delta_\tau \\ \langle\omega_{\rm rot}|\widehat{N_\tau}|\omega_{\rm rot}\rangle &= N(Z) \end{aligned} \tag{1.20}$$

with τ=(n,p). The quantities G_τ, that is the monopole pairing strengths, together with the deformation parameters (ε,γ) are fixed at $\omega_{\rm rot} = 0$ to ensure the agreement of the calculated pairing gap parameters with the experimental values. The deformation parameters (ε,γ) can be obtained following the prescription of the Strutinsky method [31] or adopting experimentally deduced values (see [32]).

Chapter 2

The RPA in a Rotating Frame

2.1 Introduction

The random phase approximation (RPA)[3, 4] is the simplest realistic microscopic treatment of nuclear excitations. It was first suggested by Bohm and Pines [12] in connection with the plasma oscillations of the electron gas. It has been applied successfully to the microscopic description of small-amplitude oscillations about an equilibrium in a number of systems, in particular the atomic nucleus. Away from closed shells, pair correlations become very important so that the RPA method is generalized to the quasiparticle random phase approximation (QPRPA) [30]. In this work we use the term RPA for both methods without distinction.

The RPA has been used to describe a large number of low-lying collective states, such as vibrations in spherical superconducting nuclei, and in deformed rare earth and actined nuclei for the description of the β-,γ-, octupole- and pairing-vibrations [28]. A basic feature of the RPA is that it takes into account ground state correlations, that is,the fact that the true ground state is not simply the Hartree-Fock particle-hole vacuum but, due to the residual interaction, it contains an admixture of particle-hole excitation states. Excited states are now a linear combination of particle-hole states generated by the operators $\widehat{c}_m^{\dagger}\widehat{c}_i (m > \varepsilon_{\mathbf{F}}$ and $i < \varepsilon_{\mathbf{F}})$ as well as by the operators $\widehat{c}_i^{\dagger}\widehat{c}_m$, which take particle-hole excitation out of the ground state. In presence of pairing correlations one talks, in both cases, of creation or annihilation of two quasiparticle excitations.

The theory of the cranked shell model extended by the RPA theory was first developed by Marshalek [20] and has been applied to high-spin β- and γ- vibrational bands [25] and to octupole bands [26]. Effects of the Coriolis force on the distinct mode of excitations are automatically taken into account in RPA solutions since the mean field is affected by the cranking term -$\omega_{\rm rot}\widehat{J}_x$.

2.2 Residual Interaction

The residual interaction between the quasiparticles in the rotating frame consistent with the single-particle Hamiltonian defined in (1.10) is composed of the monopole pairing force associated with the pairing potential (the most important pairing correlations are the one for $I = 0$ pairs) and a multipole-multipole interaction consistent with the deformed field. Since the most important deformations are of a quadrupole nature we will consider a quadrupole-quadrupole separable residual interaction. Both part of the interaction are chosen to be separable.

We consider, first of all, the residual pairing interaction associated with the pairing potential $\Delta(\widehat{P}^\dagger + \widehat{P})$, that is

$$\widehat{H}_{\rm P} = -\sum_{\tau=n,p} G_\tau \tilde{P}_\tau^\dagger \tilde{P}_\tau \qquad \tilde{P}_\tau = \widehat{P}_\tau - \langle \widehat{P}_\tau \rangle, \tag{2.1}$$

where the index τ is used to distinguish between proton and neutron pairing. The expectation value is taken with respect to a quasiparticle configuration chosen as a reference configuration and it is related to the pairing deformation Δ through the self-consistency condition $\Delta_\tau = G_\tau \langle \tilde{P}_\tau^\dagger \rangle$.

Since the residual interaction is an hermitian operator, it is more convenient to redefine the pairing interaction in such a way that the hermiticity is recovered. For this purpose one can define the following operators

$$\begin{aligned} \widehat{P}_{\tau+} &= \tilde{P}_\tau^\dagger + \tilde{P}_\tau, \\ \widehat{P}_{\tau-} &= i(\tilde{P}_\tau^\dagger - \tilde{P}_\tau), \end{aligned} \tag{2.2}$$

that satisfy the condition $\widehat{P}^{\dagger}_{\tau\pm} = \widehat{P}_{\tau\pm}$. Moreover, they are signature positive operators because

$$e^{-i\pi\widehat{J}_x}\widehat{P}_{\tau\pm}e^{i\pi\widehat{J}_x} = +\widehat{P}_{\tau\pm} \tag{2.3}$$

For the multipole-multipole interaction associated with deformation the situation is slightly more complicated. In fact, the multipole operators are defined as

$$\widehat{Q}_{LK} = \sum_{n=1}^{A}(r^L Y_{LK})_n, \tag{2.4}$$

where the spherical harmonic functions Y_{LK} are defined with respect to the symmetry axis z. We have now to remember that the K-quantum number, that is the projection of the total angular momentum along the symmetry axis, is no longer a conserved quantity at finite rotational frequency. As a consequence, it is more convenient to deal with operators defined in terms of proper quantum numbers in a rotating frame, namely the signature α (see Chapter 1). For this purpose, one can use the following definition of the multipole operators

$$\widetilde{Q}^{\alpha}_{LK} = \frac{i^{L+\alpha+K}}{\sqrt{2(1+\delta_{K0})}}\left(r^L Y_{LK} + (-1)^{L+\alpha} r^L Y_{L-K}\right), \tag{2.5}$$

where $K \geq 0$ and α can assume the values 0 and 1. The multipole operators with $\alpha = 0$ are called signature positive operators while $\alpha = 1$ corresponds to signature negative operators. This difference comes from the fact that

$$\begin{aligned} e^{-i\pi\widehat{J}_x}\widetilde{Q}^{\alpha=0}_{LK}e^{i\pi\widehat{J}_x} &= +\widetilde{Q}^{\alpha=0}_{LK} \\ e^{-i\pi\widehat{J}_x}\widetilde{Q}^{\alpha=1}_{LK}e^{i\pi\widehat{J}_x} &= -\widetilde{Q}^{\alpha=1}_{LK}. \end{aligned} \tag{2.6}$$

The factor $i^{L+\alpha+K}$ is introduced to ensure hermiticity of the multipole operators, that is $\widetilde{Q}^{\alpha\,\dagger}_{LK} = \widetilde{Q}^{\alpha}_{LK}$. Note that the K=0 quadrupole(octupole) operator $\widetilde{Q}_{20}(\widetilde{Q}_{30})$ has a unique signature $\alpha = 0(\alpha = 1)$, which corresponds to the fact that K=0 bands have no signature partners.

All the operators are defined in doubly stretched coordinates, $x_i'' \equiv (\omega_i/\omega_0)x_i$. This can be considered as an improved version of the conventional multipole-multipole interaction. Sakamoto and Kishimoto [29] have shown that the ordinary multipole-multipole interaction is not able to reproduce the prominent features of the observed data in deformed nuclei [18]. The main reason is traced back to the violation of the nuclear self-consistent condition, namely, the shape of a potential and that of a density must be the same even at the time when a nucleus undergoes collective excitations. This means that a mean-field approximation of the two-body residual interaction must not change the Hartree-Fock(HFB) field obtained, self-consistently, from the deformed one-body Hamiltonian. For small amplitudes the variation in the potential along the direction x is proportional to the amplitude γ, that is

$$\delta V = -\gamma \frac{\partial V}{\partial x} = \chi \gamma F \tag{2.7}$$

which is a mean-field approximation of the residual interaction and where F is the one-body operator generating the collective mode. Imposing the self-consistency condition the coupling constant may be derived as

$$\chi = -A\langle \frac{\partial^2 V}{\partial x^2} \rangle \tag{2.8}$$

where $<\quad>$ is to be taken at the equilibrium deformation. One can show that, due to the doubly stretched coordinates, $\langle \tilde{Q} \rangle = 0$ at the equilibrium deformation so that the mean-field approximation for these operators fulfil the condition of leaving unchanged the self-consistent Hartree-Fock field.

Since we adopt different oscillator frequency ω_0 for neutrons and protons (see Chapter 1) in the Nilsson potential, we use the following modified multipole operators

$$\tilde{Q}^{\alpha}_{LK} \rightarrow \begin{cases} \left(\frac{2Z}{A}\right)^{\frac{2}{3}} \tilde{Q}^{\alpha}_{LK} & \text{for neutrons} \\ \left(\frac{2N}{A}\right)^{\frac{2}{3}} \tilde{Q}^{\alpha}_{LK} & \text{for protons} \end{cases} \tag{2.9}$$

This was originally proposed by Baranger and Kumar [9] for quadrupole operators starting from the hypothesis that the average square radii for neutron and proton are

equal. The multiplying factors in front of the quadrupole operators tell us that the ratio between neutrons to protons remains the same everywhere in the nucleus (in an average sense). This is because one assumes that the deformation felt by the neutrons and protons is the same. Sakamoto [29] has generalized it for an arbitrary multipole operator and proved that by means of this scaling the translational symmetry is restored in the limit of the harmonic oscillator potential.

The residual interaction can then be written as

$$\widehat{H}^{\alpha}_{\rm int} = -\frac{1}{2}\sum_{\alpha}\sum_{\rho}\chi^{\alpha}_{\rho}\left\{\hat{R}^{\alpha}_{\rho}\right\}^2, \tag{2.10}$$

where $\hat{R}^{\alpha}_{\rho}$ are one-body Hermitian operators, and χ^{α}_{ρ} the corresponding coupling strengths. The indeces α and ρ represent, respectively, the signature quantum number and the different residual interactions. As explained above we adopt the following operators

$$\hat{R}^{0}_{\rho} = \tilde{P}_{n+} \quad \tilde{P}_{n-} \quad \tilde{P}_{p+} \quad \tilde{P}_{p-} \quad \tilde{Q}^{0}_{20} \quad \tilde{Q}^{0}_{21} \quad \tilde{Q}^{0}_{22}, \tag{2.11}$$

for the signature positive sector and

$$\hat{R}^{1}_{\rho} = \tilde{Q}^{1}_{21} \quad \tilde{Q}^{1}_{22}. \tag{2.12}$$

for the negative one.

The Hamiltonian describing the system expressed in terms of the quasiparticle transformation and of the signature quantum number (1.10) is defined as

$$\widehat{H} = \text{const} + \sum_{\mu} E_{\mu}\hat{a}^{\dagger}_{\mu}\hat{a}_{\mu} + \sum_{\bar{\mu}} E_{\bar{\mu}}\hat{a}^{\dagger}_{\bar{\mu}}\hat{a}_{\bar{\mu}} + \widehat{H}^{0}_{\rm int} + \widehat{H}^{(1)}_{\rm int}. \tag{2.13}$$

The coupling strengths χ should be determined by the self-consistent condition between the density distribution and the single-particle potential. For the case of the anisotropic harmonic oscillator potential [29], the values of the quadrupole strengths are given by

$$\chi^{\rm HO}_{2K} = \frac{4\pi M\omega_0^2}{5A\langle(r^2)''\rangle}, \tag{2.14}$$

with

$$A\langle(r^2)''\rangle = \langle\sum_k^A (r^2)''\rangle. \tag{2.15}$$

The notation $''$ indicates use of the doubly stretched coordinates, as explained above.

Since the cranked Nilsson potential is not a simple harmonic oscillator, we use scaling factors f_K as

$$\chi_{2K} = f_K \chi_{2K}^{\mathrm{HO}}. \tag{2.16}$$

These factors are determined by theoretical and experimental requirements. For the component K=1, we have to force a zero energy solution, called the Nambu-Goldstone mode (see Chapter 5) at $\omega_{\mathrm{rot}} = 0$, while for K=0 and K=2 one fixes the f_K in such a way to reproduce the experimental values of the β- and γ-vibration at $\omega_{\mathrm{rot}} = 0$.

We want to conclude this section performing the quasiparticle transformation of all operators that will be involved in the subsequent discussion on self-energy correction and Nambu-Goldstone modes to clarify the role played by the signature quantum number in a rotating frame. One can express the basic operators (nucleon number $\widehat{N}$, pair creation operator $\widehat{P}^\dagger$, angular momentum $\hat{J}$, quadrupole moment $\widehat{Q}$) in terms of the bilinear quasiparticle operators

$$\begin{cases} \widehat{A}^\dagger_{\mu\nu} = \widehat{a}^\dagger_\mu \widehat{a}^\dagger_\nu & \widehat{A}^\dagger_{\mu\bar{\nu}} = \widehat{a}^\dagger_\mu \widehat{a}^\dagger_{\bar{\nu}}, \\ \widehat{B}^\dagger_{\mu\nu} = \widehat{a}^\dagger_\mu \widehat{a}_\nu, & \widehat{B}^\dagger_{\mu\bar{\nu}} = \widehat{a}^\dagger_\mu \widehat{a}_{\bar{\nu}}, \end{cases} \tag{2.17}$$

and their conjugates, as listed in table (2.1), where the $\widehat{A}^\dagger$ is the creation operator of two-quasiparticles (that corresponds to an excitation of the system with respect to the quasiparticle vacuum), while $\widehat{B}^\dagger$ scatters one quasiparticle from one state to the

other.

Field	**Mean Value**	**Part A**	**Part B**
$\widehat{N} =$	$\langle\widehat{N}\rangle$	$+\sum N(\mu\bar{\nu})\left(\widehat{A}^{\dagger}_{\mu\bar{\nu}}+\widehat{A}_{\mu\bar{\nu}}\right)$	$+\sum'' N(\mu\nu)\widehat{B}^{\dagger}_{\mu\nu}$
$\widehat{P}_{\pm} =$	$\langle\widehat{P}_{\pm}\rangle$	$+\sum P_{\pm}(\mu\bar{\nu})\left(\widehat{A}^{\dagger}_{\mu\bar{\nu}}\pm\widehat{A}_{\mu\bar{\nu}}\right)$	$+\sum'' P_{\pm}(\mu\nu)\widehat{B}^{\dagger}_{\mu\nu}$
$\widehat{J}_x =$	$\langle\widehat{J}_x\rangle$	$+\sum J_x(\mu\bar{\nu})\left(\widehat{A}^{\dagger}_{\mu\bar{\nu}}+\widehat{A}_{\mu\bar{\nu}}\right)$	$+\sum'' J_x(\mu\nu)\widehat{B}^{\dagger}_{\mu\nu}$
$i\widehat{J}_y =$		$+\sum''_{\mu<\nu} J_y(\mu\bar{\nu})\left(\widehat{A}^{\dagger}_{\mu\nu}-\widehat{A}_{\mu\nu}\right)$	$+\sum J_y(\mu\bar{\nu})\left(\widehat{B}^{\dagger}_{\mu\bar{\nu}}-\widehat{B}_{\mu\bar{\nu}}\right)$
$\widehat{J}_z =$		$+\sum''_{\mu<\nu} J_z(\mu\nu)\left(\widehat{A}^{\dagger}_{\mu\nu}+\widehat{A}_{\mu\nu}\right)$	$+\sum J_z(\mu\bar{\nu})\left(\widehat{B}^{\dagger}_{\mu\bar{\nu}}+\widehat{B}_{\mu\bar{\nu}}\right)$
$\widehat{Q}^0_K =$	$\langle\widehat{Q}^0_K\rangle$	$+\sum Q^0_K(\mu\bar{\nu})\left(\widehat{A}^{\dagger}_{\mu\bar{\nu}}+(-1)^K\widehat{A}_{\mu\bar{\nu}}\right)$	$+\sum'' Q^0_K(\mu\nu)\widehat{B}^{\dagger}_{\mu\nu}$
$\widehat{Q}^1_K =$		$+\sum''_{\mu<\nu} Q^1_K(\mu\nu)\left(\widehat{A}^{\dagger}_{\mu\nu}-(-1)^K\widehat{A}_{\mu\nu}\right)$	$+\sum Q^1_K(\mu\bar{\nu})\left(\widehat{B}^{\dagger}_{\mu\bar{\nu}}-(-1)^K\widehat{B}_{\mu\bar{\nu}}\right)$
$N(\nu\mu)$	$=$	$N(\mu\nu)$,	$P_{\pm}(\nu\mu)=\pm P_{\pm}(\mu\nu)$,
$J_x(\nu\mu)$	$=$	$J_x(\mu\nu)$, $J_y(\nu\mu)=-J_y(\mu\nu)$,	$J_z(\nu\mu)=-J_z(\mu\nu)$
$Q^0_K(\nu\mu)$	$=$	$(-1)^K Q^0_K(\mu\nu)$,	$Q^1_K(\nu\mu)=-Q^1_K(\mu\nu)$

Table 2.1: Quasiparticle representation of the basic operators. All coefficients are real and satisfy the properties listed in the lower part of the Table. The double prime attached to $\sum$ indicate that when the component $(\mu\nu)$ is summed its signature partner $(\bar{\mu}\bar{\nu})$should also be summed, and the inequality $\mu<\nu$ means that the component $(\nu\mu)$ should not be counted independently of $(\mu\nu)$.

As observed from Table(2.1), the different sums over the quasiparticle states are different not only in the coefficients in front of the operators $\widehat{A}^{\dagger}$ and $\widehat{B}^{\dagger}$, but also depending on the value of the signature quantum number. We can try to understand this behaviour from the graph (2.1) in which is represented some of the outcomes the action of a one-body operator has when expressed in the quasiparticle variables.

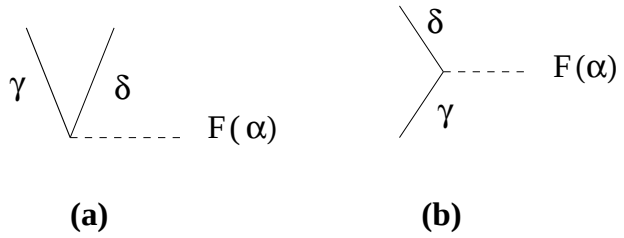

Figure 2.1: Action of one-body operator on quasiparticle states. Graph (a) correspond to the creation of two-quasiparticle excitation in the vacuum while graph (b) is the scattering of two quasiparticles

In case (a) of Fig.(2.1), the generic operator $\widehat{F}$ with signature α is acting on the vacuum to give rise to two-quasiparticle excitations. Due to the fact that the signature is a good quantum number in case we shall consider and that it is an additive quantity (see Chapter 1), one can have these following possibilities

$$\begin{aligned} \alpha &= 0 \quad \gamma+\delta=0 \quad \Longrightarrow \gamma \quad \text{and} \quad \delta \quad \text{have} \quad \text{opposite} \quad \text{signature}, \\ \alpha &= 1 \quad \gamma+\delta=1 \quad \Longrightarrow \gamma \quad \text{and} \quad \delta \quad \text{have} \quad \text{same} \quad \text{signature}. \end{aligned} \tag{2.18}$$

We consider now the scattering case depicted in graph (b) of Fig.(2.1), namely

$$\begin{aligned} \alpha &= 0 \quad \gamma=\delta+0 \quad \Longrightarrow \gamma \quad \text{and} \quad \delta \quad \text{have} \quad \text{same} \quad \text{signature}, \\ \alpha &= 1 \quad \gamma=\delta+1 \quad \Longrightarrow \gamma \quad \text{and} \quad \delta \quad \text{have} \quad \text{opposite} \quad \text{signature}. \end{aligned} \tag{2.19}$$

These different possibilities are translated in a different behaviour in the coefficients of the operators $\widehat{A}^{\dagger}$ where, for positive signature operators like $\widehat{Q}^{0}_{K}$, we have that the corresponding matrix elements contains only combinations of states of opposite signature $(\mu\bar{\nu})$ while in the signature negative operators $(\widehat{Q}^{1}_{K})$ the states can be both μ,ν and $\bar{\mu},\bar{\nu}$. In this latter case we have to impose a limitation, that is $\mu<\nu$ and $\bar{\mu}<\bar{\nu}$, to avoid double counting. This is exactly the meaning of the symbol $\sum''_{\mu\langle\nu}$. In the same way one can obtain the coefficients of the operator $\widehat{B}^{\dagger}$ corresponding to case (b).

Using these properties one can define the residual interaction $\widehat{R}^{\alpha}_{\rho}$ as a function of the signature quantum number α as

$$\widehat{R}^{0}_{\rho} = \sum_{\mu\bar{\nu}} \left\{ R^{0}_{\rho}(\mu\bar{\nu})\widehat{A}^{\dagger}_{\mu\bar{\nu}} + {R^{0}_{\rho}}^{*}(\mu\bar{\nu})\widehat{A}_{\mu\bar{\nu}} \right\}, \tag{2.20}$$

$$\widehat{R}^{1}_{\rho} = \sum''_{\mu\langle\nu} \left\{ R^{1}_{\rho}(\mu\nu)\widehat{A}^{\dagger}_{\mu\nu} + {R^{1}_{\rho}}^{*}(\mu\nu)\widehat{A}_{\mu\nu} \right\}, \tag{2.21}$$

where, in the RPA approximation, quasiparticle scattering terms as $\widehat{B}^{\dagger}$ are regarded as higher-order factor and, as a consequence, neglected.

2.3 The Coupled RPA Equation

In the present framework, the residual interaction is a sum of several separable interactions describing a coupled system of vibrations. This means that the standard eigenvalue problem cannot be transformed into a simple dispersion equation but one has to deal with coupled RPA equations.

The excitation operators of the RPA normal modes ${X^\alpha_{\boldsymbol{q}}}^\dagger (\alpha = 0, 1)$ are constructed in terms of the quasiparticle operators as

$$ {X^0_{\boldsymbol{q}}}^\dagger = \sum_{\mu\bar{\nu}} \left\{ \psi^0_{\boldsymbol{q}}(\mu\bar{\nu}) \widehat{A}^\dagger_{\mu\bar{\nu}} + \varphi^0_{\boldsymbol{q}}(\mu\bar{\nu}) \widehat{A}_{\mu\bar{\nu}} \right\}, \tag{2.22} $$

for positive-type operators and

$$ {X^1_{\boldsymbol{q}}}^\dagger = \sum_{\mu\langle\nu}{}'' \left\{ \psi^1_{\boldsymbol{q}}(\mu\nu) \widehat{A}^\dagger_{\mu\nu} + \varphi^1_{\boldsymbol{q}}(\mu\nu) \widehat{A}_{\mu\nu} \right\}, \tag{2.23} $$

for negative-type operators. The index $\mathbf{q}$ specifies excited states and $\psi^\alpha_{\boldsymbol{q}}(\gamma\delta)$ and $\varphi^\alpha_{\boldsymbol{q}}(\gamma\delta)$ are the RPA forward and backward amplitudes.

The equation of motion and the normalization condition in the RPA theory are given by

$$ [\widehat{H}, {X^\alpha_{\boldsymbol{q}}}^\dagger]_{\mathrm{RPA}} = \omega^\alpha_{\boldsymbol{q}} {X^\alpha_{\boldsymbol{q}}}^\dagger, \tag{2.24} $$

and

$$ [X^\alpha_{\boldsymbol{q}}, {X^\alpha_{\boldsymbol{q}}}^\dagger]_{\mathrm{RPA}} = \delta_{\boldsymbol{q}\boldsymbol{q}'}, \tag{2.25} $$

where the notation $[\quad]_{\mathrm{RPA}}$ means that we neglect the terms higher than the RPA order in the commutator.

Let us denote the transition matrix elements between the RPA excited states ${X^\alpha_{\boldsymbol{q}}}^\dagger$ and the yrast state as

$$ \mathcal{Q}^\alpha_\rho(\boldsymbol{q}) = \langle \omega_{\mathrm{rot}} | \widehat{R}^\alpha_{\rho'} | \mathbf{q} \rangle = \left[\widehat{R}^\alpha_{\rho'}, {X^\alpha_{\boldsymbol{q}}}^\dagger \right]_{\mathrm{RPA}}. \tag{2.26} $$

Then, the equation of motion (2.24) is equivalent to the linear homogenous equation

$$\mathcal{Q}^{\alpha}_{\rho}(\boldsymbol{q}) = \sum_{\rho'} S^{\alpha}_{\rho\rho'}(\omega)\chi^{\alpha}_{\rho}\mathcal{Q}^{\alpha}_{\rho'}(\boldsymbol{q}), \tag{2.27}$$

where the quantities $S^{\alpha}_{\rho\rho'}(\omega)$ are the so called unperturbed response functions necessary to calculate the vibrational modes. In fact, RPA solutions, the eigenergies $\omega^{\alpha}_{\boldsymbol{q}}$ are obtained by solving the equation

$$\det(\chi^{\alpha}_{\rho}S^{\alpha}_{\rho\rho'}(\omega) - \delta_{\rho\rho'}) = 0, \tag{2.28}$$

which corresponds to the condition that (2.27) has a nontrivial solution. This is a determinant equation of dimension 7×7 for signature positive sector and 2×2 for negative part , as one can see from the definitions (2.11,2.12) of the residual interactions. Each RPA eigenstate is characterized by the corresponding forward and backward amplitudes which are calculated as

$$\begin{aligned}
\psi^{\alpha}_{\boldsymbol{q}}(\gamma\delta) &= +\frac{\sum_{\rho}\chi^{\alpha}_{\rho}\mathcal{Q}^{\alpha}_{\rho}(\boldsymbol{q})R^{\alpha}_{\rho}(\gamma\delta)}{E_{\gamma}+E_{\delta}-\omega^{\alpha}_{\boldsymbol{q}}} \times N_{\boldsymbol{q}}, \\
\varphi^{\alpha}_{\boldsymbol{q}}(\gamma\delta) &= -\frac{\sum_{\rho}\chi^{\alpha}_{\rho}\mathcal{Q}^{\alpha}_{\rho}(\boldsymbol{q})R^{\alpha}_{\rho}{}^{*}(\gamma\delta)}{E_{\gamma}+E_{\delta}+\omega^{\alpha}_{\boldsymbol{q}}} \times N_{\boldsymbol{q}},
\end{aligned} \tag{2.29}$$

where $N_{\boldsymbol{q}}$ is the normalization constant defined by

$$\sum_{\boldsymbol{q}} \left\{ \psi^{\alpha^2}_{\boldsymbol{q}}(\gamma\delta) - \varphi^{\alpha^2}_{\boldsymbol{q}}(\gamma\delta) \right\} = 1. \tag{2.30}$$

The transition matrix elements between the RPA excited states $\mathbf{q}$ and the yrast state for any of the residual interaction can be expressed in terms of the amplitudes $\psi^{\alpha}_{\boldsymbol{q}}(\gamma\delta)$ and $\varphi^{\alpha}_{\boldsymbol{q}}(\gamma\delta)$

$$\mathcal{Q}^{\alpha}_{\rho}(\boldsymbol{q}) = \sum_{\gamma\delta} \left[R^{\alpha}_{\rho}{}^{*}(\gamma\delta)\psi^{\alpha}_{\boldsymbol{q}}(\gamma\delta) - R^{\alpha}_{\rho}(\gamma\delta)\varphi^{\alpha}_{\boldsymbol{q}}(\gamma\delta) \right]. \tag{2.31}$$

The expression for the unperturbed response functions for positive and negative signature is given by

$$
\begin{aligned}
S^0_{\rho\rho'}(\omega) &= \sum_{\mu\bar{\nu}} \left(\frac{R^{0\,*}_{\rho}(\mu\bar{\nu}) R^0_{\rho'}(\mu\bar{\nu})}{E_{\mu\bar{\nu}} - \omega} + \frac{R^0_{\rho}(\mu\bar{\nu}) R^{0\,*}_{\rho'}(\mu\bar{\nu})}{E_{\mu\bar{\nu}} + \omega} \right), \\
S^1_{\rho\rho'}(\omega) &= {\sum_{\mu\langle\nu}}'' \left(\frac{R^{1\,*}_{\rho}(\mu\nu) R^1_{\rho'}(\mu\nu)}{E_{\mu\nu} - \omega} + \frac{R^1_{\rho}(\mu\nu) R^{1\,*}_{\rho'}(\mu\nu)}{E_{\mu\nu} + \omega} \right),
\end{aligned}
\tag{2.32}
$$

where the quantities $E_{\mu\bar{\nu}} = E_\mu + E_{\bar{\nu}}$ and $E_{\mu\nu} = E_\mu + E_\nu$ are the two-quasiparticle excitations in the positive and negative sector respectively. In the case of a non-superconducting system these energies correspond to the usual particle-hole excitations.

The coupled RPA equation (2.28) presents numerical difficulties, connected to the fact that the number of the two-quasiparticle excitations $E_{\mu\bar{\nu}}(E_{\mu\nu})$ in a deformed rotating system is more than thousands due to the loss of degeneracy in the single-particle spectrum. Moreover, the spectrum of these two-quasiparticle excitations is very dense leading to a difficult search of the coherent RPA solution, because each vibrational solution of (2.28) lies between two of these two-quasiparticle excitations.

In what follows we are going to show in a realistic case the difficulties met in looking for each individual RPA roots. We have chosen a well-deformed nucleus, ^{168}Yb and calculated the two-quasiparticle excitations entering in the definition of the unperturbed response function (see Eq.(2.32)). In this case we have two sectors, one for signature positive with dimension of 7×7 and a signature negative part of 2×2 dimension. We consider, for simplicity only one case, namely the positive one and in particular the two-quasiparticle energies and corresponding transition matrix elements for β-vibration. We take now the same quantities but for a spherical nucleus, that is ^{98}Mo and we plot the results in the same picture (see Fig.(2.2)) for comparison. From graph (a) it is clear that the number of transitions is considerably increased (we are in presence of ∼16000 different transitions for ^{168}Yb while we have only 200 for ^{98}Mo in the same range of energy) and, moreover, the difference between two of these two-quasiparticle excitation can be so tiny that it is not resolvable in the plot (grey region). Thinking in terms of the simple RPA dispersion relation this means

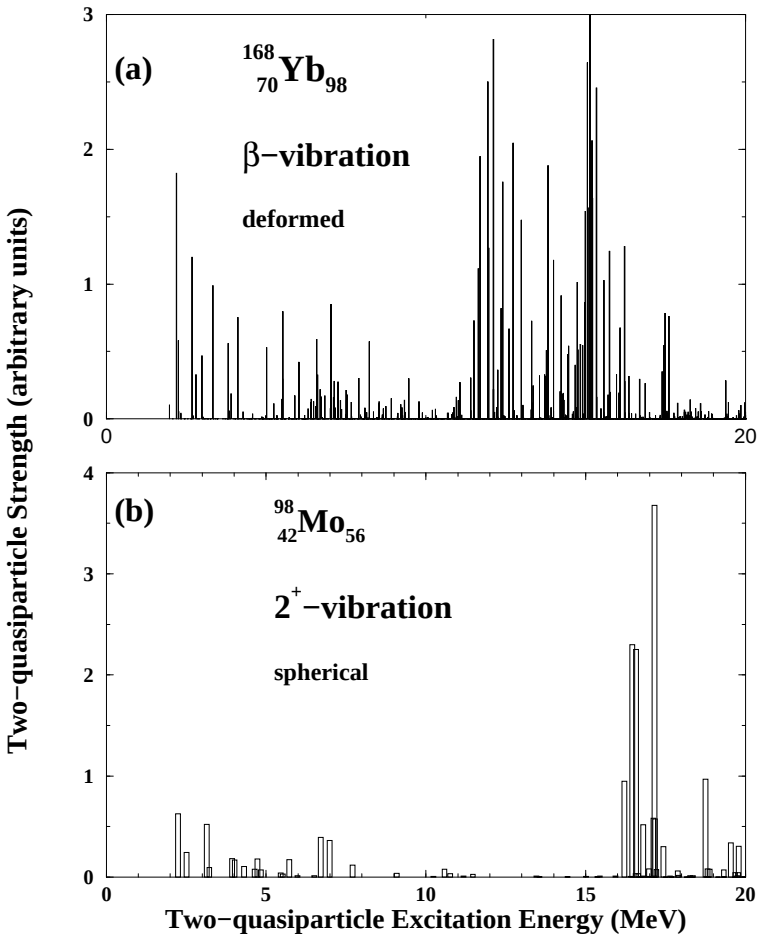

Figure 2.2: Two-quasiparticle excitation energies for a deformed (case (a)) and spherical nucleus (case (b)).

that one should be able to find a number of RPA roots equal to the number of the two-quasiparticle excitation energies, because each of the individual RPA solutions are sandwiched between two of the two-quasiparticle-like excitations. This represents a numerical challenge in the coupled RPA equation especially in connection with the determination of the spurious states associated with Nambu-Goldstone modes (see Chapters 5).

We are then left with the problem of finding the RPA solutions without solving numerically eq.(2.28) and the corresponding transition matrix elements (2.26). This is possible within the framework of the linear response theory. As an example, the RPA ground state correlation energy has been calculated by using this technique,

without explicitly solving the RPA equations [23].

2.4 Linear Response Theory

The expression for the response function, in case of separable residual interactions, can be written as

$$\mathcal{R} = (1 - S\chi)^{-1} S, \tag{2.33}$$

where $\mathcal{R}$, S and χ, in the actual case of coupled RPA, are $N \times N$ matrices, where N is the total number of the residual interactions in a specific sector of signature. The matrix S is the unperturbed response function defined in terms of two-quasiparticle excitations given by (2.32). It is convenient to have the explicit expression for the response function, namely its spectral representation, (see [3]). For this purpose we need to calculate the resolvent operator

$$\widehat{G}(\omega) = \frac{1}{\widehat{H} - \omega}. \tag{2.34}$$

The matrix $G(\omega)$ corresponding to the above resolvent is easily obtained once the RPA eigenvalue problem is solved. The RPA spectrum consists of complex energies. However, one can show that only the real ones correspond to physical solutions, while the complex ones are sign of the instability of the system. For non-zero real solutions, the eigenvalues and eigenvectors of the RPA can be written as

$$(\omega_{\boldsymbol{q}}, X_{\boldsymbol{q}}), (-\omega_{\boldsymbol{q}}, \bar{X}_{\boldsymbol{q}}), \tag{2.35}$$

where the eigenvectors are defined by

$$\begin{aligned} X^{\alpha}_{\boldsymbol{q}} &= \begin{pmatrix} \psi^{\alpha}_{\boldsymbol{q}}(\gamma\delta) \\ \varphi^{\alpha}_{\boldsymbol{q}}(\gamma\delta) \end{pmatrix} \rightarrow {X^{\alpha}_{\boldsymbol{q}}}^{\dagger} = \sum_{\gamma<\delta} \left[\psi^{\alpha}_{\boldsymbol{q}}(\gamma\delta) \widehat{A}^{\dagger}_{\gamma\delta} + \varphi^{\alpha}_{\boldsymbol{q}}(\gamma\delta) \widehat{A}_{\gamma\delta} \right], \\ \bar{X^{\alpha}_{\boldsymbol{q}}} &= \begin{pmatrix} {\varphi^{\alpha}_{\boldsymbol{q}}}^{*}(\gamma\delta) \\ {\psi^{\alpha}_{\boldsymbol{q}}}^{*}(\gamma\delta) \end{pmatrix} \rightarrow {\bar{X}^{\alpha}_{\boldsymbol{q}}}^{\dagger} = \sum_{\gamma<\delta} \left[{\varphi^{\alpha}_{\boldsymbol{q}}}^{*}(\gamma\delta) \widehat{A}^{\dagger}_{\gamma\delta} + {\psi^{\alpha}_{\boldsymbol{q}}}^{*}(\gamma\delta) \widehat{A}_{\gamma\delta} \right]. \end{aligned} \tag{2.36}$$

Due to the normalization condition (2.25) we have that

$$[X^{\alpha}_{\boldsymbol{q}}, X^{\alpha}_{\boldsymbol{q}}{}^{\dagger}]_{RPA} = \delta_{\boldsymbol{qq'}} = -[\bar{X}^{\alpha}_{\boldsymbol{q}}, \bar{X}^{\alpha}_{\boldsymbol{q}}{}^{\dagger}]_{\rm RPA} = \delta_{\boldsymbol{qq'}} \tag{2.37}$$

The spectral representation of the resolvent expressed in terms of these eigenvectors is

$$G(\omega) = \sum_{\boldsymbol{q}} \left[\frac{X^{\alpha}_{\boldsymbol{q}} * X^{\alpha}_{\boldsymbol{q}}{}^{\dagger}}{\omega^{\alpha}_{\boldsymbol{q}} - \omega} + \frac{\bar{X}^{\alpha}_{\boldsymbol{q}} \bar{X}^{\alpha}_{\boldsymbol{q}}{}^{\dagger}}{\omega^{\alpha}_{\boldsymbol{q}} + \omega} \right] \tag{2.38}$$

where the notation $X * Y$ represents a matrix constructed from the product of two vectors X and Y (Notice that this is valid only when we do not have zero-energy solutions, that is the Nambu-Goldstone modes(see Chapter 5)).

The resolvent matrix can be used to evaluate the spectral representation of the RPA response, because

$$\mathcal{R}^{\alpha}_{\rm AB}(\omega) \equiv \langle \widehat{A}^{\dagger} G(\omega) B \rangle, \tag{2.39}$$

where A and B are two generic operators and the notation $\langle \quad \rangle$ means that we are considering the vacuum expectation value, that is $\langle \omega_{\rm rot}| \quad |\omega_{\rm rot}\rangle$. This means that the numerators of the response function will contains terms as $\widehat{A}^{\dagger}\widehat{X} * \widehat{Y}^{\dagger}\widehat{B}$ that, in the framework of the RPA response, can be written as

$$\langle \widehat{A}^{\dagger}\widehat{X} * \widehat{Y}^{\dagger}\widehat{B} \rangle = [\widehat{A}^{\dagger}_{,}\widehat{X}]_{\rm RPA}[\widehat{Y}^{\dagger}_{,}\widehat{B}]_{\rm RPA}. \tag{2.40}$$

We remember now the definition of the transition matrix elements between excited and ground state (see Eq.(2.26)), so that the expression above can be written as

$$\langle \widehat{A}^{\dagger}\widehat{X} * \widehat{Y}^{\dagger}\widehat{B} \rangle = \mathcal{Q}^{\alpha}_{\widehat{A}}{}^{*}(\boldsymbol{q}) \mathcal{Q}^{\alpha}_{\widehat{B}}(\boldsymbol{q}). \tag{2.41}$$

Introducing this last equality in the spectral representation of the RPA response function we obtain

$$\mathcal{R}^{\alpha}_{\rho\rho'}(\omega) = \sum_{\boldsymbol{q}} \left(\frac{\mathcal{Q}^{\alpha}_{\rho}{}^{*}(\boldsymbol{q}) \mathcal{Q}^{\alpha}_{\rho'}(\boldsymbol{q})}{\omega^{\alpha}_{\boldsymbol{q}} - \omega} + \frac{\mathcal{Q}^{\alpha}_{\rho}(\boldsymbol{q}) \mathcal{Q}^{\alpha}_{\rho'}{}^{*}(\boldsymbol{q})}{\omega^{\alpha}_{\boldsymbol{q}} + \omega} \right), \tag{2.42}$$

where the indexes ρ and ρ' are used to label the operators $\widehat{A}$ and $\widehat{B}$.

Chapter 3

Single-Particle Self-Energy

3.1 Introduction

We can summarize the content of the former Chapters saying that the nuclear system is built up of single-particle(quasiparticle) plus surface vibrations. In fact, we have seen in Chapter 1, that the quasiparticles can be considered as independent elementary excitations of the HFB vacuum state, while the collective modes are elementary (independent) excitations of the RPA vacuum (see Chapter 2). The next step is to consider states which are made up from two excitation modes. If one of the excitations has a collective character while the second has a single particle nature (as in the nucleus case), one can define an interaction Hamiltonian which is linear in the collective and particle variables. The density variations associated with the surface mode produce corresponding variations in the average nuclear potential, leading to a coupling between the vibrational degrees of freedom and those of the individual particles which plays a similar role in the nucleus as the particle-phonon or particle-plasmon couplings in condensed matter. One may consider the various effects which arise from the coupling, for example the renormalization of the properties of both the particles and the vibrations, the effective interactions between those elementary excitations and so on.

In a nucleus shape oscillations are the most important low-lying collective motion. In this case the average potential can be approximately obtained by a deformation of the static potential which has a surface $R(\hat{r})$ defined by

$$R(\hat{r}) = R_0 \left[1 + \sum_{\lambda\mu\mathbf{q}} \alpha_{\lambda\mu}(\mathbf{q}) Y^*_{\lambda\mu}(\hat{r}) \right] \qquad \lambda \geq 2. \tag{3.1}$$

In the above definition the quantities $\alpha_{\lambda\mu}(\mathbf{q})$ are time-dependent amplitudes of the collective deformation(excitations) of the nuclear surface. For each multipolarity λ we have a set of $(2\lambda + 1)$ variables μ=0,$\pm$ 1,...,$\pm\lambda$. The corresponding wave-like excitations (in number of $\mathbf{q}$ for each multipolarity λ) carry the angular momentum λ, its projection μ onto an arbitrary quantization axis z fixed in space, and *natural parity* $(-1)^\lambda$.

3.2 Particle-Vibration Coupling

The fluctuation of the nuclear surface around the equilibrium radius R_0 is then given by

$$\widehat{V}(r) = \widehat{V}_0(r) + H_{\text{coupl}}, \tag{3.2}$$

where the first term on the right hand side represents the average static one-body potential while the second one, defined by

$$\widehat{H}_{\text{coupl}} = -R_0 \frac{\partial \widehat{V}_0}{\partial r} \sum_{\lambda\mu\boldsymbol{q}} \widehat{\alpha}_{\lambda\mu}(\boldsymbol{q}) \widehat{Y^*}_{\lambda\mu}(\hat{r}), \tag{3.3}$$

is the particle-vibration coupling Hamiltonian. From its definition (see Eq.3.3) one can see that $\widehat{H}_{\text{coupl}}$, due to the amplitudes $\alpha_{\lambda\mu}(\boldsymbol{q})$, introduces an explicitly time-dependence (energy-dependence) into the one-body potential, hence modifying the Hartree-Fock (or HFB) predictions of single-particles properties in several respects. It turns out that it is not possible to reproduce the essential features of the experimental data on bound and scattering states if one assumes that this potential is local and independent of energy. It was shown [39] that the particle-vibration coupling strongly shifts these states surrounding the Fermi-level and increases the single-particle density. This level shift can also be discussed in terms of an effective mass m^*. It was already pointed out by Brown et al [38] that the experimental single-particles energies are better reproduced if one allows the ratio m^*/m to be close to or larger than 1 around

the Fermi level whereas it should be about 0.6-0.7 for the deeper states. Brueckner HF calculations in nuclear matter [35] and second-order calculations in finite nuclei [36] indicate that the energy dependence of the one-body potential, or mass operator, leads to an enhancement of m^*/m around the Fermi energy. On the other hand, the values of m^*/m predicted for example by HF calculations with Skyrme III [37] are smaller than one. One can show that m^*/m becomes larger than one for states in the vicinity of the Fermi level when the particle-vibration coupling is included. We will come back to the definition of the effective mass and how to evaluate it later on (see Chapter 8). Now we are interested in studying the energy correction to the one-body potential generated by the coupling of the single-particle degrees of freedom with the collective motion.

We start looking at the main vertices originating by the coupling (3.3) which are depicted in Fig.(3.1), where case(a) represents a particle(hole) exciting a vibration by means of an inelastic bouncing off the surface while case(b) is the annihilation of the surface modes with production of a particle-hole pair.

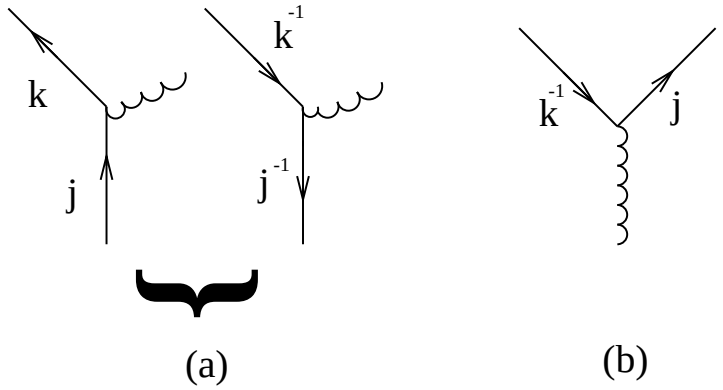

Figure 3.1: Basic couplings between particles and phonons which contribute to the self-energies of single-particle states. A line marked with an arrow pointing up represents a particle, while one pointing down represents a hole. A wavy line stands for a surface vibration. In (a) a particle (hole) bounces inelastically off the surface and creates a surface vibration. In (b) the annihilation of a surface modes is followed by the creation of a particle-hole pair.

The lowest (second) order dynamical contributions in the particle-vibration model to the mass operator renormalizing the single-particle motion are given in Fig.(3.2)

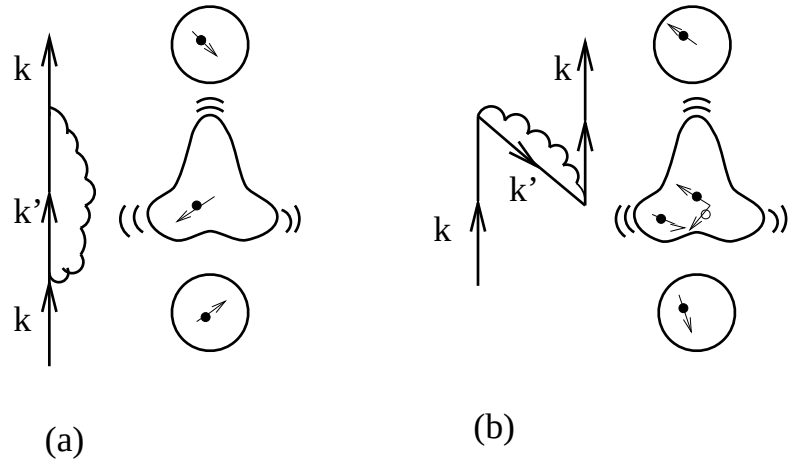

Figure 3.2: The lowest(second)order processes by which the single-particle motion is renormalized by the coupling to surface modes. The intermediate state is a particle (case (a)) while graph (b) represents a hole intermediate state.

The associated expression of the self-energy operator is

$$\sum_{\rm sp}(\mathbf{1},\omega)=\sum_{2,\boldsymbol{q}}\left\{\frac{V^2(\mathbf{1},\mathbf{2};\lambda,\boldsymbol{q})}{\omega-(\varepsilon_{\mathbf{2}}+\omega_{\boldsymbol{q}})}+\frac{V^2(\mathbf{1},\mathbf{2};\lambda,\boldsymbol{q})}{\omega-(\varepsilon_{\mathbf{2}}-\omega_{\boldsymbol{q}})}\right\}. \tag{3.4}$$

The notation $\sum_{\rm sp}(\mathbf{1},\omega)$ means self-energy correction of the single-particle state $\mathbf{1}$ while

$$V(\mathbf{1},\mathbf{2};\lambda,\boldsymbol{q})=\langle(\mathbf{2};\mathbf{q}(\lambda))\mathbf{1}|\widehat{H}_{\rm coupl}|\mathbf{1}\rangle=\pm\frac{\beta_{\boldsymbol{q}}(\lambda)}{\sqrt{(2j_{\mathbf{1}}+1)(2\lambda+1)}}\langle\mathbf{1}||\widehat{T}_\lambda||\mathbf{2}\rangle, \tag{3.5}$$

are the matrix elements controlling the coupling mechanism (cf. Fig.(3.1) case(a)) and where the term

$$\widehat{T}_{\lambda\mu}=R_0\frac{\partial\widehat{V}_0}{\partial r}\widehat{Y^*}_{\lambda\mu}(\hat{r}), \tag{3.6}$$

is the field generating the collective modes $\widehat{\alpha}_{\lambda\mu}$. The plus and minus sign corresponds to a particle or to a hole scattering respectively. In the above notation

$|(\mathbf{2};\mathbf{q}(\lambda))\mathbf{1}>$ means that the coupling (3.3) gives rise to an intermediate state built up as a particle **2** coupled to the vibration **q** of multipolarity λ in such a way that the quantum numbers of the initial state **1** are conserved. Each term of the self-energy expression has the typical structure of an energy correction in second order perturbation theory, that is, a square matrix element divided by an energy denominator, given by the difference between the initial and intermediate states.

The quantity $\beta_{\boldsymbol{q}}(\lambda)$ defined as

$$M_{\lambda\boldsymbol{q}}(T) = |\langle 1_{\lambda\mu\mathbf{q}}|\widehat{\alpha}_{\lambda\mu}(\mathbf{q})|0\rangle|^2 = \frac{\beta^2_{\boldsymbol{q}}(\lambda)}{2\lambda+1}. \tag{3.7}$$

is the deformation parameter associated with the **q**'th surface vibration. In the above definition we have used the notation $1_{\lambda\mu\mathbf{q}}$ to label a one-phonon state of multipolarity λ and projection μ. In the framework of the linear response function, this parameter represents, for each RPA solutions, the transition matrix element between the excited state and the ground state (see Chapter 2), so that one can write

$$\mathcal{R}_\lambda(\omega) = \sum_{\boldsymbol{q}} \left[\frac{M_{\lambda\boldsymbol{q}}(T)}{\omega^\lambda_{\boldsymbol{q}} - \omega} + \frac{M_{\lambda\boldsymbol{q}}(T)}{\omega^\lambda_{\boldsymbol{q}} + \omega}\right] = \sum_{\boldsymbol{q}} M_{\lambda\boldsymbol{q}}(T)\frac{-2\omega^\lambda_{\boldsymbol{q}}}{\omega^2 - {\omega^\lambda_{\boldsymbol{q}}}^2}. \tag{3.8}$$

In this case we are dealing with only one residual interaction, so that ${\mathcal{Q}^\alpha_\rho}^*(\boldsymbol{q})\mathcal{Q}^\alpha_{\rho'}(\boldsymbol{q})$ and $\mathcal{Q}^\alpha_\rho(\boldsymbol{q}){\mathcal{Q}^\alpha_{\rho'}}^*(\boldsymbol{q})$, appearing in Eq.(2.42), coincide because $\rho = \rho' = 1$ and they are called $M_{\lambda\boldsymbol{q}}(T)$. We will see in Chapter 4 that this, in a more general framework, is not possible leading to extra terms in the self-energy expression.

3.3 Self-Energy at Finite Temperature

The finite temperature method we shall use was developed by Matsubara and one can find the details in textbooks [5, 7, 8]. Here we recall only some of the important properties that we will use in the development of the self-energy correction in a rotating frame. First of all, the Matsubara's method is based on the treatment of time t and temperature $\beta(= 1/KT)$ as real and imaginary parts of a complex variable. As a consequence, the frequencies associated with single-particle states are discrete quantities.

The fermion Green's function representing the free propagation of a particle with momentum $\mathbf{p}$ and energy $\varepsilon_{\mathbf{p}}$ (the energies are always considered referred to the Fermi energy) is defined as

$$\mathcal{G}^0(\boldsymbol{p}, ip_n) = \frac{1}{ip_n - \varepsilon_{\mathbf{p}}}, \tag{3.9}$$

while the propagation of a phonon with momentum $\mathbf{q}$ and frequency $\omega_{\boldsymbol{q}}$ is given by the phonon Green's function

$$\mathcal{D}^0_\lambda(\boldsymbol{q}, i\omega_n) = \left(\frac{1}{i\omega_n - \omega^\lambda_{\boldsymbol{q}}} - \frac{1}{i\omega_n + \omega^\lambda_{\boldsymbol{q}}} \right). \tag{3.10}$$

The label λ is used to distinguish between different multipolarity of the vibrational modes. The temperature information are contained in the frequencies ip_n and $i\omega_n$ defined as

$$\begin{aligned} ip_n &= i\frac{(2n+1)\pi}{\beta}, \\ i\omega_n &= i\frac{2n\pi}{\beta}, \end{aligned} \tag{3.11}$$

where n is an integer number, that can be positive, negative or zero. This means that the fermion and phonon frequencies take discrete values and, in particular, the fermion frequencies are odd multiples of $\frac{\pi}{\beta}$ while the phonon frequencies are even multiples.

The basic self-energy contribution originating from the particle-vibration coupling is shown in Fig.(3.3) and the analytic expression is given by

$$\sum_{\text{sp}}(\mathbf{1}, ip_n) = -\frac{1}{\beta} \sum_{\lambda, \boldsymbol{q}, \mathbf{2}} V^2(\mathbf{1}, \mathbf{2}; \lambda, \boldsymbol{q}) \sum_{i\omega_n} \mathcal{D}^0_\lambda(\boldsymbol{q}, i\omega_n) \mathcal{G}^0(\mathbf{2}, ip_n - i\omega_n). \tag{3.12}$$

One can try to give a simple explanation to this expression looking at Fig.(3.3). The initial state is a particle with frequency ip_n, labelled $\mathbf{1}$, moving in the mean field that can emit or absorb a phonon with frequency $i\omega_n$ (phonon free propagation given by $\mathcal{D}^0_\lambda(\boldsymbol{q}, i\omega_n)$). This induces the initial particle to change its state of motion

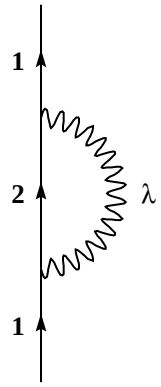

Figure 3.3: Self-energy diagram for the single-particle state at finite temperature. An arrowed line describes the particle propagation while a wavy line indicates a surface mode.

going into another state with frequency $ip_n - i\omega_n$, labelled **2** (fermion propagation represented by $\mathcal{G}^0(\mathbf{2}, ip_n - i\omega_n)$). The phonon is re-absorbed or re-emitted bringing the configuration to the same initial state. One can notice that at the vertex there is conservation of the oddness and eveness of the fermion and phonon frequencies, respectively. In fact, $ip_n - i\omega_n$ is the difference between an odd and an even number. This means that the result is an odd number as it should be because the intermediate state **2** is a fermion.

3.4 Matsubara Frequency Summation

The following section develops in details the Matsubara's method of summation over combinations of unperturbed Green's functions. We have decided to report here all steps of calculations to compare it with the new procedure that will be discussed in the next section. We simplify the notation of (3.12) introducing the function S that contains the sum in which we are interested in, namely

$$S = -\frac{1}{\beta}\sum_{i\omega_n} \mathcal{D}^0_\lambda(\boldsymbol{q}, i\omega_n)\mathcal{G}^0(\mathbf{2}, ip_n - i\omega_n), \tag{3.13}$$

since we can rewrite the self-energy in the compact form

$$\sum_{\rm sp}(\mathbf{1}, ip_n) = \sum_{\lambda,\boldsymbol{q},\mathbf{2}} V^2(\mathbf{1},\mathbf{2};\lambda,\boldsymbol{q})S. \tag{3.14}$$

The function S, after substituting the definition of the fermion and phonon Green's functions, can be written as

$$S = -\frac{1}{\beta}\sum_{n=-\infty}^{+\infty} f(i\omega_n) = -\frac{1}{\beta}\sum_{n=-\infty}^{+\infty} \frac{2\omega_{\boldsymbol{q}}^{\lambda}}{(i\omega_n)^2 - \omega_{\boldsymbol{q}}^{\lambda}} \frac{1}{ip_n - i\omega_n - \varepsilon_{\mathbf{2}}}. \tag{3.15}$$

We consider now the following contour integration

$$I = \lim_{R\to\infty} \frac{1}{2\pi i}\oint_C dz f(z) n_B(z), \tag{3.16}$$

where the path C corresponds to a large circle of radius R in the limit as R $\to \infty$ and the function f is exactly the one defined in Eq.(3.15) with the substitution $i\omega_n \to z$. The function $n_B(z)$ is chosen to generate poles at the points $i\omega_n$ for all even integer n. The function which does this is the boson factor

$$n_B(z) = \frac{1}{\mathrm{e}^{\beta z} - 1}. \tag{3.17}$$

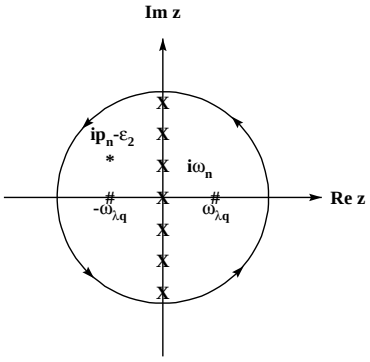

Figure 3.4: Contour integration and poles of the function $f(z)$. The mark **X** is used for the boson factor poles while # indicates the phonon Green's function poles. For the fermion case the symbol * is used.

The poles of $n_B(z)$ are the points $i\frac{2n\pi}{\beta}$ for all positive, negative integer n included

n=0. The residue at each of these poles is $\frac{1}{\beta}$. In Fig.(3.4), these poles are drawn using **X** marks evenly spaced on the vertical axis. The function $f(z)$ has poles at the points $\pm\omega_{\boldsymbol{q}}^{\lambda}$, (labelled by # in the same figure) which originate from the phonon Green's function. The last pole is $ip_n - \varepsilon_{\mathbf{2}}$, (labelled by * where it is considered the case $\varepsilon_{\mathbf{2}} > 0$)) due to the fermion Green's function.

In the following we summarize the calculated residues at each pole, namely

$$\begin{aligned}
z_n &= i\frac{2n\pi}{\beta} & R_n &= \frac{1}{\beta} f(i\omega_n) \\
z_1 &= \omega_{\boldsymbol{q}}^{\lambda} & R_1 &= \frac{-n_B(\omega_{\boldsymbol{q}}^{\lambda})}{+\omega_{\boldsymbol{q}}^{\lambda} - ip_n + \varepsilon_{\mathbf{2}}} \\
z_2 &= -\omega_{\boldsymbol{q}}^{\lambda} & R_2 &= \frac{n_B(-\omega_{\boldsymbol{q}}^{\lambda})}{-\omega_{\boldsymbol{q}}^{\lambda} - ip_n + \varepsilon_{\mathbf{2}}} \\
z_3 &= ip_n - \varepsilon_{\mathbf{2}} & R_3 &= \frac{-2\omega_{\boldsymbol{q}}^{\lambda} n_B(ip_n - \varepsilon_{\mathbf{2}})}{(ip_n - \varepsilon_{\mathbf{2}})^2 - {\omega_{\boldsymbol{q}}^{\lambda}}^2}
\end{aligned} \tag{3.18}$$

It is important to remember some useful properties of the boson and fermion function that we will use below to simplify as much as possible the formulations. We can start with the relation existing between the values of the function $n_B(z)$ at the point $-z$ and its opposite $+z$, that is

$$n_B(-z) = \frac{1}{e^{-\beta z} - 1} = \frac{e^{\beta z}}{1 - e^{\beta z}} = -e^{\beta z} n_B(z). \tag{3.19}$$

But

$$e^{\beta z} = 1 + n_B(z)^{-1} = \frac{1 + n_B(z)}{n_B(z)}, \tag{3.20}$$

so that

$$n_B(-z) = -\frac{1 + n_B(z)}{n_B(z)} n_B(z) = -\left[1 + n_B(z)\right]. \tag{3.21}$$

We want to find the equivalent relation for the fermion function, that is

$$n_F(-z) = \frac{1}{e^{-\beta z}+1} = \frac{e^{\beta z}}{e^{\beta z}+1} = e^{\beta z} n_F(z). \tag{3.22}$$

We notice that

$$e^{\beta z} = n_F(z)^{-1} - 1 = \frac{1-n_F(z)}{n_F(z)}, \tag{3.23}$$

which allows us to write

$$n_F(-z) = \frac{1-n_F(z)}{n_F(z)} n_F(z) = 1 - n_F(z). \tag{3.24}$$

We now observe that the exponential function has an important property

$$e^{im\pi} = \cos m\pi + i \sin m\pi = (-1)^m, \tag{3.25}$$

if m is an integer number. We can use these results to write that

$$n_B(ip_n - \varepsilon_{\mathbf{2}}) = -n_F(-\varepsilon_{\mathbf{2}}), \tag{3.26}$$

because, using (3.11,3.19-3.25), we have that

$$\begin{aligned} n_B(ip_n - \varepsilon_{\mathbf{2}}) &= \frac{1}{e^{\beta i p_n} e^{-\beta\varepsilon_{\mathbf{2}}} - 1} = \frac{1}{e^{i(2n+1)\pi} e^{-\beta\varepsilon_{\mathbf{2}}} - 1} = \\ &= \frac{1}{(-1)^{(2n+1)} e^{-\beta\varepsilon_{\mathbf{2}}} - 1} = \frac{1}{-e^{-\beta\varepsilon_{\mathbf{2}}} - 1} = -\frac{1}{e^{-\beta\varepsilon_{\mathbf{2}}} + 1} = -n_F(-\varepsilon_{\mathbf{2}}). \end{aligned} \tag{3.27}$$

We can now rewrite the residues R_2 and R_3, using the relations found above, that is

$$R_2 = \frac{-n_B(\omega^\lambda_{\boldsymbol{q}}) - 1}{-\omega^\lambda_{\boldsymbol{q}} - ip_n + \varepsilon_{\mathbf{2}}} \tag{3.28}$$

$$R_3 = \frac{2\omega^\lambda_{\boldsymbol{q}} n_F(-\varepsilon_{\mathbf{2}})}{(ip_n - \varepsilon_{\mathbf{2}})^2 - \omega^{\lambda^2}_{\boldsymbol{q}}} = \frac{2\omega^\lambda_{\boldsymbol{q}} \left[1 - n_F(\varepsilon_{\mathbf{2}})\right]}{(ip_n - \varepsilon_{\mathbf{2}})^2 - \omega^{\lambda^2}_{\boldsymbol{q}}}. \tag{3.29}$$

The last residue can be reduced to a more useful form because its denominator is the difference of two squared numbers. This means that

$$\frac{2\omega_{\mathbf{q}}^{\lambda}}{(ip_n-\varepsilon_{\mathbf{2}})^2-{\omega_{\mathbf{q}}^{\lambda}}^2} = \frac{2\omega_{\mathbf{q}}^{\lambda}}{\left(ip_n-\varepsilon_{\mathbf{2}}-\omega_{\mathbf{q}}^{\lambda}\right)\times\left(ip_n-\varepsilon_{\mathbf{2}}+\omega_{\mathbf{q}}^{\lambda}\right)} = = \left(\frac{1}{ip_n-\varepsilon_{\mathbf{2}}-\omega_{\mathbf{q}}^{\lambda}}-\frac{1}{ip_n-\varepsilon_{\mathbf{2}}+\omega_{\mathbf{q}}^{\lambda}}\right), \tag{3.30}$$

leading to this expression for the residue R_3

$$R_3=\left[\frac{1-n_F(\varepsilon_{\mathbf{2}})}{ip_n-\varepsilon_{\mathbf{2}}-\omega_{\mathbf{q}}^{\lambda}}-\frac{1-n_F(\varepsilon_{\mathbf{2}})}{ip_n-\varepsilon_{\mathbf{2}}+\omega_{\mathbf{q}}^{\lambda}}\right]. \tag{3.31}$$

We insert back R_n, R_1, R_2, and R_3 in the definition of the contour integration I taking into account that, by definition, it is simply the sum of all the residues included in the chosen path. For convenience, we change sign in the denominators of R_1 and R_2 to have similar terms in the sum. The value of the contour integration I is then

$$I=\sum_{n=-\infty}^{+\infty}R_n+R_1+R_2+R_3, \tag{3.32}$$

that means

$$I = \sum_{n=-\infty}^{+\infty}\frac{1}{\beta}f(i\omega_n)+\frac{n_B(\omega_{\mathbf{q}}^{\lambda})}{ip_n-\varepsilon_{\mathbf{2}}-\omega_{\mathbf{q}}^{\lambda}}+\frac{1+n_B(\omega_{\mathbf{q}}^{\lambda})}{ip_n-\varepsilon_{\mathbf{2}}+\omega_{\mathbf{q}}^{\lambda}}+ + \left[\frac{1-n_F(\varepsilon_{\mathbf{2}})}{ip_n-\varepsilon_{\mathbf{2}}-\omega_{\mathbf{q}}^{\lambda}}-\frac{1-n_F(\varepsilon_{\mathbf{2}})}{ip_n-\varepsilon_{\mathbf{2}}+\omega_{\mathbf{q}}^{\lambda}}\right]. \tag{3.33}$$

We can simplify this integral adding the terms with the same denominator and using the definition of S given in Eq.(3.13),

$$I=-S+\frac{1+n_{\mathrm{B}}(\omega_{\mathbf{q}}^{\lambda})-n_{\mathrm{F}}(\varepsilon_{\mathbf{2}})}{ip_n-\varepsilon_{\mathbf{2}}-\omega_{\mathbf{q}}^{\lambda}}+\frac{n_{\mathrm{B}}(\omega_{\mathbf{q}}^{\lambda})+n_{\mathrm{F}}(\varepsilon_{\mathbf{2}})}{ip_n-\varepsilon_{\mathbf{2}}+\omega_{\mathbf{q}}^{\lambda}}. \tag{3.34}$$

Due to the fact that the function $f(z)$, defined in Eq.(3.15), goes to zero when $R\to\infty$, the integral I, in this limit, approaches the zero-value. This result is important, because in this way we can find the expression of S, that is the function containing the sum over the frequencies. The result is

$$S=\frac{1}{\beta}\sum_{n=-\infty}^{+\infty}f(i\omega_n)=\frac{1+n_{\mathrm{B}}(\omega_{\mathbf{q}}^{\lambda})-n_{\mathrm{F}}(\varepsilon_{\mathbf{2}})}{ip_n-\varepsilon_{\mathbf{2}}-\omega_{\mathbf{q}}^{\lambda}}+\frac{n_{\mathrm{B}}(\omega_{\mathbf{q}}^{\lambda})+n_{\mathrm{F}}(\varepsilon_{\mathbf{2}})}{ip_n-\varepsilon_{\mathbf{2}}+\omega_{\mathbf{q}}^{\lambda}}. \tag{3.35}$$

The expression of the self-energy is then (3.12)

$$\sum_{\rm sp}(\mathbf{1}, ip_n) = \sum_{\lambda,\boldsymbol{q},\mathbf{2}} V^2(\mathbf{1},\mathbf{2};\lambda,\boldsymbol{q}) \left[\frac{1 + n_{\rm B}(\omega^\lambda_{\boldsymbol{q}}) - n_{\rm F}(\varepsilon_{\mathbf{2}})}{ip_n - \varepsilon_{\mathbf{2}} - \omega^\lambda_{\boldsymbol{q}}} + \frac{n_{\rm B}(\omega^\lambda_{\boldsymbol{q}}) + n_{\rm F}(\varepsilon_{\mathbf{2}})}{ip_n - \varepsilon_{\mathbf{2}} + \omega^\lambda_{\boldsymbol{q}}} \right]. \quad (3.36)$$

We have to connect this function defined in term of discrete fermion frequencies ip_n with retarded functions. This is possible through an analytic continuation of the form $ip_n \to \varepsilon + i\eta$. The retarded self-energy is then

$$\sum_{\rm ret}(\mathbf{1}, \varepsilon + i\eta) = \sum_{\lambda,\boldsymbol{q},\mathbf{2}} V^2(\mathbf{1},\mathbf{2};\lambda,\boldsymbol{q}) \left[\frac{1 + n_{\rm B}(\omega^\lambda_{\boldsymbol{q}}) - n_{\rm F}(\varepsilon_{\mathbf{2}})}{\varepsilon + i\eta - \varepsilon_{\mathbf{2}} - \omega^\lambda_{\boldsymbol{q}}} + \frac{n_{\rm B}(\omega^\lambda_{\boldsymbol{q}}) + n_{\rm F}(\varepsilon_{\mathbf{2}})}{\varepsilon + i\eta - \varepsilon_{\mathbf{2}} + \omega^\lambda_{\boldsymbol{q}}} \right]. \quad (3.37)$$

The structure of the equation above contains two terms coming from the fact that an intermediate state can be formed either by creation or annihilation of a vibrational quantum. Taking into account that the Matsubara Green's function includes both particle and hole propagation, one can give a straightforward interpretation of the single graph in Fig.(3.3) showing that it contains the time-ordered processes at *T=0* (see [13]).

Equation (3.37) is a transparent and simple expression limited by the fact that we need to know exactly all the phonon energies $\omega^\lambda_{\boldsymbol{q}}$ and the corresponding transition matrix elements. This can be done in the framework of the RPA theory at finite temperature [24]. Since in a rotating frame we are dealing, as explained in Chapter 2, with a sum over several interactions corresponding to different vibrational modes, we will end up with a coupled RPA equation with numerical complications. Only a drastic reduction of the number of possible phonon excitations can allow us to use the formula given in (3.37). One can ask the following question: is it possible to obtain the retarded self-energy using a different expression in which the detailed knowledge of the vibrational modes is not necessary ? The linear response theory gives us an affirmative answer because the excitations are, in a sense, "hidden" in the response function(see Chapter 2)

3.5 New Frequency Summation

This new method is based exactly on the original Matsubara's procedure with an important inversion on the order of steps. In fact, while in the usual method one starts solving the frequency summation followed by an analytic continuation, in this new procedure we do the inverse, that is we perform immediately the analytic continuation and, successively, we treat the sum over the frequencies. As we will show below, this inversion leads to a modification in the fermion pole and its corresponding residue that change in an important way the technical details and the computational difficulties in arriving to the same results as Matsubara.

Our starting point is, as in the former section, the self-energy (3.12)

$$\sum_{\rm sp}(\mathbf{1}, ip_n) = -\frac{1}{\beta}\sum_{\lambda,\boldsymbol{q},\mathbf{2}} V^2(\mathbf{1},\mathbf{2};\lambda,\boldsymbol{q})\sum_{i\omega_n}\mathcal{D}^0_\lambda(\boldsymbol{q}, i\omega_n)\mathcal{G}^0(\mathbf{2}, ip_n - i\omega_n). \tag{3.38}$$

We proceed immediately with the analytic continuation $ip_n \to \varepsilon + i\eta$ so that we can write

$$\sum_{\rm sp}(\mathbf{1}, \varepsilon + i\eta) = -\frac{1}{\beta}\sum_{\lambda,\boldsymbol{q},\mathbf{2}} V^2(\mathbf{1},\mathbf{2};\lambda,\boldsymbol{q})\sum_{i\omega_n}\mathcal{D}^0_\lambda(\boldsymbol{q}, i\omega_n)\mathcal{G}^0(\mathbf{2}, \varepsilon + i\eta - i\omega_n). \tag{3.39}$$

The main point in these calculations is to recognize the following inequality

$$\sum_{\rm sp}(\mathbf{1}, ip_n) \quad ip_n \to \varepsilon + i\eta \quad \text{after} \quad \text{summation} \quad \neq \sum_{\rm sp}(\mathbf{1}, \varepsilon + i\eta) \tag{3.40}$$

As in the former section, the self-energy (3.12) can be written in terms of a function containing the sum over the phonon frequencies, that is

$$\sum_{\rm sp}(\mathbf{1}, \varepsilon + i\eta) = -\frac{1}{\beta}\sum_{\lambda,\boldsymbol{q},\mathbf{2}} V^2(\mathbf{1},\mathbf{2};\lambda,\boldsymbol{q})G \tag{3.41}$$

where

$$G = -\frac{1}{\beta}\sum_{i\omega_n} g(i\omega_n) = -\frac{1}{\beta}\sum_{n=-\infty}^{+\infty}\frac{2\omega^\lambda_{\boldsymbol{q}}}{(i\omega_n)^2 - \omega^{\lambda^2}_{\boldsymbol{q}}}\frac{1}{\varepsilon + i\eta - i\omega_n - \varepsilon_{\mathbf{2}}}. \tag{3.42}$$

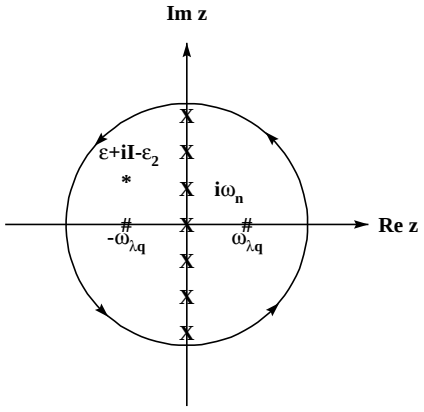

Figure 3.5: Contour integration and poles of the function $g(z)$. See caption of Fig.(3.4) for details.

We need to choose a proper contour integration, as in the former section, defined as

$$J = \lim_{R\to\infty} \frac{1}{2\pi i} \oint_C dz g(z) n_B(z), \tag{3.43}$$

where the path of integration is a large circle of radius R in the limit as $R \to \infty$. The contour of integration and the poles of the function $g(z)$ are represented in Fig.(3.5) for $(\varepsilon - \varepsilon_{\mathbf{2}} < 0)$

The function $g(z)$ is defined as (see 3.42)

$$g(z) = \frac{2\omega_{\boldsymbol{q}}^{\lambda}}{z^2 - \omega_{\boldsymbol{q}}^{\lambda\,2}} \frac{1}{\varepsilon + i\eta - z - \varepsilon_{\mathbf{2}}} = -\frac{2\omega_{\boldsymbol{q}}^{\lambda}}{z^2 - \omega_{\boldsymbol{q}}^{\lambda\,2}} \frac{1}{z - \varepsilon - iI + \varepsilon_{\mathbf{2}}}. \tag{3.44}$$

This function has the same poles of the $f(z)$ except the one originating from the fermion Green's function, namely $\varepsilon + i\eta - \varepsilon_{\mathbf{2}}$. We can write the poles and corresponding residues in the table

$$
\begin{aligned}
z'_n &= i\frac{2n\pi}{\beta} & R'_n &= \frac{1}{\beta}g(i\omega_n) \\
z'_1 &= \omega^\lambda_{\mathbf{q}} & R'_1 &= \frac{-n_B(\omega^\lambda_{\mathbf{q}})}{+\omega^\lambda_{\mathbf{q}} - \varepsilon - iI + \varepsilon_{\mathbf{2}}} \\
z'_2 &= -\omega^\lambda_{\mathbf{q}} & R'_2 &= \frac{n_B(-\omega^\lambda_{\mathbf{q}})}{-\omega^\lambda_{\mathbf{q}} - \varepsilon - iI + \varepsilon_{\mathbf{2}}} \\
z'_3 &= \varepsilon + i\eta - \varepsilon_{\mathbf{2}} & R'_3 &= \frac{-2\omega^\lambda_{\mathbf{q}} n_B(\varepsilon + i\eta - \varepsilon_{\mathbf{2}})}{(\varepsilon + i\eta - \varepsilon_{\mathbf{2}})^2 - {\omega^\lambda_{\mathbf{q}}}^2}
\end{aligned}
\tag{3.45}
$$

We now use the relations (3.19) to simplify the residue R'_2 in the form

$$
R'_2 = \frac{n_B(\omega^\lambda_{\mathbf{q}}) + 1}{\varepsilon + i\eta - \varepsilon_{\mathbf{2}} + \omega^\lambda_{\mathbf{q}}}. \tag{3.46}
$$

The definition of the residues R_3 and R'_3 given, respectively, in (3.18) and (3.45), do not have the same numerators. This difference comes from the fact that we can not use the identity (3.26) because the argument of the boson factor has a continuous value, namely

$$
n_B(\varepsilon + i\eta - \varepsilon_{\mathbf{2}}) \neq -n_F(-\varepsilon_{\mathbf{2}}), \tag{3.47}
$$

This is the main difference in this new procedure compared with the standard one. It is this inequality that change the final result and, as one can see, it comes directly from the "order" in which the analytic continuation is performed.

We are going to look for the final expression of the self-energy and this will take some algebraic steps. First of all, we modify the residue R'_3, adding and subtracting the same quantity, i.e. we define

$$
\begin{aligned}
R'_3 = R'_3 \quad &+ \quad \left[\frac{1 - n_F(\varepsilon_{\mathbf{2}})}{\varepsilon + i\eta - \varepsilon_{\mathbf{2}} - \omega^\lambda_{\mathbf{q}}} - \frac{1 - n_F(\varepsilon_{\mathbf{2}})}{\varepsilon + i\eta - \varepsilon_{\mathbf{2}} + \omega^\lambda_{\mathbf{q}}}\right] \\
&- \quad \left[\frac{1 - n_F(\varepsilon_{\mathbf{2}})}{\varepsilon + i\eta - \varepsilon_{\mathbf{2}} - \omega^\lambda_{\mathbf{q}}} - \frac{1 - n_F(\varepsilon_{\mathbf{2}})}{\varepsilon + i\eta - \varepsilon_{\mathbf{2}} + \omega^\lambda_{\mathbf{q}}}\right].
\end{aligned}
\tag{3.48}
$$

We can write now the result of integration as the sum of all residues $R'_n, R'_1, R'_2$and R'_3. The value of the integral J is then

$$J = \sum_{n=-\infty}^{+\infty} R'_n + R'_1 + R'_2 + R'_3, \tag{3.49}$$

that means

$$\begin{aligned} J &= \sum_{n=-\infty}^{+\infty} \frac{1}{\beta} g(i\omega_n) + \frac{n_B(\omega_{\mathbf{q}}^{\lambda})}{\varepsilon + i\eta - \varepsilon_{\mathbf{2}} - \omega_{\mathbf{q}}^{\lambda}} + \frac{1 + n_B(\omega_{\mathbf{q}}^{\lambda})}{\varepsilon + i\eta - \varepsilon_{\mathbf{2}} + \omega_{\mathbf{q}}^{\lambda}} + \\ &- \left[\frac{n_B(\varepsilon + i\eta - \varepsilon_{\mathbf{2}})}{\varepsilon + i\eta - \varepsilon_{\mathbf{2}} - \omega_{\mathbf{q}}^{\lambda}} - \frac{n_B(\varepsilon + i\eta - \varepsilon_{\mathbf{2}})}{\varepsilon + i\eta - \varepsilon_{\mathbf{2}} + \omega_{\mathbf{q}}^{\lambda}} \right] + \\ &+ \left[\frac{1 - n_F(\varepsilon_{\mathbf{2}})}{\varepsilon + i\eta - \varepsilon_{\mathbf{2}} - \omega_{\mathbf{q}}^{\lambda}} - \frac{1 - n_F(\varepsilon_{\mathbf{2}})}{\varepsilon + i\eta - \varepsilon_{\mathbf{2}} + \omega_{\mathbf{q}}^{\lambda}} \right] \\ &- \left[\frac{1 - n_F(\varepsilon_{\mathbf{2}})}{\varepsilon + i\eta - \varepsilon_{\mathbf{2}} - \omega_{\mathbf{q}}^{\lambda}} - \frac{1 - n_F(\varepsilon_{\mathbf{2}})}{\varepsilon + i\eta - \varepsilon_{\mathbf{2}} + \omega_{\mathbf{q}}^{\lambda}} \right]. \end{aligned} \tag{3.50}$$

We can simplify this integral adding the terms with the same denominator

$$\begin{aligned} J &= -G + \frac{1 + n_{\mathrm{B}}(\omega_{\mathbf{q}}^{\lambda}) - n_{\mathrm{F}}(\varepsilon_{\mathbf{2}})}{\varepsilon + i\eta - \varepsilon_{\mathbf{2}} - \omega_{\mathbf{q}}^{\lambda}} + \frac{n_{\mathrm{B}}(\omega_{\mathbf{q}}^{\lambda}) + n_{\mathrm{F}}(\varepsilon_{\mathbf{2}})}{\varepsilon + i\eta - \varepsilon_{\mathbf{2}} + \omega_{\mathbf{q}}^{\lambda}} + \\ &- \frac{1 - n_F(\varepsilon_{\mathbf{2}}) + n_B(\varepsilon + i\eta - \varepsilon_{\mathbf{2}})}{\varepsilon + i\eta - \varepsilon_{\mathbf{2}} - \omega_{\mathbf{q}}^{\lambda}} + \frac{n_F(\varepsilon_{\mathbf{2}}) + n_B(\varepsilon + i\eta - \varepsilon_{\mathbf{2}})}{\varepsilon + i\eta - \varepsilon_{\mathbf{2}} + \omega_{\mathbf{q}}^{\lambda}} = \\ &= -G + \frac{1 + n_{\mathrm{B}}(\omega_{\mathbf{q}}^{\lambda}) - n_{\mathrm{F}}(\varepsilon_{\mathbf{2}})}{\varepsilon + i\eta - \varepsilon_{\mathbf{2}} - \omega_{\mathbf{q}}^{\lambda}} + \frac{n_{\mathrm{B}}(\omega_{\mathbf{q}}^{\lambda}) + n_{\mathrm{F}}(\varepsilon_{\mathbf{2}})}{\varepsilon + i\eta - \varepsilon_{\mathbf{2}} + \omega_{\mathbf{q}}^{\lambda}} + \\ &- \left[1 - n_F(\varepsilon_{\mathbf{2}}) + n_B(\varepsilon + i\eta - \varepsilon_{\mathbf{2}})\right] \frac{2\omega_{\mathbf{q}}^{\lambda}}{(\varepsilon + i\eta - \varepsilon_{\mathbf{2}})^2 - \omega_{\mathbf{q}}^{\lambda^2}}. \end{aligned} \tag{3.51}$$

Due to the fact that the function $g(z) \to 0$ when $R \to \infty$, the integral J, in this limit, is zero. This property allows us to find the value of the function G, that contains the sum over the discrete frequencies $i\omega_n$, that is

$$\begin{aligned} G &= \frac{1 + n_{\mathrm{B}}(\omega_{\mathbf{q}}^{\lambda}) - n_{\mathrm{F}}(\varepsilon_{\mathbf{2}})}{\varepsilon + i\eta - \varepsilon_{\mathbf{2}} - \omega_{\mathbf{q}}^{\lambda}} + \frac{n_{\mathrm{B}}(\omega_{\mathbf{q}}^{\lambda}) + n_{\mathrm{F}}(\varepsilon_{\mathbf{2}})}{\varepsilon + i\eta - \varepsilon_{\mathbf{2}} + \omega_{\mathbf{q}}^{\lambda}} + \\ &- \left[1 - n_F(\varepsilon_{\mathbf{2}}) + n_B(\varepsilon + i\eta - \varepsilon_{\mathbf{2}})\right] \frac{2\omega_{\mathbf{q}}^{\lambda}}{(\varepsilon + i\eta - \varepsilon_{\mathbf{2}})^2 - \omega_{\mathbf{q}}^{\lambda^2}}. \end{aligned} \tag{3.52}$$

This means that the self-energy can be written as

$$\begin{aligned}\sum_{\rm sp}(\mathbf{1},\varepsilon+i\eta) &= \sum_{\lambda,\boldsymbol{q},\mathbf{2}} V^2(\mathbf{1},\mathbf{2};\lambda,\boldsymbol{q})\left[\frac{1+n_{\rm B}(\omega^\lambda_{\boldsymbol{q}})-n_{\rm F}(\varepsilon_{\mathbf{2}})}{\varepsilon+i\eta-\varepsilon_{\mathbf{2}}-\omega^\lambda_{\boldsymbol{q}}}+\frac{n_{\rm B}(\omega^\lambda_{\boldsymbol{q}})+n_{\rm F}(\varepsilon_{\mathbf{2}})}{\varepsilon+i\eta-\varepsilon_{\mathbf{2}}+\omega^\lambda_{\boldsymbol{q}}}\right]\\ &- \sum_{\lambda,\boldsymbol{q},\mathbf{2}} V^2(\mathbf{1},\mathbf{2};\lambda,\boldsymbol{q})\frac{[1-n_F(\varepsilon_{\mathbf{2}})+n_B(\varepsilon+i\eta-\varepsilon_{\mathbf{2}})]\,2\omega^\lambda_{\boldsymbol{q}}}{(\varepsilon+i\eta-\varepsilon_{\mathbf{2}})^2-{\omega^\lambda_{\boldsymbol{q}}}^2}\\ &= \sum_{\rm ret}(\mathbf{1},\varepsilon+i\eta)+\\ &- \sum_{\lambda,\boldsymbol{q},\mathbf{2}} V^2(\mathbf{1},\mathbf{2};\lambda,\boldsymbol{q})\frac{[1-n_F(\varepsilon_{\mathbf{2}})+n_B(\varepsilon+i\eta-\varepsilon_{\mathbf{2}})]\,2\omega^\lambda_{\boldsymbol{q}}}{(\varepsilon+i\eta-\varepsilon_{\mathbf{2}})^2-{\omega^\lambda_{\boldsymbol{q}}}^2}\end{aligned} \tag{3.53}$$

We can compare now the analytic continued expression of (3.36) and this last one. While in the first case the result is exactly the retarded self energy, in the latter one, obtained with our new method, we have an additional term, that we can express by means of the response function. To achieve this goal we have to come back to the definition of the vertex matrix elements(3.5) and separate the vibration contribution from the particle one, using (3.7), that is

$$V^2(\mathbf{1},\mathbf{2};\lambda,\boldsymbol{q}) = \frac{|\langle\mathbf{1}||\widehat{T}_\lambda||\mathbf{2}\rangle|^2}{2j_{\mathbf{1}}+1}M_{\lambda\boldsymbol{q}}(T). \tag{3.54}$$

At this point, using the definition of response function (3.8), we obtain

$$\begin{aligned}\sum_{\rm sp}(\mathbf{1},\varepsilon+i\eta) &= \sum_{\rm ret}(\mathbf{1},\varepsilon+i\eta)+\sum_{\lambda,\mathbf{2}}\frac{\langle\mathbf{1}||\widehat{T}_\lambda||\mathbf{2}\rangle}{2j_{\mathbf{1}}+1}\times\\ &\times\ [1-n_F(\varepsilon_{\mathbf{2}})+n_B(\varepsilon+i\eta-\varepsilon_{\mathbf{2}})]\,\mathcal{R}_\lambda(\varepsilon+i\eta-\varepsilon_{\mathbf{2}}).\end{aligned} \tag{3.55}$$

The result of this new procedure is then

$$\begin{aligned}\sum_{\rm ret}(\mathbf{1},\varepsilon+i\eta) &= \sum_{\rm sp}(\mathbf{1},\varepsilon+i\eta)-\sum_{\lambda,\mathbf{2}}\frac{\langle\mathbf{1}||\widehat{T}_\lambda||\mathbf{2}\rangle}{2j_{\mathbf{1}}+1}\times\\ &\times\ [1-n_F(\varepsilon_{\mathbf{2}})+n_B(\varepsilon+i\eta-\varepsilon_{\mathbf{2}})]\,\mathcal{R}_\lambda(\varepsilon+i\eta-\varepsilon_{\mathbf{2}}).\end{aligned} \tag{3.56}$$

This is not yet our final answer because we need to write down in a useful form the first term on the right hand side of the last equation. For this purpose, we have to

remember the relation existing between the response function(3.8) and the phonon Green's function (3.10), that is

$$\mathcal{R}_\lambda(i\omega_n, T) = -\sum_{\boldsymbol{q}} M_{\lambda\boldsymbol{q}}(T)\mathcal{D}^0_\lambda(\boldsymbol{q}, i\omega_n). \tag{3.57}$$

Using this expression and (3.54) in the definition of the self-energy (3.39), we obtain

$$\sum_{\rm sp}(\mathbf{1}, \varepsilon + i\eta) = \frac{1}{\beta}\sum_{\lambda,\mathbf{2}} \frac{\langle \mathbf{1}||\widehat{T}_\lambda||\mathbf{2}\rangle}{2j_{\mathbf{1}}+1} \sum_{i\omega_n} \mathcal{R}_\lambda(i\omega_n, T)\mathcal{G}^0(\mathbf{2}, \varepsilon + i\eta - i\omega_n). \tag{3.58}$$

Using this last result inside (3.56), after substituting the expression of the fermion Green's function, we reach our aim, that is

$$\begin{aligned}\sum_{\rm ret}(\mathbf{1}, \varepsilon + i\eta) &= \sum_{\lambda,\mathbf{2}} \frac{\langle \mathbf{1}||\widehat{T}_\lambda||\mathbf{2}\rangle}{2j_{\mathbf{1}}+1}\Bigg\{ \frac{1}{\beta}\sum_{i\omega_n} \frac{\mathcal{R}_\lambda(i\omega_n)}{\varepsilon + i\eta - \varepsilon_{\mathbf{2}} - i\omega_n} \\ &- \left[1 - n_F(\varepsilon_{\mathbf{2}}) + n_B(\varepsilon + i\eta - \varepsilon_{\mathbf{2}})\right]\mathcal{R}_\lambda(\varepsilon + i\eta - \varepsilon_{\mathbf{2}})\Bigg\}. \end{aligned} \tag{3.59}$$

This is the expression of the retarded self-energy at finite temperature in terms of the response function. The advantage of this formula compared with the standard one is that one needs only to work within the chosen single-particle space where it is possible to evaluate the energies $\varepsilon_{\mathbf{2}}$,the matrix elements $\langle \mathbf{1}||\widehat{T}_\lambda||\mathbf{2}\rangle$ and the response function.

This new method doesn't solve completely the phonon frequency sum, as one can see from the first term on the right hand side of Eq.(3.59). However, this sum can be easily evaluated numerically because we do not need to take into account an infinite summation. This is because the response function tends rapidly to zero with increasing energy. This means that when n is big enough, $i\omega_n$ corresponds to an energy for which the response function is absolutely zero. We have checked that the range $(-500, 500)$ for the integer variable n is a reasonable choice, because it corresponds to evaluate the response function inside the energy range $(-3000T, 3000T)$ MeV. Outside this interval one can be completely sure that there are no contributions from $\sum_{i\omega_n}$.

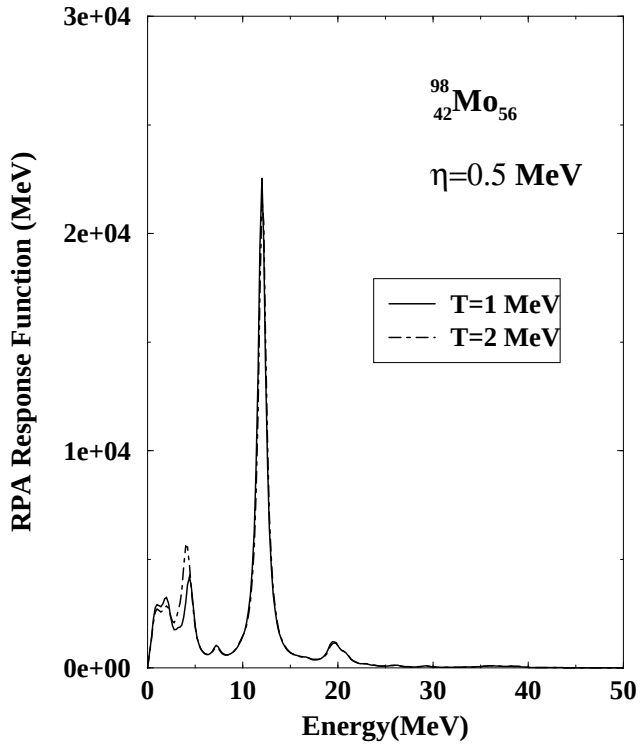

Figure 3.6: Quadrupole RPA response function for ^{98}Mo at different temperatures. The used averaging parameter is $\eta = 0.5$ MeV.

To understand much better this truncation in the infinite sum we present in Fig.(3.6) the RPA response function for the 2^+-vibration at two different values of temperature (T=1 MeV and T=2 MeV) for the nucleus ^{98}Mo. These results are obtained using a spherical Woods-Saxon mean-field potential with standard parameters. As one can see from Fig.(3.6), the response function dies out already at 40 MeV of excitation energy so that our condition on the n-value, taking into account a much larger range, does not neglect any important contributions.

Using the calculations known in literature[14] on self-energy at finite temperature for spherical nuclei, it was possible to check the validity of the new formulation (Eq.(3.59). In Fig.(3.7) we present the self-energy of a specific single-particle state evaluated with the usual definition in terms of RPA solutions (3.37) and the one obtained with the new expression (Eq.(3.59)), showing that there is perfect agreement between the two different procedures.

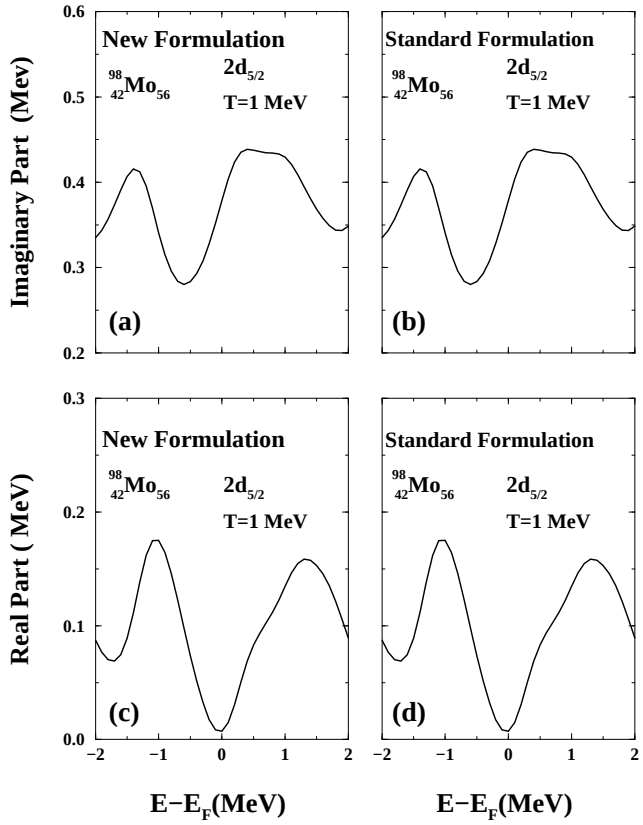

Figure 3.7: Self-energy of the single-particle state $2d_{5/2}$ in ^{98}Mo at T=1 MeV. Graphs (a) and (c) are obtained using Eq.(3.37), while for graphs (b) and (d) use was made of Eq.(3.59). The upper line contains the imaginary part while the lower one the real part of the self-energy. The averaging parameter used is η=0.5 MeV.

As one can see from Eq.(3.59), the retarded self-energy is the sum of two terms, where the first one (that we call term a) reminds to the original Matsubara's self-energy while the second one (term b) contains explicitly the dependence on temperature because of the boson and fermi factors. Below we will show that one cannot neglect any of these terms but that they both contribute in an important way to the total retarded self-energy. The example given in Fig.(3.8) refers to the self-energy of the same single-particle state $2d_{5/2}$ analyzed in the former picture.

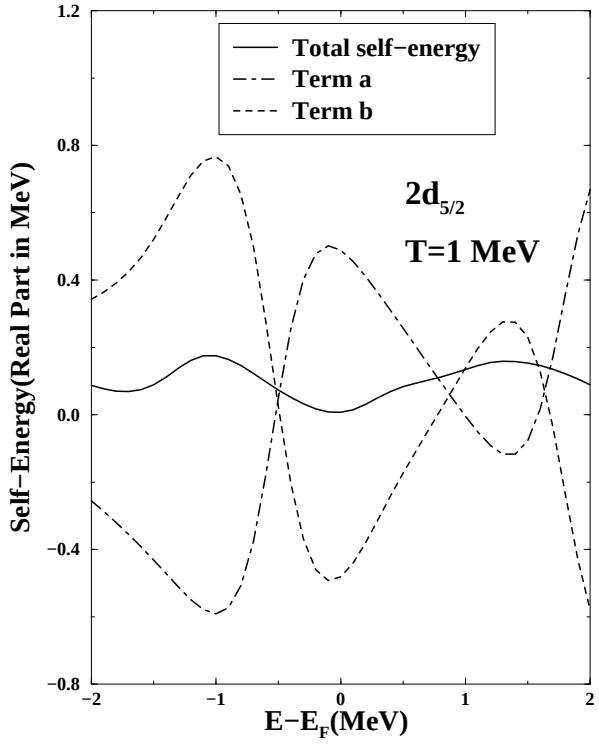

Figure 3.8: Self-energy contributions of terms (a) and (b) to the total retarded self-energy (see Eq.(3.56) and text for explanation).

3.6 Self-Energy at Zero Temperature

We shall now show that the self-energy at zero temperature is only a limiting case of the results obtained at finite temperature. We start considering the standard expression of the self-energy (3.37) using the consideration that the boson factor cancels out when $T \to 0$ (because its argument is a positive qunatity). The self energy becomes

$$\sum_{\text{ret}}(\mathbf{1}, \varepsilon + i\eta) = \sum_{\lambda,\boldsymbol{q},\mathbf{2}} V^2(\mathbf{1},\mathbf{2};\lambda,\boldsymbol{q}) \left[\frac{1 - n_F(\varepsilon_{\mathbf{2}})}{\varepsilon + i\eta - \varepsilon_{\mathbf{2}} - \omega^{\lambda}_{\boldsymbol{q}}} + \frac{n_F(\varepsilon_{\mathbf{2}})}{\varepsilon + i\eta - \varepsilon_{\mathbf{2}} + \omega^{\lambda}_{\boldsymbol{q}}} \right], \quad (3.60)$$

where the two terms originate from the fact that the intermediate state $\mathbf{2}$ can be a particle ($n_F(\varepsilon_{\mathbf{2}}) = 0$) or a hole ($n_F(\varepsilon_{\mathbf{2}}) = 1$). This is the usual expression of the self-energy at zero temperature, as one can check in literature([5],[13]).

For the reasons already explained in the previous section, we would like to have

the expression of the retarded self-energy in terms of the response function also at zero temperature. This can be done starting from the result (3.59) obtained at finite temperature and going to the limit of zero temperature. We will show that the expression that one obtain in this limit coincides with the one given in Eq.(3.60) in terms of the RPA solutions.

In the Matsubara's formalism, the limit of zero temperature is equivalent to perform the following substitution

$$\frac{1}{\beta}\sum_{i\omega_n} f(i\omega_n) \to \frac{1}{2\pi}\int_{-\infty}^{+\infty} d\omega f(i\omega). \tag{3.61}$$

Differently from the first case, the boson factor included in (3.59) doesn't cancel out automatically in the limit of zero temperature because its argument can change sign, that is

$$n_B(\varepsilon + i\eta - \varepsilon_{\mathbf{2}}) = \frac{1}{\mathrm{e}^{\beta\varepsilon + i\eta - \varepsilon_{\mathbf{2}}} - 1} \quad \beta \to \infty \quad \begin{cases} 0 & \varepsilon - \varepsilon_{\mathbf{2}} > 0 \\ \\ -1 & \varepsilon - \varepsilon_{\mathbf{2}} < 0 \end{cases}, \tag{3.62}$$

where the details of this derivation are given in appendix A. As a consequence, we have to distinguish between two different intervals of energy, so that the self-energy can be written as

$$\begin{aligned} \sum_{\mathrm{ret}}(\mathbf{1}, \varepsilon + i\eta) &= \frac{1}{2\pi}\int_{-\infty}^{+\infty} d\omega \frac{\mathcal{R}_\lambda(i\omega)}{\varepsilon + i\eta - \varepsilon_{\mathbf{2}} - i\omega} + \\ &+ \begin{cases} n_F(\varepsilon_{\mathbf{2}})\mathcal{R}_\lambda(\varepsilon + i\eta - \varepsilon_{\mathbf{2}}) & \varepsilon - \varepsilon_{\mathbf{2}} < 0 \\ \\ -[1 - n_F(\varepsilon_{\mathbf{2}})]\mathcal{R}_\lambda(\varepsilon + i\eta - \varepsilon_{\mathbf{2}}) & \varepsilon - \varepsilon_{\mathbf{2}} > 0 \end{cases} \end{aligned} \tag{3.63}$$

We shall show that the above expression is equivalent to the standard one given in Eq.(3.60). For this purpose, we start with the integral term and write down the response function in terms of the RPA solutions (3.8). This brings us to the following expression

$$
\begin{aligned}
I &= \frac{1}{2\pi}\int_{-\infty}^{+\infty} d\omega \sum_{\boldsymbol{q}} M_{\lambda \boldsymbol{q}}(T)\left[\frac{1}{\omega_{\boldsymbol{q}}^{\lambda}-i\omega}+\frac{1}{\omega_{\boldsymbol{q}}^{\lambda}+i\omega}\right]\frac{1}{\varepsilon+i\eta-\varepsilon_{\boldsymbol{2}}-i\omega} = \\
&= \frac{1}{2\pi}\left\{\sum_{\boldsymbol{q}}\frac{M_{\lambda \boldsymbol{q}}(T)}{\varepsilon+i\eta-\varepsilon_{\boldsymbol{2}}-\omega_{\boldsymbol{q}}^{\lambda}}\int_{-\infty}^{+\infty} d\omega\left[\frac{1}{\omega_{\boldsymbol{q}}^{\lambda}-i\omega}-\frac{1}{\varepsilon+i\eta-\varepsilon_{\boldsymbol{2}}-i\omega}\right]+\right. \\
&+ \left.\sum_{\boldsymbol{q}}\frac{M_{\lambda \boldsymbol{q}}(T)}{\varepsilon+i\eta-\varepsilon_{\boldsymbol{2}}+\omega_{\boldsymbol{q}}^{\lambda}}\int_{-\infty}^{+\infty} d\omega\left[\frac{1}{\omega_{\boldsymbol{q}}^{\lambda}+i\omega}+\frac{1}{\varepsilon+i\eta-\varepsilon_{\boldsymbol{2}}-i\omega}\right]\right\}.
\end{aligned}
\tag{3.64}
$$

The final result depends on the solution of three different integrals

$$
\begin{aligned}
I_1 &= \int_{-\infty}^{+\infty} d\omega \frac{1}{\omega_{\boldsymbol{q}}^{\lambda}-i\omega} \\
I_2 &= \int_{-\infty}^{+\infty} d\omega \frac{1}{\omega_{\boldsymbol{q}}^{\lambda}+i\omega} \\
I_3 &= \int_{-\infty}^{+\infty} d\omega \frac{1}{\varepsilon+i\eta-\varepsilon_{\boldsymbol{2}}-i\omega}.
\end{aligned}
\tag{3.65}
$$

The first two integrals, I_1 and I_2, are very easy to evaluate while the third one is slightly more involved. However, we are able to give their analytic solutions, as one can check in appendix A, namely

$$
\begin{aligned}
I_1 &= \pi \\
I_2 &= \pi \\
I_3 &= \begin{cases} \pi & \varepsilon-\varepsilon_{\boldsymbol{2}}>0 \\ -\pi & \varepsilon-\varepsilon_{\boldsymbol{2}}<0 \end{cases}
\end{aligned}
\tag{3.66}
$$

We can now use these results to write the value of the integral I

$$
I = \frac{1}{2\pi}\sum_{\boldsymbol{q}} M_{\lambda \boldsymbol{q}}(T)\left\{\frac{\pi-\pi\mathrm{sign}(\varepsilon-\varepsilon_{\boldsymbol{2}})}{\varepsilon+i\eta-\varepsilon_{\boldsymbol{2}}-\omega_{\boldsymbol{q}}^{\lambda}}+\frac{\pi+\pi\mathrm{sign}(\varepsilon-\varepsilon_{\boldsymbol{2}})}{\varepsilon+i\eta-\varepsilon_{\boldsymbol{2}}+\omega_{\boldsymbol{q}}^{\lambda}}\right\} =
$$

$$= \begin{cases} \sum_{\boldsymbol{q}} \dfrac{M_{\lambda \boldsymbol{q}}(T)}{\varepsilon + i\eta - \varepsilon_{\boldsymbol{2}} - \omega^{\lambda}_{\boldsymbol{q}}} & \varepsilon - \varepsilon_{\boldsymbol{2}} < 0 \\ \sum_{\boldsymbol{q}} \dfrac{M_{\lambda \boldsymbol{q}}(T)}{\varepsilon + i\eta - \varepsilon_{\boldsymbol{2}} + \omega^{\lambda}_{\boldsymbol{q}}} & \varepsilon - \varepsilon_{\boldsymbol{2}} > 0 \end{cases} \tag{3.67}$$

Using these expressions and the definition of the response function(3.8) inside eq(3.63), we obtain

$$\sum_{\text{ret}}(\mathbf{1}, \varepsilon + i\eta) = \sum_{\lambda, \boldsymbol{q}, \mathbf{2}} V^2(\mathbf{1}, \mathbf{2}; \lambda, \boldsymbol{q}) \begin{cases} \dfrac{1 - n_F(\varepsilon_{\boldsymbol{2}})}{\varepsilon + i\eta - \varepsilon_{\boldsymbol{2}} - \omega^{\lambda}_{\boldsymbol{q}}} + \dfrac{n_F(\varepsilon_{\boldsymbol{2}})}{\varepsilon + i\eta - \varepsilon_{\boldsymbol{2}} + \omega^{\lambda}_{\boldsymbol{q}}} & \varepsilon - \varepsilon_{\boldsymbol{2}} < 0 \\ \dfrac{1 - n_F(\varepsilon_{\boldsymbol{2}})}{\varepsilon + i\eta - \varepsilon_{\boldsymbol{2}} - \omega^{\lambda}_{\boldsymbol{q}}} + \dfrac{n_F(\varepsilon_{\boldsymbol{2}})}{\varepsilon + i\eta - \varepsilon_{\boldsymbol{2}} + \omega^{\lambda}_{\boldsymbol{q}}} & \varepsilon - \varepsilon_{\boldsymbol{2}} > 0 \end{cases} \tag{3.68}$$

This is the retarded self-energy defined in the standard way.

Chapter 4

Self-Energy in a Rotating Frame

4.1 Introduction

The formalism developed in the last Chapter applies only to normal systems. In order to generalize the particle-vibration coupling in a rotating frame, we have to consider that we are in presence of two different properties compared to the normal case, that is pairing correlations and rotation.

It is common to describe a superfluid system where the ground state is built up of paired states through a canonical transformation from bare particles to quasiparticles (see Chapter 1 for details). In this way we are dealing with an Hamiltonian of independent quasiparticles where the elementary excitations are created by the operators $\widehat{a}^{\dagger}_{\mu}$. These excitations are neither particles nor holes but they belong to both types at the same time. To understand the main difference compared with the normal case is convenient to use the one quasiparticle Green's function (see [6]) which is defined as in the normal system with the exception that the field operators correspond to quasiparticles creation operators. One can write that

$$\mathcal{G}_0(k,t) = i\mathrm{e}^{-iE_k t}\Theta(t), \tag{4.1}$$

where $\Theta(t)$ is a step function

$$\Theta(t) = \begin{cases} 1 & t > 0 \\ 0 & t < 0 \end{cases} . \tag{4.2}$$

This means that a quasiparticle cannot move backward in time while, conversely, a

bare particle can propagate either forward or backward. This will produce in the expression of the self-energy a difference in the definition of the denominators, that is in the energy of the intermediate state that can be generated by the coupling of a quasiparticle with a vibration.

As we have seen in Chapter 1, the introduction of Coriolis and inertial forces bring us to a different way to label states, that is we have to use the signature quantum number α. While in a normal system at the vertices of the particle-vibration coupling one has to impose angular momentum conservation, in a rotating frame we have to conserve signature. This will introduce a furthermore complication in the final expression of the retarded self-energy.

4.2 Quasiparticle-Vibration Coupling

The starting point for defining the self-energy is, of course, the quasiparticle-vibration coupling Hamiltonian representing the coupling between quasiparticles $\widehat{a}_\mu^\dagger$ and the surface normal modes $X_{\boldsymbol{q}}^{\alpha\,\dagger}$ (see Chapter 2).

For this purpose we go back to the coupling Hamiltonian defined in the Chapter 3 Eq.(3.3) and see that it can be written as

$$\widehat{H}_{\text{coupl}} = -\chi F \alpha. \tag{4.3}$$

In second quantization the field F will be expressed in terms of quasiparticle operators (because it is a one-body operator) exactly as it was done in Chapter 1 in Table (2.1), while $\widehat{\alpha}$, which represents the collective coordinate, by means of vibrational modes, in such a way that the quasiparticle vibration coupling can be written as

$$\widehat{H}_{\text{coupl}} = -\chi \widehat{F}_{\text{qp}} \widehat{F}_{\text{vib}}. \tag{4.4}$$

The effective Hamiltonian describing the total system built up of single quasiparticles plus surface vibration can be written, in a rotating frame, as

$$\widehat{H} = \sum_\mu E_\mu \widehat{a}_\mu^\dagger \widehat{a}_\mu + \sum_{\bar{\mu}} E_{\bar{\mu}} \widehat{a}_{\bar{\mu}}^\dagger \widehat{a}_{\bar{\mu}} + \sum_\alpha \sum_{\boldsymbol{q}} \hbar\omega_{\boldsymbol{q}}^{(\alpha)} X_{\boldsymbol{q}}^{\alpha\,\dagger} X_{\boldsymbol{q}}^\alpha + \sum_\alpha \widehat{H}_{\text{coupl}}^\alpha, \tag{4.5}$$

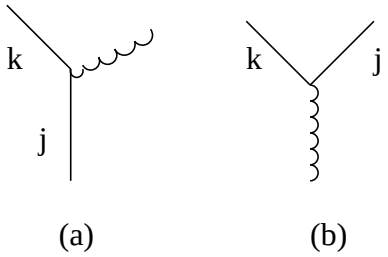

Figure 4.1: Basic couplings between a quasiparticle and a surface mode which contribute to the self-energy.

where $\widehat{H}^{\alpha}_{\rm coupl}$ is the quasiparticle-vibration coupling Hamiltonian with signature quantum number α

$$\widehat{H}^{\alpha}_{\rm coupl} = -\sum_{\rho} \chi^{\alpha}_{\rho} \widehat{h}^{\alpha}_{\rho}({\rm vib}) \widehat{h}^{\alpha}_{\rho}({\rm qp}). \tag{4.6}$$

The expressions of the vibration and quasiparticle Hamiltonian (both Hermitian operators) for different signature are given by

$$\begin{aligned}
h^{\alpha}_{\rho}({\rm vib}) &= \sum_{\boldsymbol{q}} \left[\mathcal{Q}^{\alpha}_{\rho}(\boldsymbol{q}) {X^{\alpha}_{\boldsymbol{q}}}^{\dagger} + {\rm h.c} \right], \\
\widehat{h}^{(0)}_{\rho}({\rm qp}) &= \sum_{\mu\bar{\nu}} \left[R^{0A}_{\rho}(\mu\bar{\nu}) \widehat{A}^{\dagger}_{\mu\bar{\nu}} + {\rm h.c} \right] + \sum_{\mu\nu}{}'' R^{0B}_{\rho}(\mu\nu) \widehat{B}^{\dagger}_{\mu\nu} \\
\widehat{h}^{(1)}_{\rho}({\rm qp}) &= \sum_{\mu\langle\nu}{}'' \left[R^{1A}_{\rho}(\mu\nu) \widehat{A}^{\dagger}_{\mu\nu} + {\rm h.c} \right] + \sum_{\mu\bar{\nu}} \left[R^{1B}_{\rho}(\mu\bar{\nu}) \widehat{B}^{\dagger}_{\mu\bar{\nu}} + {\rm h.c} \right].
\end{aligned} \tag{4.7}$$

The main vertices of this quasiparticle-vibration coupling are depicted in Fig.(4.1) At first glance one doesn't notice any difference compared to the normal case (see Fig.(3.1) except that these vertices are generated by different operators, that is $\widehat{B}^{\dagger}$ and $\widehat{A}^{\dagger}$ in case (a) and (b) respectively that have different matrix elements. The former one represents a scattering of two quasiparticles with creation of a surface mode while the latter is the annihilation of a collective excitation with creation of a two quasiparticle-like excitation. This means that we have to keep track of this difference in our formulation and, for this reason, we will draw two distinct self-energy diagrams representing this situation, as shown in Fig.(4.2)

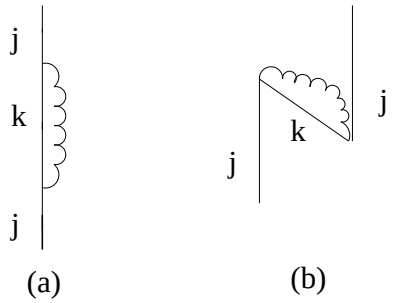

Figure 4.2: The lowest second-order processes by which the quasiparticle motion is renormalized by the coupling to the surface vibrational mode.

While the first diagram is completely equivalent to the normal case , the second one contains the impossibility of a quasiparticle to propagate backward in time, as we have explained in the introduction of this Chapter. In fact, the energy of the quasiparticle labelled by k in graph (b) of Fig.(4.2) is E_k while in the normal case it would be -ε_k because, in that situation, k is a hole state, that is the propagation backward in time of a particle. This will result in a different definition of the corresponding energy denominator, that is $E + E_k + \omega_{\boldsymbol{q}}$ for a condensate system and $\varepsilon - \varepsilon_k + \omega_{\boldsymbol{q}}$ in a normal case.

We have now to be more specific introducing the correct quantum number, that is the signature α. As we have seen in Chapter 2 and, in particular, in Table (2.1), the operator $\widehat{A}^\dagger$ can create a two quasiparticle-like excitation where the quasiparticle involved has the same signature if the considered one-body operator has signature negative while for signature positive operators the two quasiparticle have opposite α. For the operator $\widehat{B}^\dagger$ the situation is opposite. This will introduce a further distinction in the self-energy diagrams as one can check in Fig.(4.3) where at each vertex was imposed conservation of the signature quantum number. In fact, for a particle of signature $\alpha = 1/2(r = -i)$ the intermediate state k in diagram (a) of Fig.(4.2) has the same value of α if the surface mode has positive signature while it has opposite signature when the collective mode has $\alpha = 1$ (graphs (a) and (c) of Fig.(4.3). The situation is inverted when one considers diagram (b) of Fig.(4.2) where it is involved the operator $\widehat{A}^\dagger$. The conservation of α produces graphs (b) and (d) of Fig.(4.3).

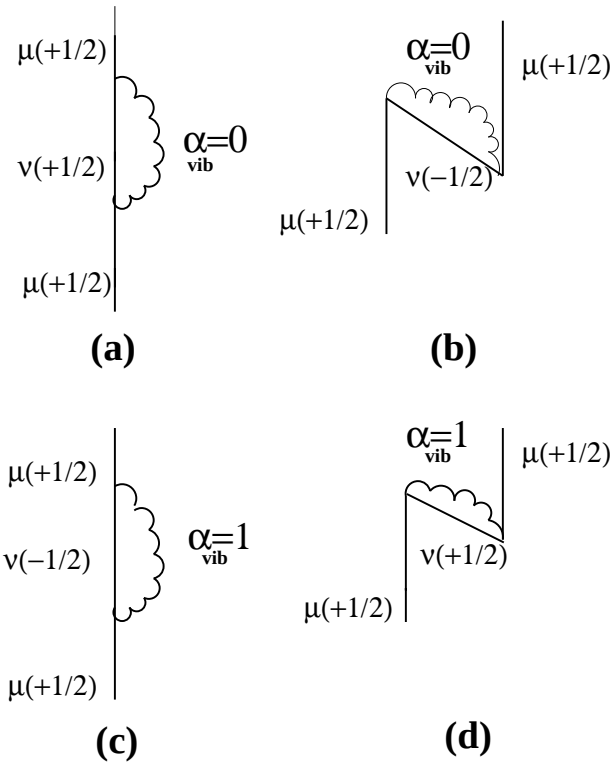

Figure 4.3: Basic diagrams representing the self-energy of a quasiparticle state in a rotating frame. A wavy line stands for a surface vibration. Graphs (a) and (b) correspond to the case of vibrations with positive signature ($\alpha = 0$) while graphs (c) and (d) are associated with vibrations with negative signature ($\alpha = 1$).

4.3 Self-Energy at Finite Temperature

Taking into account the four possible diagrammatic contributions to the self-energy in a rotating frame, one can generalize the corresponding expression of Matsubara and write

$$\sum_{\rm qp}(\boldsymbol{\mu}, ip_n) = -\frac{1}{\beta}\sum_{\lambda}\sum_{i\omega_n,\boldsymbol{q},\rho\rho'} \mathcal{S}^{i\omega_n,\boldsymbol{q}}_{\mu,\rho\rho'}(\lambda), \tag{4.8}$$

where the notation $\sum_{\rm qp}(\boldsymbol{\mu}, ip_n)$ means self-energy correction of a quasiparticle state μ with frequency ip_n. The function $\mathcal{S}$ is defined as

$$\mathcal{S}^{i\omega_n,\mathbf{q}}_{\mu,\rho\rho'}(\lambda) \;=\; \left\{\sum_{\nu} \frac{\chi^0_\rho R^{0B^*}_\rho(\mu\nu)\mathcal{Q}^{0^*}_\rho(\boldsymbol{q})\mathcal{Q}^0_{\rho'}(\boldsymbol{q})R^{0B}_{\rho'}(\mu\nu)\chi^0_{\rho'}}{ip_n - E_\nu - i\omega_n}\left[\frac{1}{i\omega_n - \omega^0_{\boldsymbol{q}}} - \frac{1}{i\omega_n + \omega^0_{\boldsymbol{q}}}\right]\right.$$

$$
\begin{aligned}
&+ \sum_{\bar{\nu}} \frac{\chi^0_\rho R^{0A}_\rho{}^*(\mu\bar{\nu})\mathcal{Q}^0_\rho{}^*(\boldsymbol{q})\mathcal{Q}^0_{\rho'}(\boldsymbol{q})R^{0A}_{\rho'}(\mu\bar{\nu})\chi^0_{\rho'}}{ip_n + E_{\bar{\nu}} - i\omega_n}\left[\frac{1}{i\omega_n - \omega^0_{\boldsymbol{q}}} - \frac{1}{i\omega_n + \omega^0_{\boldsymbol{q}}}\right] \\
&+ \sum_{\bar{\nu}} \frac{\chi^1_\rho R^{1B}_\rho{}^*(\mu\bar{\nu})\mathcal{Q}^1_\rho{}^*(\boldsymbol{q})\mathcal{Q}^1_{\rho'}(\boldsymbol{q})R^{1B}_{\rho'}(\mu\bar{\nu})\chi^1_{\rho'}}{ip_n - E_{\bar{\nu}} - i\omega_n}\left[\frac{1}{i\omega_n - \omega^1_{\boldsymbol{q}}} - \frac{1}{i\omega_n + \omega^1_{\boldsymbol{q}}}\right] \\
&+ \sum_{\nu} \frac{\chi^1_\rho R^{1A}_\rho{}^*(\mu\nu)\mathcal{Q}^1_\rho{}^*(\boldsymbol{q})\mathcal{Q}^1_{\rho'}(\boldsymbol{q})R^{1A}_{\rho'}(\mu\nu)\chi^1_{\rho'}}{ip_n + E_{\nu} - i\omega_n}\left[\frac{1}{i\omega_n - \omega^1_{\boldsymbol{q}}} - \frac{1}{i\omega_n + \omega^1_{\boldsymbol{q}}}\right]\Bigg\}.
\end{aligned}
\tag{4.9}
$$

The index λ indicates the possibility to have coupling with vibrational mode of different multipolarity, as quadrupole and octupole. The symbols 0 and 1 represent the value of the signature quantum number α, namely positive for $\alpha = 0$ and negative for $\alpha = 1$. Independently of its complexity, the self-energy in a rotating frame has exactly the same structure as that of Eq.(3.12) so that one can write right away its retarded expression, namely

$$
\begin{aligned}
\sum_{\text{ret}}(\mathbf{1}, \varepsilon + i\eta) &= \sum_{\lambda}\Bigg\{\sum_{\nu}\mathcal{T}^{0B}_{\rho\rho'}(\mu\nu)\left[\frac{1 + n_B(\omega^0_{\boldsymbol{q}}) - n_F(E_\nu)}{E + i\eta - E_\nu - \omega^0_{\boldsymbol{q}}} + \frac{n_B(\omega^0_{\boldsymbol{q}}) + n_F(E_\nu)}{E + i\eta - E_\nu + \omega^0_{\boldsymbol{q}}}\right] + \\
&+ \sum_{\bar{\nu}}\mathcal{T}^{0A}_{\rho\rho'}(\mu\bar{\nu})\left[\frac{1 + n_B(\omega^0_{\boldsymbol{q}}) - n_F(-E_{\bar{\nu}})}{E + i\eta + E_{\bar{\nu}} - \omega^0_{\boldsymbol{q}}} + \frac{n_B(\omega^0_{\boldsymbol{q}}) + n_F(-E_{\bar{\nu}})}{E + i\eta + E_{\bar{\nu}} + \omega^0_{\boldsymbol{q}}}\right] + \\
&+ \sum_{\bar{\nu}}\mathcal{T}^{1B}_{\rho\rho'}(\mu\bar{\nu})\left[\frac{1 + n_B(\omega^1_{\boldsymbol{q}}) - n_F(E_{\bar{\nu}})}{E + i\eta - E_{\bar{\nu}} - \omega^1_{\boldsymbol{q}}} + \frac{n_B(\omega^1_{\boldsymbol{q}}) + n_F(E_{\bar{\nu}})}{E + i\eta - E_{\bar{\nu}} + \omega^1_{\boldsymbol{q}}}\right] + \\
&+ \sum_{\nu}\mathcal{T}^{1A}_{\rho\rho'}(\mu\nu)\left[\frac{1 + n_B(\omega^1_{\boldsymbol{q}}) - n_F(-E_\nu)}{E + i\eta + E_\nu - \omega^1_{\boldsymbol{q}}} + \frac{n_B(\omega^1_{\boldsymbol{q}}) + n_F(-E_\nu)}{E + i\eta + E_\nu + \omega^1_{\boldsymbol{q}}}\right]\Bigg\}.
\end{aligned}
\tag{4.10}
$$

In the above expression, use was made of the definition

$$
\mathcal{T}^{\alpha}_{\rho\rho'}(\mu\gamma) = \chi^\alpha_\rho R^\alpha_\rho{}^*(\mu\gamma)R^\alpha_{\rho'}(\mu\gamma)\chi^\alpha_{\rho'} \tag{4.11}
$$

to simplify the notation. The minus sign in the Fermi factor in the square parenthesis appearing in the second and third line reflects the processes depicted in Fig.(4.3). Using the property of the Fermi distribution, $n_F(-x) = 1 - n_F(x)$, one can write that

$$
\begin{aligned}
\sum_{\text{ret}}(\mathbf{1}, \varepsilon + i\eta) &= \sum_{\lambda}\Bigg\{\sum_{\nu}\mathcal{T}^{0B}_{\rho\rho'}(\mu\nu)\left[\frac{1 + n_B(\omega^0_{\boldsymbol{q}}) - n_F(E_\nu)}{E + i\eta - E_\nu - \omega^0_{\boldsymbol{q}}} + \frac{n_B(\omega^0_{\boldsymbol{q}}) + n_F(E_\nu)}{E + i\eta - E_\nu + \omega^0_{\boldsymbol{q}}}\right] +
\end{aligned}
$$

$$
\begin{aligned}
&+ \sum_{\bar{\nu}} \mathcal{T}^{0A}_{\rho\rho'}(\mu\bar{\nu}) \left[\frac{n_B(\omega^0_{\boldsymbol{q}}) + n_F(E_{\bar{\nu}})}{E + i\eta + E_{\bar{\nu}} - \omega^0_{\boldsymbol{q}}} + \frac{1 + n_B(\omega^0_{\boldsymbol{q}}) + n_F(E_{\bar{\nu}})}{E + i\eta + E_{\bar{\nu}} + \omega^0_{\boldsymbol{q}}} \right] + \\
&+ \sum_{\bar{\nu}} \mathcal{T}^{1B}_{\rho\rho'}(\mu\bar{\nu}) \left[\frac{1 + n_B(\omega^1_{\boldsymbol{q}}) - n_F(E_{\bar{\nu}})}{E + i\eta - E_{\bar{\nu}} - \omega^1_{\boldsymbol{q}}} + \frac{n_B(\omega^1_{\boldsymbol{q}}) + n_F(E_{\bar{\nu}})}{E + i\eta - E_{\bar{\nu}} + \omega^1_{\boldsymbol{q}}} \right] + \\
&+ \sum_{\nu} \mathcal{T}^{1A}_{\rho\rho'}(\mu\nu) \left[\frac{n_B(\omega^1_{\boldsymbol{q}}) + n_F(E_{\nu})}{E + i\eta + E_{\nu} - \omega^1_{\boldsymbol{q}}} + \frac{1 + n_B(\omega^1_{\boldsymbol{q}}) - n_F(E_{\nu})}{E + i\eta + E_{\nu} + \omega^1_{\boldsymbol{q}}} \right] \Bigg\} .
\end{aligned}
\tag{4.12}
$$

As already pointed out, the RPA equations are too involved to be solved by finding each individual root, and consequently Eq.(4.12) cannot be used directly. We have to rewrite it using the same procedure given in Chapter 3, that is introducing the RPA response given in Eq.(2.42), with the further complication of the multidimensionality of this function. In the present case we cannot substitute directly the spectral representation of the RPA response, as we did in Chapter 3, because the terms in Eq. (4.9) contain only one of the numerator $\mathcal{Q}^{\alpha}_{\rho}{}^{*}(q)\mathcal{Q}^{\alpha}_{\rho'}(q)$ entering in the definition given in Eq. (2.42) and we can not consider the equality $\mathcal{Q}^{\alpha}_{\rho}{}^{*}(q)\mathcal{Q}^{\alpha}_{\rho'}(q) = \mathcal{Q}^{\alpha}_{\rho}(q)\mathcal{Q}^{\alpha}_{\rho'}{}^{*}(q)$ because of the difference in the residual interaction when using $\rho \neq \rho'$. To be able to use the method developed in Chapter 3, some algebraic manipulations have to be carried out. For this reason we prefer to simplify the notation writing Eq.(4.9) as

$$
\sum_{\mathrm{qp}} (\boldsymbol{\mu}, ip_n) = -\frac{1}{\beta} \sum_{\lambda} \sum_{i\omega_n, \boldsymbol{q}, \rho\rho'} \sum_{\alpha=0}^{1} \sum_{\gamma=1}^{2} \frac{q^{\alpha}_{\rho\rho'}(\gamma) \mathcal{Q}^{\alpha}_{\rho}{}^{*}(q) \mathcal{Q}^{\alpha}_{\rho'}(q)}{ip_n - E_{\gamma} - i\omega_n} \left[\frac{1}{i\omega_n - \omega^{\alpha}_{\boldsymbol{q}}} - \frac{1}{i\omega_n + \omega^{\alpha}_{\boldsymbol{q}}} \right] ,
\tag{4.13}
$$

where we have introduced the index γ with the following convention

$$
\begin{aligned}
\gamma &= 1 \quad \begin{cases} E_{\gamma} = +E_{\nu} & q^{\alpha}_{\rho\rho'}(\gamma) = \mathcal{T}^{0B}_{\rho\rho'}(\mu\nu) \qquad \alpha = 0 \\ E_{\gamma} = -E_{\bar{\nu}} & q^{\alpha}_{\rho\rho'}(\gamma) = \mathcal{T}^{1B}_{\rho\rho'}(\mu\bar{\nu}) \qquad \alpha = 1 \end{cases} , \\
\gamma &= 2 \quad \begin{cases} E_{\gamma} = +E_{\bar{\nu}} & q^{\alpha}_{\rho\rho'}(\gamma) = \mathcal{T}^{0A}_{\rho\rho'}(\mu\bar{\nu}) \qquad \alpha = 0 \\ E_{\gamma} = -E_{\nu} & q^{\alpha}_{\rho\rho'}(\gamma) = \mathcal{T}^{1A}_{\rho\rho'}(\mu\nu) \qquad \alpha = 1 \end{cases} .
\end{aligned}
\tag{4.14}
$$

This is exactly the expression of the self-energy in the Matsubara's formalism used in Chapter 3. To express this quantity in terms of the RPA response we add and subtract the term $\frac{\mathcal{Q}^{\alpha}_{\rho}(\boldsymbol{q})\mathcal{Q}^{\alpha}_{\rho'}{}^{*}(\boldsymbol{q})}{i\omega_n+\omega^{\alpha}_{\boldsymbol{q}}}$, obtaining

$$\begin{aligned}\sum_{\rm qp}(\boldsymbol{\mu}, ip_n) &= \frac{1}{\beta}\sum_{\lambda}\sum_{i\omega_n,\boldsymbol{q},\rho\rho'}\sum_{\alpha=0}^{1}\sum_{\gamma=1}^{2}\times \\ &\times \left\{\frac{q^{\alpha}_{\rho\rho'}(\gamma)}{ip_n - E_\gamma - i\omega_n}\left[\frac{\mathcal{Q}^{\alpha}_{\rho}{}^{*}(\boldsymbol{q})\mathcal{Q}^{\alpha}_{\rho'}(\boldsymbol{q})}{\omega^{\alpha}_{\boldsymbol{q}} - i\omega_n} + \frac{\mathcal{Q}^{\alpha}_{\rho}(\boldsymbol{q})\mathcal{Q}^{\alpha}_{\rho'}{}^{*}(\boldsymbol{q})}{i\omega_n + \omega^{\alpha}_{\boldsymbol{q}}}\right]\right. \\ &+ \left.\left[\frac{q^{\alpha}_{\rho\rho'}(\gamma)}{ip_n - E_\gamma - i\omega_n}\frac{\mathcal{Q}^{\alpha}_{\rho}{}^{*}(\boldsymbol{q})\mathcal{Q}^{\alpha}_{\rho'}(\boldsymbol{q}) - \mathcal{Q}^{\alpha}_{\rho}(\boldsymbol{q})\mathcal{Q}^{\alpha}_{\rho'}{}^{*}(\boldsymbol{q})}{\omega^{\alpha}_{\boldsymbol{q}} + i\omega_n}\right]\right\} + \end{aligned} \tag{4.15}$$

We can now use the definition of the spectral response function given in Eq.(4.15) and the usual substitution $ip_n \to E + i\eta$ to obtain

$$\begin{aligned}\sum_{\rm qp}(\boldsymbol{\mu}, E+i\eta) &= \frac{1}{\beta}\sum_{\lambda,i\omega_n,\rho\rho'}\sum_{\alpha=0}^{1}\sum_{\gamma=1}^{2}\times \\ &\times \left\{\frac{\mathcal{R}^{\alpha}_{\rho\rho'}(i\omega_n)q^{\alpha}_{\rho\rho'}(\gamma)}{E+i\eta - E_\gamma - i\omega_n} + \right. \\ &+ \left.\sum_{\boldsymbol{q}}\frac{q^{\alpha}_{\rho\rho'}(\gamma)}{E+i\eta - E_\gamma - i\omega_n}\frac{\mathcal{Q}^{\alpha}_{\rho}{}^{*}(\boldsymbol{q})\mathcal{Q}^{\alpha}_{\rho'}(\boldsymbol{q}) - \mathcal{Q}^{\alpha}_{\rho}(\boldsymbol{q})\mathcal{Q}^{\alpha}_{\rho'}{}^{*}(\boldsymbol{q})}{\omega^{\alpha}_{\boldsymbol{q}} + i\omega_n}\right\}. \end{aligned} \tag{4.16}$$

This is equivalent to the expression given in Eq.(3.58) with the exception of the extra term (the second one on the right hand side of the above equation) due to the different distinct residual interactions.

We can now apply the technique developed in Chapter 3 starting from Eq.(4.9) following exactly the same steps. Due to the similarity of Eq.(4.9) and Eq.(3.12), we do not repeat all calculations and use directly the result (3.53), that is

$$\sum_{\rm qp}(\mathbf{1}, E+i\eta) = \sum_{\rm ret}(\boldsymbol{\mu}, E+i\eta) +$$

$$- \sum_{\lambda,\rho\rho',\mathbf{q}} \sum_{\alpha=0}^{1} \sum_{\gamma=1}^{2} \frac{\mathcal{Q}_\rho^{\alpha\,*}(q)\mathcal{Q}_{\rho'}^{\alpha}(q) q_{\rho\rho'}^{\alpha}(\gamma) 2\omega_{\boldsymbol{q}}^{\alpha}}{(\varepsilon + i\eta - \varepsilon_{\boldsymbol{\gamma}})^2 - {\omega_{\boldsymbol{q}}^{\alpha}}^2} \left[1 + n_B(E + i\eta - E_\gamma) - n_F(E_\gamma)\right]. \tag{4.17}$$

After inverting this equation to calculate the retarded self-energy as a function of $\sum_{\rm qp}(\mathbf{1}, E + i\eta)$ and using the result (4.16) for this last quantity, we obtain

$$\begin{aligned}
\sum_{\rm ret}(\boldsymbol{\mu}, E + i\eta) &= \sum_{\lambda,\rho\rho'} \sum_{\alpha=0}^{1} \sum_{\gamma=1}^{2} \times \\
&\times \left\{ \frac{1}{\beta} \sum_{i\omega_n} \frac{\mathcal{R}_{\rho\rho'}^{\alpha}(i\omega_n) q_{\rho\rho'}^{\alpha}(\gamma)}{E + i\eta - E_\gamma - i\omega_n} + \right. \\
&+ \frac{1}{\beta} \sum_{i\omega_n,\mathbf{q}} \frac{q_{\rho\rho'}^{\alpha}(\gamma)}{E + i\eta - E_\gamma - i\omega_n} \frac{\mathcal{Q}_\rho^{\alpha\,*}(q)\mathcal{Q}_{\rho'}^{\alpha}(q) - \mathcal{Q}_\rho^{\alpha}(q)\mathcal{Q}_{\rho'}^{\alpha\,*}(q)}{\omega_{\boldsymbol{q}}^{\alpha} + i\omega_n} + \\
&+ \left. \sum_{\mathbf{q}} \frac{\mathcal{Q}_\rho^{\alpha\,*}(q)\mathcal{Q}_{\rho'}^{\alpha}(q) q_{\rho\rho'}^{\alpha}(\gamma) 2\omega_{\boldsymbol{q}}^{\alpha}}{(E + i\eta - E_\gamma)^2 - {\omega_{\boldsymbol{q}}^{\alpha}}^2} \left[1 + n_B(E + i\eta - E_\gamma) - n_F(E_\gamma)\right] \right\}.
\end{aligned} \tag{4.18}$$

The last term in this equation needs to be transformed in terms of the RPA response function. In fact we can write

$$\begin{aligned}
F_{\rho\rho',\gamma}^{\alpha} &= -\sum_{\mathbf{q}} \frac{\mathcal{Q}_\rho^{\alpha\,*}(q)\mathcal{Q}_{\rho'}^{\alpha}(q) 2\omega_{\boldsymbol{q}}^{\alpha}}{(E + i\eta - E_\gamma)^2 - {\omega_{\boldsymbol{q}}^{\alpha}}^2} \\
&= \sum_{\mathbf{q}} \left[\frac{\mathcal{Q}_\rho^{\alpha\,*}(q)\mathcal{Q}_{\rho'}^{\alpha}(q)}{\omega_{\boldsymbol{q}}^{\alpha} - E - iI + E_\gamma} + \frac{\mathcal{Q}_\rho^{\alpha\,*}(q)\mathcal{Q}_{\rho'}^{\alpha}(q)}{\omega_{\boldsymbol{q}}^{\alpha} + E + i\eta - E_\gamma} \right] \\
&= \sum_{\mathbf{q}} \left[\frac{\mathcal{Q}_\rho^{\alpha\,*}(q)\mathcal{Q}_{\rho'}^{\alpha}(q)}{\omega_{\boldsymbol{q}}^{\alpha} - E - iI + E_\gamma} + \frac{\mathcal{Q}_\rho^{\alpha}(q)\mathcal{Q}_{\rho'}^{\alpha\,*}(q)}{\omega_{\boldsymbol{q}}^{\alpha} + E + i\eta - E_\gamma} \right] + \\
&+ \sum_{\mathbf{q}} \left[\frac{\mathcal{Q}_\rho^{\alpha\,*}(q)\mathcal{Q}_{\rho'}^{\alpha}(q) - \mathcal{Q}_\rho^{\alpha}(q)\mathcal{Q}_{\rho'}^{\alpha\,*}(q)}{\omega_{\boldsymbol{q}}^{\alpha} + E + i\eta - E_\gamma} \right] \\
&= \mathcal{R}_{\rho\rho'}^{\alpha}(E + i\eta - E_\gamma) + \\
&+ \sum_{\mathbf{q}} \left[\frac{\mathcal{Q}_\rho^{\alpha\,*}(q)\mathcal{Q}_{\rho'}^{\alpha}(q) - \mathcal{Q}_\rho^{\alpha}(q)\mathcal{Q}_{\rho'}^{\alpha\,*}(q)}{\omega_{\boldsymbol{q}}^{\alpha} + E + i\eta - E_\gamma} \right]
\end{aligned} \tag{4.19}$$

Inserting back this term in (4.18) and, after rearrangement of similar terms, we find

$$\begin{aligned}
\sum_{\text{ret}}(\boldsymbol{\mu}, E+i\eta) &= \sum_{\lambda,\rho\rho'}\sum_{\alpha=0}^{1}\sum_{\gamma=1}^{2}\times \\
&\times \left\{\frac{1}{\beta}\sum_{i\omega_n}\frac{\mathcal{R}^{\alpha}_{\rho\rho'}(i\omega_n)q^{\alpha}_{\rho\rho'}(\gamma)}{E+i\eta-E_\gamma-i\omega_n}+\right. \\
&- q^{\alpha}_{\rho\rho'}(\gamma)\left[1+n_B(E+i\eta-E_\gamma)-n_F(E_\gamma)\right]\mathcal{R}^{\alpha}_{\rho\rho'}(E+i\eta-E_\gamma)+ \\
&+ \frac{1}{\beta}\sum_{i\omega_n,\mathbf{q}}\frac{q^{\alpha}_{\rho\rho'}(\gamma)}{E+i\eta-E_\gamma-i\omega_n}\frac{\mathcal{Q}^{\alpha}_{\rho}{}^{*}(\boldsymbol{q})\mathcal{Q}^{\alpha}_{\rho'}(\boldsymbol{q})-\mathcal{Q}^{\alpha}_{\rho}(\boldsymbol{q})\mathcal{Q}^{\alpha}_{\rho'}{}^{*}(\boldsymbol{q})}{\omega^{\alpha}_{\boldsymbol{q}}+i\omega_n}+ \\
&- \sum_{\mathbf{q}} q^{\alpha}_{\rho\rho'}(\gamma)\left[1+n_B(E+i\eta-E_\gamma)-n_F(E_\gamma)\right]\times \\
&\times \left.\left[\frac{\mathcal{Q}^{\alpha}_{\rho}{}^{*}(\boldsymbol{q})\mathcal{Q}^{\alpha}_{\rho'}(\boldsymbol{q})-\mathcal{Q}^{\alpha}_{\rho}(\boldsymbol{q})\mathcal{Q}^{\alpha}_{\rho'}{}^{*}(\boldsymbol{q})}{\omega^{\alpha}_{\boldsymbol{q}}+E+i\eta-E_\gamma}\right]\right\}.
\end{aligned} \tag{4.20}$$

The first two terms of this expression coincide with the retarded self energy found in Chapter 3 while the last two are due to the different residual interactions used to describe different vibrational modes, such as β- and γ- vibrations and the Nambu-Goldstone modes. The other important difference is the sum over γ and α, that is now we are in presence of four different diagrams due to signature conservation. Using particular integrals containing the RPA response function in the integrand, we can evaluate the two extra terms. To avoid lengthly calculations, we prefer to give here only the final result leaving the detailed derivation in Appendix C.

We need two different integral forms to solve our problem, that is

$$\begin{aligned}
I^{\alpha}_{\rho\rho'}(E+i\eta) &= \int_{-\infty}^{+\infty} d\omega \frac{\mathcal{R}^{\alpha}_{\rho\rho'}(i\omega)}{E+i\eta-i\omega}, \\
J^{\alpha}_{\rho\rho'}(i\omega_n) &= \int_{-\infty}^{+\infty} d\omega \frac{\mathcal{R}^{\alpha}_{\rho\rho'}(i\omega)}{i\omega_n-i\omega}.
\end{aligned} \tag{4.21}$$

The important results that we obtain using these integrals (C.6,C.7,C.14,C.15) are

$$\sum_{\boldsymbol{q}} \frac{\mathcal{Q}_{\rho}^{\alpha}{}^{*}(\boldsymbol{q})\mathcal{Q}_{\rho'}^{\alpha}(\boldsymbol{q})}{E+i\eta-\omega_{\boldsymbol{q}}^{\lambda}} = \begin{cases} \frac{1}{2\pi}\int_{-\infty}^{+\infty} d\omega \frac{\mathcal{R}_{\rho\rho'}^{\alpha}(i\omega)}{E+i\eta-i\omega} & \mathrm{E}<0 \\ \frac{1}{2\pi}\int_{-\infty}^{+\infty} d\omega \frac{\mathcal{R}_{\rho\rho'}^{\alpha}(i\omega)}{E+i\eta-i\omega} - \mathcal{R}_{\rho\rho'}^{\alpha}(E+i\eta) & \mathrm{E}>0 \end{cases},$$

$$\sum_{\boldsymbol{q}} \frac{\mathcal{Q}_{\rho}^{\alpha}(\boldsymbol{q})\mathcal{Q}_{\rho'}^{\alpha}{}^{*}(\boldsymbol{q})}{E+i\eta+\omega_{\boldsymbol{q}}^{\lambda}} = \begin{cases} \frac{1}{2\pi}\int_{-\infty}^{+\infty} d\omega \frac{\mathcal{R}_{\rho\rho'}^{\alpha}(i\omega)}{E+i\eta-i\omega} & \mathrm{E}>0 \\ \frac{1}{2\pi}\int_{-\infty}^{+\infty} d\omega \frac{\mathcal{R}_{\rho\rho'}^{\alpha}(i\omega)}{E+i\eta-i\omega} + \mathcal{R}_{\rho\rho'}^{\alpha}(E+i\eta) & \mathrm{E}<0 \end{cases},$$

$$\sum_{\boldsymbol{q}} \frac{\mathcal{Q}_{\rho}^{\alpha}{}^{*}(\boldsymbol{q})\mathcal{Q}_{\rho'}^{\alpha}(\boldsymbol{q})}{\omega_{\boldsymbol{q}}^{\alpha}-i\omega_n} = \frac{1}{2}\left\{\mathcal{R}_{\rho\rho'}^{\alpha}(i\omega_n) - \frac{1}{\pi}\int_{-\infty}^{+\infty} d\omega \frac{\mathcal{R}_{\rho\rho'}^{\alpha}(i\omega)}{i\omega_n-i\omega}\right\}, \tag{4.22}$$

$$\sum_{\boldsymbol{q}} \frac{\mathcal{Q}_{\rho}^{\alpha}(\boldsymbol{q})\mathcal{Q}_{\rho'}^{\alpha}{}^{*}(\boldsymbol{q})}{\omega_{\boldsymbol{q}}^{\alpha}+i\omega_n} = \frac{1}{2}\left\{\mathcal{R}_{\rho\rho'}^{\alpha}(i\omega_n) + \frac{1}{\pi}\int_{-\infty}^{+\infty} d\omega \frac{\mathcal{R}_{\rho\rho'}^{\alpha}(i\omega)}{i\omega_n-i\omega}\right\}. \tag{4.23}$$

The extra terms can be written then as

$$\sum_{\boldsymbol{q}} \frac{\mathcal{Q}_{\rho}^{\alpha}{}^{*}(\boldsymbol{q})\mathcal{Q}_{\rho'}^{\alpha}(\boldsymbol{q}) - \mathcal{Q}_{\rho}^{\alpha}(\boldsymbol{q})\mathcal{Q}_{\rho'}^{\alpha}{}^{*}(\boldsymbol{q})}{\omega_{\boldsymbol{q}}^{\alpha}+i\omega_n} = \frac{1}{2}\left[\mathcal{R}_{\rho'\rho}^{\alpha}(i\omega_n) - \mathcal{R}_{\rho\rho'}^{\alpha}(i\omega_n)\right] + \\ + \frac{1}{2\pi}\int_{-\infty}^{+\infty} d\omega \frac{\left[\mathcal{R}_{\rho'\rho}^{\alpha}(i\omega_n) - \mathcal{R}_{\rho\rho'}^{\alpha}(i\omega_n)\right]}{i\omega_n-i\omega}, \tag{4.24}$$

and

$$\sum_{\boldsymbol{q}} \frac{\mathcal{Q}_{\rho}^{\alpha}{}^{*}(\boldsymbol{q})\mathcal{Q}_{\rho'}^{\alpha}(\boldsymbol{q}) - \mathcal{Q}_{\rho}^{\alpha}(\boldsymbol{q})\mathcal{Q}_{\rho'}^{\alpha}{}^{*}(\boldsymbol{q})}{\omega_{\boldsymbol{q}}^{\alpha}+E+i\eta-E_\gamma} = \frac{1}{2\pi}\int_{-\infty}^{+\infty} d\omega \frac{\mathcal{R}_{\rho'\rho}^{\alpha}(i\omega) - \mathcal{R}_{\rho\rho'}^{\alpha}(i\omega)}{E+i\eta-E_\gamma-i\omega} + \\ + \begin{cases} 0 & \mathrm{E}-\mathrm{E}_\gamma>0 \\ +\mathcal{R}_{\rho'\rho}^{\alpha}(E+i\eta-E_\gamma) - \mathcal{R}_{\rho\rho'}^{\alpha}(E+i\eta-E_\gamma) & \mathrm{E}-\mathrm{E}_\gamma<0 \end{cases} \tag{4.25}$$

After substituting these expression in (4.20)(see appendix C for details), we obtain that the retarded self-energy becomes

$$
\begin{aligned}
\sum_{\text{ret}}(\boldsymbol{\mu}, E+i\eta) &= \sum_{\lambda,\rho\rho'}\sum_{\alpha=0}^{1}\sum_{\gamma=1}^{2} q^{\alpha}_{\rho\rho'}(\gamma)\times \\
&\times \left\{ \frac{1}{2\beta}\sum_{i\omega_n} \frac{\left[\mathcal{R}^{\alpha}_{\rho\rho'}(i\omega_n)+\mathcal{R}^{\alpha}_{\rho'\rho}(i\omega_n)\right]}{E+i\eta-E_\gamma-i\omega_n} + \right. \\
&+ \frac{1}{\beta}\sum_{i\omega_n}\frac{1}{E+i\eta-E_\gamma-i\omega_n}\frac{1}{2\pi}\int_{-\infty}^{+\infty} d\omega \frac{\mathcal{R}^{\alpha}_{\rho'\rho}(i\omega)-\mathcal{R}^{\alpha}_{\rho\rho'}(i\omega)}{i\omega_n-i\omega} + \\
&- \frac{[1+n_B(E+i\eta-E_\gamma)-n_F(E_\gamma)]}{2\pi}\int_{-\infty}^{+\infty} d\omega \frac{\mathcal{R}^{\alpha}_{\rho'\rho}(i\omega)-\mathcal{R}^{\alpha}_{\rho\rho'}(i\omega)}{E+i\eta-E_\gamma-i\omega} + \\
&+ \left. [1+n_B(E+i\eta-E_\gamma)-n_F(E_\gamma)] \begin{cases} \mathcal{R}^{\alpha}_{\rho\rho'}(E+i\eta-E_\gamma) & \text{E}-\text{E}_\gamma>0 \\ \mathcal{R}^{\alpha}_{\rho'\rho}(E+i\eta-E_\gamma) & \text{E}-\text{E}_\gamma<0 \end{cases} \right\}
\end{aligned}
\tag{4.26}
$$

We have to face another problem connected with the second term in the above expression, because we have an integration contained in an infinite sum. It is not difficult to simplify this term into a convenient form but we prefer to give here only the final answer leaving all the algebraic steps to the Appendix C. The new form of this term is

$$
\begin{aligned}
G^{\alpha}_{\rho\rho'}(i\omega) &= \frac{1}{\beta}\sum_{i\omega_n}\frac{1}{E+i\eta-E_\gamma-i\omega_n}\frac{1}{2\pi}\int_{-\infty}^{+\infty} d\omega \frac{\mathcal{R}^{\alpha}_{\rho'\rho}(i\omega)-\mathcal{R}^{\alpha}_{\rho\rho'}(i\omega)}{i\omega_n-i\omega} = \\
&= \frac{1}{2\pi}\int_{-\infty}^{+\infty} d\omega \frac{\mathcal{R}^{\alpha}_{\rho\rho'}(i\omega)-\mathcal{R}^{\alpha}_{\rho\rho'}(i\omega)}{E+i\eta-E_\gamma-i\omega}\left[n_B(E+i\eta-E_\gamma)-n_B(i\omega)\right].
\end{aligned}
\tag{4.27}
$$

Inserting this result in (4.26) and summing up similar terms (see Appendix C for all steps) we obtain the final expression for the retarded self-energy in a rotating frame

$$
\begin{aligned}
\sum_{\text{ret}}(\boldsymbol{\mu}, E+i\eta) &= \sum_{\lambda,\rho\rho'}\sum_{\alpha=0}^{1}\sum_{\gamma=1}^{2} q^{\alpha}_{\rho\rho'}(\gamma)\times \\
&\times \left\{ \frac{1}{2\beta}\sum_{i\omega_n} \frac{\left[\mathcal{R}^{\alpha}_{\rho\rho'}(i\omega_n)+\mathcal{R}^{\alpha}_{\rho'\rho}(i\omega_n)\right]}{E+i\eta-E_\gamma-i\omega_n} + \right.
\end{aligned}
$$

$$
\begin{aligned}
- \quad & \frac{1}{2\pi}\int_{-\infty}^{+\infty} d\omega \frac{\mathcal{R}^{\alpha}_{\rho'\rho}(i\omega) - \mathcal{R}^{\alpha}_{\rho\rho'}(i\omega)}{E + i\eta - E_\gamma - i\omega}\left[1 + n_B(i\omega) - n_F(E_\gamma)\right] + \\
- \quad & \left[1 + n_B(E + i\eta - E_\gamma) - n_F(E_\gamma)\right] \left\{ \begin{array}{ll} \mathcal{R}^{\alpha}_{\rho\rho'}(E + i\eta - E_\gamma) & E - E_\gamma > 0 \\ \mathcal{R}^{\alpha}_{\rho'\rho}(E + i\eta - E_\gamma) & E - E_\gamma < 0 \end{array} \right\}
\end{aligned}
\tag{4.28}
$$

This is a quite complicated expression that looks quite different corresponding to the one in Chapter 3. However one can show that Eqs.(4.28) and (3.59) coincide in the case of only one separable interaction where $\rho = \rho' = 1$, and, as a consequence, $\mathcal{R}^{\alpha}_{\rho\rho'}(z) = \mathcal{R}^{\alpha}_{\rho'\rho}(z)$. In this situation the extra terms in Eq.(4.28) cancel out and it is not necessary distinguish between $E - E_\gamma > 0$ and $E - E_\gamma < 0$, so that the expression becomes

$$
\begin{aligned}
\sum_{\text{ret}}(\boldsymbol{\mu}, E + i\eta) \quad = \quad & \sum_{\lambda}\sum_{\alpha=0}^{1}\sum_{\gamma=1}^{2} q^{\alpha}(\gamma) \times \\
& \times \quad \left\{ \frac{1}{\beta}\sum_{i\omega_n} \frac{\mathcal{R}^{\alpha}(i\omega_n)}{E + i\eta - E_\gamma - i\omega_n} + \right. \\
& - \quad \left. \mathcal{R}^{\alpha}(E + i\eta - E_\gamma)\left[1 + n_B(E + i\eta - E_\gamma) - n_F(E_\gamma)\right] . \right.
\end{aligned}
\tag{4.29}
$$

This has the same structure of Eq.(3.59) of Chapter 3 except for the sum over γ, that comes from the conservation of the signature quantum number.

4.4 Self-Energy at Zero Temperature

As explained in Chapter 3, the limiting case of zero temperature can be obtained from the expression at finite temperature substituting the sum over frequencies with a proper integration. Applying this rule to eq (4.28) and keeping into account the properties of the boson factor (see appendix A) we can write

$$
\sum_{\text{ret}}(\mathbf{1}, \varepsilon + i\eta) \quad = \quad \sum_{\lambda,\rho\rho'}\sum_{\alpha=0}^{1}\sum_{\gamma=1}^{2} q^{\alpha}_{\rho\rho'}(\gamma) \times
$$

$$
\begin{aligned}
&\times \quad \left\{ \frac{1}{2}\frac{1}{2\pi}\int_{-\infty}^{+\infty} d\omega \frac{\left[\mathcal{R}^{\alpha}_{\rho\rho'}(i\omega)+\mathcal{R}^{\alpha}_{\rho'\rho}(i\omega)\right]}{E+i\eta-E_\gamma-i\omega} + \right. \\
&- \quad \frac{1}{2\pi}\int_{-\infty}^{+\infty} d\omega \frac{\mathcal{R}^{\alpha}_{\rho'\rho}(i\omega)-\mathcal{R}^{\alpha}_{\rho\rho'}(i\omega)}{E+i\eta-E_\gamma-i\omega}\left[1-\frac{1}{2}-n_F(E_\gamma)\right] + \\
&- \quad \left. \begin{cases} [1-n_F(E_\gamma)]\,\mathcal{R}^{\alpha}_{\rho\rho'}(E+i\eta-E_\gamma) & E-E_\gamma>0 \\ -n_F(E_\gamma)\mathcal{R}^{\alpha}_{\rho'\rho}(E+i\eta-E_\gamma) & E-E_\gamma<0 \end{cases} \right\}.
\end{aligned}
\tag{4.30}
$$

Combining together the integrals, one obtains

$$
\begin{aligned}
\sum_{\rm ret}(\mathbf{1},\varepsilon+i\eta) \quad &= \quad \sum_{\lambda,\rho\rho'}\sum_{\alpha=0}^{1}\sum_{\gamma=1}^{2} q^{\alpha}_{\rho\rho'}(\gamma)\times \\
&\times \quad \left\{ \frac{[1-n_F(E_\gamma)]}{2\pi}\int_{-\infty}^{+\infty} d\omega \frac{\mathcal{R}^{\alpha}_{\rho\rho'}(i\omega)}{E+i\eta-E_\gamma-i\omega} + \right. \\
&+ \quad \frac{n_F(E_\gamma)}{2\pi}\int_{-\infty}^{+\infty} d\omega \frac{\mathcal{R}^{\alpha}_{\rho'\rho}(i\omega)}{E+i\eta-E_\gamma-i\omega} + \\
&- \quad \left. \begin{cases} [1-n_F(E_\gamma)]\,\mathcal{R}^{\alpha}_{\rho\rho'}(E+i\eta-E_\gamma) & E-E_\gamma>0 \\ -n_F(E_\gamma)\mathcal{R}^{\alpha}_{\rho'\rho}(E+i\eta-E_\gamma) & E-E_\gamma<0 \end{cases} \right\}.
\end{aligned}
\tag{4.31}
$$

We have to remember now the convention on the γ index because the result will depend on the sign of E_γ, that is we have that for $\gamma = 2(4)$ $E_\gamma \to -E_{\bar{\nu}}(-E_\nu)$. This observation is very important because, in case of a condensate state at zero temperature, the quasiparticle energies are, per definition, positive quantities so that the Fermi factor behaves as

$$
n_F(E_\gamma)=0, \qquad n_F(-E_\gamma)=1. \tag{4.32}
$$

Introducing this result in the equation above we find that

$$
\sum_{\rm ret}(\mathbf{1},\varepsilon+i\eta)=\sum_{\lambda,\rho\rho'}\sum_{\alpha=0}^{1}\sum_{\gamma=1}^{2} q^{\alpha}_{\rho\rho'}(\gamma)I^{\alpha}_{\rho\rho'}(\gamma), \tag{4.33}
$$

where, to simplify the notation, we have introduced the function $I^{\alpha}_{\rho\rho'}(\gamma)$ defined as

$$I^{\alpha}_{\rho\rho'}(\gamma) = \frac{1}{2\pi}\int_{-\infty}^{+\infty} d\omega \frac{\mathcal{R}^{\alpha}_{\rho\rho'}(i\omega)}{E+i\eta-E_\gamma-i\omega} + \begin{cases} -\mathcal{R}^{\alpha}_{\rho\rho'}(E+i\eta-E_\gamma) & E-E_\gamma>0, \\ 0 & E-E_\gamma<0, \end{cases} \tag{4.34}$$

for $\gamma = 1, 3$ and

$$I^{\alpha}_{\rho\rho'}(\gamma) = \frac{1}{2\pi}\int_{-\infty}^{+\infty} d\omega \frac{\mathcal{R}^{\alpha}_{\rho'\rho}(i\omega)}{E+i\eta-E_\gamma-i\omega} + \begin{cases} 0 & E-E_\gamma>0, \\ \mathcal{R}^{\alpha}_{\rho'\rho}(E+i\eta-E_\gamma) & E-E_\gamma<0, \end{cases} \tag{4.35}$$

for $\gamma = 2, 4$, keeping the same convention defined in (4.14). This is the final expression of the retarded self-energy in terms of the RPA response.

We want to translate the former equation in the standard way using RPA solutions, For this purpose, we observe that the integrals above were already used for the extra terms problem (Appendix C Eqs.C.6,C.7,C.14, C.15) so that we can write

$$\begin{aligned} I^{\alpha}_{\rho\rho'}(\gamma) &= \sum_{\boldsymbol{q}} \frac{\mathcal{Q}^{\alpha}_{\rho}{}^{*}(\boldsymbol{q})\mathcal{Q}^{\alpha}_{\rho'}(\boldsymbol{q})}{E+i\eta-E_\gamma-\omega^{\alpha}_{\boldsymbol{q}}}, \qquad (\gamma=1,3) \\ I^{\alpha}_{\rho\rho'}(\gamma) &= \sum_{\boldsymbol{q}} \frac{\mathcal{Q}^{\alpha}_{\rho}{}^{*}(\boldsymbol{q})\mathcal{Q}^{\alpha}_{\rho'}(\boldsymbol{q})}{E+i\eta-E_\gamma+\omega^{\alpha}_{\boldsymbol{q}}} \qquad (\gamma=2,4) \end{aligned} \tag{4.36}$$

The self-energy in terms of the vibrational energies, that is RPA solutions, can be written as

$$\begin{aligned} \sum_{\text{ret}}(\boldsymbol{\mu}, E+i\eta) &= \sum_{\lambda,\rho\rho'}\sum_{\boldsymbol{q}} \times \\ &\times \left\{ \sum_{\nu} \chi^0_\rho R^{0B}_{\rho}{}^{*}(\mu\nu) R^{0B}_{\rho'}(\mu\nu)\chi^0_{\rho'} \frac{\mathcal{Q}^{0}_{\rho}{}^{*}(\boldsymbol{q})\mathcal{Q}^{0}_{\rho'}(\boldsymbol{q})}{E+i\eta-E_\nu-\omega^0_{\boldsymbol{q}}} + \right. \\ &+ \left. \sum_{\bar{\nu}} \chi^0_\rho R^{0A}_{\rho}{}^{*}(\mu\bar{\nu}) R^{0A}_{\rho'}(\mu\bar{\nu})\chi^0_{\rho'} \frac{\mathcal{Q}^{0}_{\rho}{}^{*}(\boldsymbol{q})\mathcal{Q}^{0}_{\rho'}(\boldsymbol{q})}{E+i\eta+E_{\bar{\nu}}+\omega^0_{\boldsymbol{q}}} + \right. \end{aligned}$$

$$
\begin{aligned}
&+ \quad \sum_{\bar{\nu}} \chi^1_\rho R^{1B^*}_\rho(\mu\bar{\nu}) R^{1B}_{\rho'}(\mu\bar{\nu}) \chi^1_{\rho'} \frac{\mathcal{Q}^{1^*}_\rho(q)\mathcal{Q}^1_{\rho'}(q)}{E + i\eta - E_{\bar{\nu}} - \omega^1_{\boldsymbol{q}}} + \\
&+ \quad \sum_{\nu} \chi^1_\rho R^{1A^*}_\rho(\mu\nu) R^{1A}_{\rho'}(\mu\nu) \chi^1_{\rho'} \frac{\mathcal{Q}^{1^*}_\rho(q)\mathcal{Q}^1_{\rho'}(q)}{E + i\eta + E_{\nu} + \omega^1_{\boldsymbol{q}}} \Bigg\} .
\end{aligned}
\tag{4.37}
$$

In the limit of zero rotational frequency, we are in presence of degeneracy in signature and in different component of separable interactions so that we can write

$$
\begin{aligned}
\sum_{\text{ret}}(\mathbf{1}, \varepsilon + i\eta) \quad &= \quad \sum_{\lambda,\nu} \sum_{\boldsymbol{q}} \times \\
&\times \quad \Bigg\{ \chi R^{B^*}(\mu\nu) R^B(\mu\nu) \chi \frac{\mathcal{Q}^*(q)\mathcal{Q}(q)}{E + i\eta - E_\nu - \omega_{\boldsymbol{q}}} + \\
&+ \quad \chi R^{A^*}(\mu\nu) R^A(\mu\nu) \chi \frac{\mathcal{Q}^*(q)\mathcal{Q}(q)}{E + i\eta + E_\nu + \omega_{\boldsymbol{q}}} \Bigg\} ,
\end{aligned}
\tag{4.38}
$$

an expression which coincides with the known self-energy for a condensate state at zero temperature used for spherical nuclei [15, 14]. We want to show now that this expression coincide, in the limit of zero pairing correlations, to the result of Chapter 3. From the diagrams of Fig.(4.4) , one can write

$$
\begin{aligned}
R^B(\mu\nu) \quad &\rightarrow \quad F^2_{\mu\nu}(u_\mu u_\nu \pm u_\nu u_\mu)^2 \\
R^A(\mu\nu) \quad &\rightarrow \quad F^2_{\mu\nu}(u_\mu v_\nu \mp u_\nu v_\mu)^2
\end{aligned}
\tag{4.39}
$$

where u and v are the occupation factors defined as

$$
\begin{aligned}
u^2_\gamma \quad &= \quad \frac{1}{2}\left[\frac{1}{2} + \frac{\varepsilon_{\boldsymbol{\gamma}} - \varepsilon_{\boldsymbol{F}}}{E_\gamma}\right] \\
v^2_\gamma \quad &= \quad \frac{1}{2}\left[\frac{1}{2} - \frac{\varepsilon_{\boldsymbol{\gamma}} - \varepsilon_{\boldsymbol{F}}}{E_\gamma}\right] ,
\end{aligned}
\tag{4.40}
$$

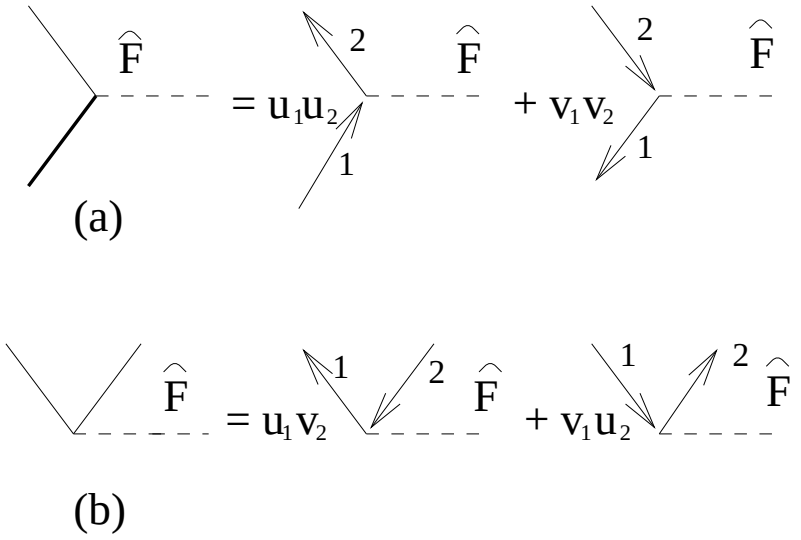

Figure 4.4: Matrix elements of one-particle operator between quasiparticle states. Graph (a) corresponds to the scattering while graph (b) is the creation of two quasiparticles.

and $E_\gamma = \sqrt{(\varepsilon_{\boldsymbol{\gamma}} - \varepsilon_{\boldsymbol{F}})^2 + \Delta^2}$. The $\pm$ sign is related with the time-reversal property of the operator $\widehat{F}$. The above expressions for the quasiparticle matrix elements are consequence of the Bogoliubov transformation where a quasiparticle is a linear combination of particle and hole.

At this point we can study the limit of no pairing correlations, that is $\Delta = 0$. Choosing, as an example, μ as particle state, we get that

$$\begin{aligned} R^B(\mu\nu) &\rightarrow F^2_{\mu\nu} u^2_\nu \\ R^A(\mu\nu) &\rightarrow F^2_{\mu\nu} v^2_\nu. \end{aligned} \tag{4.41}$$

This means that, if ν is a particle state , $u^2_\nu = 1$, $v^2_\nu = 0$ and $E_\nu = \varepsilon'_\nu = \varepsilon_{\boldsymbol{\nu}} - \varepsilon_{\boldsymbol{F}}$, so that the only surviving term is the one with matrix elements $R^B(\mu\nu)$

$$\sum_{\rm sp}(\boldsymbol{\mu}, \varepsilon + i\eta) = \sum_\lambda \sum_\nu \sum_{\boldsymbol{q}} \chi R^{B^*}(\mu\nu) R^B(\mu\nu) \chi \frac{\mathcal{Q}^*(\boldsymbol{q})\mathcal{Q}(\boldsymbol{q})}{\varepsilon + i\eta - \varepsilon'_\nu - \omega_{\boldsymbol{q}}}, \tag{4.42}$$

while if ν is an hole state, $u^2_\nu = 0$, $v^2_\nu = 1$ and $E_\nu = -\varepsilon'_\nu = -(\varepsilon_{\boldsymbol{\nu}} - \varepsilon_{\boldsymbol{F}})$, the self-energy

coincides with the $R^A(\mu\nu)$ term, namely

$$\sum_{\rm sp}(\boldsymbol{\mu},\varepsilon+i\eta) \;=\; \sum_{\lambda}\sum_{\nu}\sum_{\boldsymbol{q}}\chi R^{A^*}(\mu\nu)R^A(\mu\nu)\chi\frac{\mathcal{Q}^*(\boldsymbol{q})\mathcal{Q}(\boldsymbol{q})}{\varepsilon+i\eta-\varepsilon'_\nu+\omega_{\boldsymbol{q}}}, \tag{4.43}$$

Combining these two results we get

$$\begin{aligned}\sum_{\rm sp}(\boldsymbol{\mu},\varepsilon+i\eta) \;&=\; \sum_{\lambda}\sum_{\nu}\sum_{\boldsymbol{q}}\chi F^2(\mu\nu)\chi\mathcal{Q}^*(\boldsymbol{q})\mathcal{Q}(\boldsymbol{q})\times\\ &\times\;\left[\frac{1-n_F(\varepsilon_{\boldsymbol{\nu}})}{\varepsilon+i\eta-\varepsilon'_\nu-\omega_{\boldsymbol{q}}}+\frac{n_F(\nu)}{\varepsilon+i\eta-\varepsilon'_\nu+\omega_{\boldsymbol{q}}}\right].\end{aligned} \tag{4.44}$$

This is exactly the same expression of Chapter 3(Eq.(3.60)) with

$$V^2(\mathbf{1},\mathbf{2};\lambda,\boldsymbol{q})\rightarrow\chi F^2(\mu\nu)\chi\mathcal{Q}^*(\boldsymbol{q})\mathcal{Q}(\boldsymbol{q}). \tag{4.45}$$

Chapter 5

Broken Symmetries

5.1 Introduction

The exact many-body Hamiltonian $\widehat{H}$ is invariant under a number of symmetry operations that is, it commutes with the corresponding generator of symmetry $\widehat{P}$:

$$[\widehat{H}, \widehat{P}] = 0. \tag{5.1}$$

This property is very important because it allows us to look for wave functions that are simultaneous eigenfunctions of $\widehat{H}$ and $\widehat{P}$. In the general case of many-particles and strong correlations, the proper treatment of symmetries is a serious problem because it is a generally accepted procedure that correlations are treated by symmetry violating mean field approach. The correlations we are interested in are of two kinds, long-range correlations causing stable deformation (violation of rotational invariance due to the possible choice of orientation) and short-range correlations which provide super-fluid solutions (violation of particle number).

We have already seen in Chapter 1 that these correlations can be treated in HFB theory, that is a mean field approach that violates angular momentum and particle number conservation. In this approximation, the ground state of the system is referred to as a state of broken symmetry and can be viewed as an intrinsic state which defines a privileged orientation in three-dimensional and gauge space. Eliminating the corresponding spurious state by taking into account the appropriate particle-vibration coupling, one is led with a zero-energy mode orthogonal with all the others

in the spectrum and which has zero matrix elements for all physical operators. The rotational band displaying the moment of inertia associated with this ω=0 state is known, in analogy with relativistic field theory. as the Nambu-Goldstone mode.

5.2 Restoration of Broken Symmetries in RPA

The RPA theory, which goes beyond the static mean field approach, includes higher order correlations and leads to a restoration of the symmetry in the harmonic approximation. We are not interested in all details (see [3, 2, 21]). What we want to show here is how the presence of a Nambu-Goldstone mode influences the RPA response function when the restoration of the symmetry is carried out within this approximation.

We start with the Hamiltonian $\widehat{H}$, invariant under a continuous symmetry operation generated by a Hermitian one-body operator $\widehat{P}$. We assume that the HFB solution violates this symmetry, namely $[\widehat{H}_{\rm HFB}, \widehat{P}] \neq 0$. We note an essential property of the RPA, that is conservation laws possessed by the original Hamiltonian are preserved. We know that any one-body operator can be written, in RPA approximation, as

$$\widehat{P} = \sum_{\gamma,\delta} [P(\gamma,\delta)\widehat{A}^{\dagger}_{\gamma\delta} + P^{*}(\gamma,\delta)\widehat{A}_{\gamma\delta}] \tag{5.2}$$

The commutator relation in RPA becomes

$$[\widehat{H}, \widehat{P}]_{\rm RPA} = \sum_{\gamma,\delta} \left(\langle 0|[\widehat{A}_{\delta\gamma}, [\widehat{H}, \widehat{P}]]|0\rangle \widehat{A}^{\dagger}_{\gamma\delta} + \langle 0|[[\widehat{H}, \widehat{P}], \widehat{A}^{\dagger}_{\gamma\delta}]|0\rangle \widehat{A}_{\gamma\delta} \right), \tag{5.3}$$

from which one can check that if $[\widehat{H}, \widehat{P}] = 0$ then $[\widehat{H}, \widehat{P}]_{\rm RPA} = 0$.

The relation above means that $\widehat{P}$ is an exact but *spurious solution* of the RPA equation with zero energy as eigenvalue. We use the word spurious to indicate RPA solutions corresponding to a broken symmetry in the HFB state. From the properties of the RPA solutions one can check that the spurious solutions are completely orthogonal to the other(physical)excitations, where physical means intrinsic excitations of the system as, for example, β- and γ- vibrations.

In what follows we want to analyze the behaviour of the constant of motions of our system in the case where the generator $\widehat{P}$ coincides with the particle number $\widehat{N}_\tau$, $(\tau = n, p)$ or with the angular momentum $\mathbf{J}$. The corresponding conservation laws are lead to

$$[\widehat{H}, \widehat{N}_\tau] = 0, \tag{5.4}$$

$$[\widehat{H}, \boldsymbol{J}] = 0. \tag{5.5}$$

In the case under discussion, the Hamiltonian is defined as

$$\widehat{H'} = \widehat{H} - \lambda\widehat{N} - \omega_{\rm rot}\widehat{J}_x, \tag{5.6}$$

so that the conservations laws connected with the existence of zero-frequency solutions should satisfy the following relations

$$[\widehat{H'}, \widehat{N}_\tau] = 0, \tag{5.7}$$

$$[\widehat{H'}, \widehat{J}_x] = 0. \tag{5.8}$$

$$[\widehat{H'}, \widehat{J}_y - i\widehat{J}_z] = \omega_{\rm rot}(\widehat{J}_y - i\widehat{J}_z) \tag{5.9}$$

$$[\widehat{H'}, \widehat{J}_y + i\widehat{J}_z] = -\omega_{\rm rot}(\widehat{J}_y + i\widehat{J}_z). \tag{5.10}$$

For convenience we define the operators $\widehat{J}_\pm = \widehat{J}_y \pm i\widehat{J}_z$. As we have seen in Chapter 2, it is convenient to work with good signature operators so that the RPA Hamiltonian is actually divided in two parts, a positive and negative subspace. Looking at the Table (2.1), we see that the number operators $\widehat{N}_\tau$ and $\widehat{J}_x$ lie in the positive sector while $\widehat{J}_\pm$ are negative signature operators.

5.3 Nambu-Goldstone Modes in the Positive Signature Sector

As we have seen above we are in presence of three different zero solutions corresponding to spurious states violating number conservation (proton and neutron separately) and rotational invariance(x-component of the angular momentum).

Using a standard procedure (see [21, 3]) one can define the canonical conjugate operators of $\hat{J}_x$ and $\widehat{N}_\tau$, namely

$$[\widehat{J}_x, \widehat{\phi}_x] = -i \tag{5.11}$$

$$[\widehat{N}_N, \widehat{\phi}_N] = -i \tag{5.12}$$

$$[\widehat{N}_Z, \widehat{\phi}_Z] = -i. \tag{5.13}$$

Generally speaking, one can express the creation operator of normal modes in terms of canonically conjugate variables P and Q in the form

$$\widehat{X} = \frac{1}{\sqrt{2\omega\mathcal{I}}}(P + i\omega\mathcal{I}Q), \tag{5.14}$$

where the quantity $\mathcal{I}$ is the moment of inertia and $[P, Q] = -i$. With $\omega \to 0$, the contribution of the mode (5.14) to the response function (see Eq.(2.42)) is given by

$$\mathcal{R}_{\hat{A}\hat{B}} = \frac{1}{\mathcal{I}}\left\{\frac{[\hat{A}, \hat{P}]_{\mathrm{RPA}}[\hat{P}, \hat{B}]_{\mathrm{RPA}}}{\omega^2} + \frac{[\hat{A}, \hat{Q}]_{\mathrm{RPA}}[\hat{P}, \hat{B}]_{\mathrm{RPA}} + [\hat{A}, \hat{P}]_{\mathrm{RPA}}[\hat{Q}, \hat{B}]_{\mathrm{RPA}}}{\omega}\right\}, \tag{5.15}$$

where $\hat{A}$ and $\hat{B}$ correspond to the distinct residual interaction taking into account. From equation above one can see that this term is quadratically divergent when $\omega \to 0$. This divergence cancels out only when $[\hat{A}, \hat{P}]_{\mathrm{RPA}} = 0$ exactly.

Applying this result to our three Nambu-Goldstone modes, we see that P corresponds, respectively to $\hat{J}_x$ and $\widehat{N}_\tau$. This means that the corresponding three spurious states will give divergent contributions to the response function (2.42) for all the operators $\widehat{A}$ that do not commute with them, that is for operators $\hat{A}(\hat{B})$ such that

$$[\widehat{A}, \widehat{J}_x]_{\mathrm{RPA}} \neq 0 \tag{5.16}$$

$$[\widehat{A}, \widehat{N}_\tau]_{\mathrm{RPA}} \neq 0. \tag{5.17}$$

From Table (2.1), one can see that the operators $\widehat{P}_{\tau-}$ do not commute with particle number operator while $\widehat{Q}^0_{21}$ does not commute with angular momentum operator. This is because

$$[\widehat{P}_{\tau-}, \widehat{N}_{\tau}]_{\mathrm{RPA}} = -2 \sum P_{\tau}(\mu\bar{\nu}) N_{\tau}(\mu\bar{\nu}), \tag{5.18}$$

$$[\widehat{Q}^{0}_{21}, \widehat{J}_{x}]_{\mathrm{RPA}} = -2 \sum Q^{0}_{21}(\mu\bar{\nu}) J_{x}(\mu\bar{\nu}). \tag{5.19}$$

This means that the following response functions will contain divergent contributions due to the Nambu-Goldstone modes, that is

$$\mathcal{R}^{0}_{AB}(\omega) \qquad A = B = \widehat{P}_{\tau-}, \tag{5.20}$$

$$\mathcal{R}^{0}_{AB}(\omega) \qquad A = B = \widehat{Q}^{0}_{21}. \tag{5.21}$$

5.4 Nambu-Goldstone Modes in the Negative Signature Sector

The operators $\widehat{J}_{\pm}$ lie in the negative signature sector and , as seen above, they do not give zero excitation energy. However, defining new operators as

$$\Gamma = \frac{\widehat{J}_{y} + i\widehat{J}_{z}}{\sqrt{2I_{0}}} \qquad \widehat{\Gamma}^{\dagger} = \frac{\widehat{J}_{y} - i\widehat{J}_{z}}{\sqrt{2I_{0}}}, \quad \text{with} \quad I_{0} = \langle \widehat{J}_{x} \rangle, \tag{5.22}$$

we can write

$$[\widehat{H}, \widehat{\Gamma}^{\dagger}] = \omega_{\mathrm{rot}} \widehat{\Gamma}^{\dagger}. \tag{5.23}$$

This means that $\widehat{\Gamma}^{\dagger}$ creates a normal mode with frequency ω_{rot}. This excitation is a spurious mode induced by the Coriolis term -$\omega_{\mathrm{rot}} \widehat{J}_{x}$. In fact $\widehat{\Gamma}^{\dagger}$ re-orients the angular momentum from its alignment along the x-axis (cf. ref.[21]) in keeping with the fact that

$$\widehat{\Gamma}^{\dagger}\widehat{\Gamma} \rightarrow \widehat{I} - \langle \widehat{J}_{x} \rangle, \tag{5.24}$$

where $\widehat{I}$ is the total angular momentum operator. Only when $\omega_{\mathrm{rot}} = 0$ one can infer that $\widehat{J}_{x} \pm i\widehat{J}_{z}$ corresponds to a zero frequency mode. As in the positive signature case, the operator that does not commute with $\widehat{\Gamma}^{\dagger}$ is $\widehat{Q}^{1}_{21}$ because

$$[\widehat{Q}^1_{21}, \widehat{J}_y - i\widehat{J}_z] = -2\sum Q^1_{21}(\mu\nu)J_y(\mu\nu), \tag{5.25}$$

so that the $\mathcal{R}^1_{AB}(\omega)$ response with A=B=$\widehat{Q}^1_{21}$ will present a divergent contribution in the zero energy region.

Chapter 6

Removal of Nambu-Goldstone Modes

6.1 Introduction

As we have seen in Chapter 5, the Nambu-Goldstone modes contribute to the RPA response function producing giant bumps at $\omega = 0$ and, moreover, by mixing with the physical modes at $\omega \approx 0$. Therefore, it is necessary to find a proper procedure for the removal of their contributions. A method was proposed some years ago [22] based on the introduction of an effective Hamiltonian defined in terms of canonically conjugate operators associated with the generators of the Nambu-Goldstone modes. The basic idea of this technique is to shift the energy of the spurious states towards a region of non physical interest for the RPA response. However, we have decided to develop an alternative method based simply on the RPA response function in such a way that it has a very general applicability because it is not subject to the choice of effective operators.

6.2 General Method

The underlying idea of the method we propose is based on the Cauchy's integral formula, that is the integration of an analytic function on a closed contour where the function is bounded. The problem of evaluating contour integrals can be replaced by the algebraic computation of residues at singular points, that is

$$\frac{1}{2\pi i}\oint_C dz f(z) \rightarrow \sum_i \mathrm{Res_i}, \tag{6.1}$$

where the integration path C is chosen in such a way that all poles of the function $f(z)$ lie inside the contour of integration and the notation $\mathrm{Res_i}$ means the residue of the function $f(z)$ corresponding to the pole i. Our method follows the inverse strategy, namely we start with a function $f(z)$ for which we do not know the poles and, as a consequence, the corresponding residues so that we are forced to evaluate the contour integral numerically that is

$$\frac{1}{2\pi i}\oint_C dz f(z) \leftarrow \sum_i \mathrm{Res_i}. \tag{6.2}$$

In what follows we assume that $f(z)$ is an analytic function with real poles(see fig.(6.1)). Our problem is to evaluate one of the poles (marked with # in the Fig.(6.1) and labelled with the letter a) and its residue without knowing the value of the pole itself. To achieve this goal, one can apply the Cauchy's theorem twice using two different contours which, respectively, include or not the pole a.

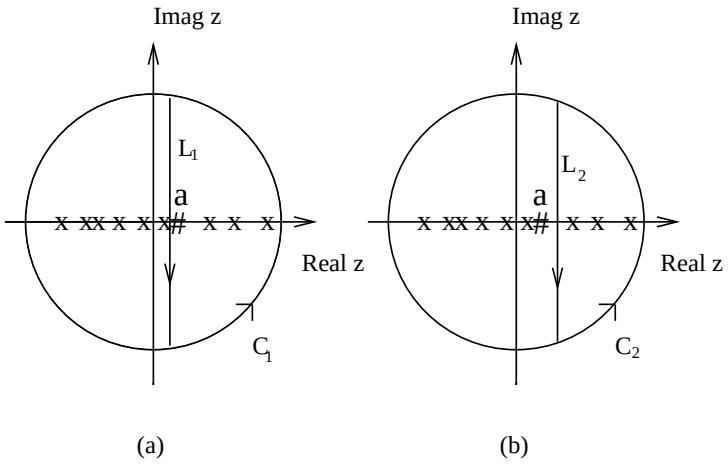

Figure 6.1: Real poles of a generic function $f(z)$. The contour encircles the unknown pole a (b) The contour does not encircle the pole a

We start by explaining our method taking into account the path $C_1 + L_1$ that includes the pole a (see Fig.(6.1(a)). The result of the integration on this path is

$$\frac{1}{2\pi i}\oint_{C_1+L_1} dz f(z) = \sum_{p_+} Res_{p_+}, \tag{6.3}$$

where p_+ means sum over positive poles encircled by the path. We consider now a second path, indicated by $C_2 + L_2$ (see fig.6.1(b)), that excludes the pole a. Cauchy's theorem gives

$$\frac{1}{2\pi i}\oint_{C_2+L_2} dz f(z) = \sum_{p_+} Res_{p_+} - Res_a. \tag{6.4}$$

Subtracting the result of these integrations, one obtain

$$I_a = Res_a = \frac{1}{2\pi i}\oint_{C_1+L_1} dz f(z) - \frac{1}{2\pi i}\oint_{C_2+L_2} dz f(z). \tag{6.5}$$

This last expression allows us to evaluate the residue of the singularity a without knowing its value. The idea is to find an equivalent expression that can be used to calculate the pole itself. This can be done using, as integrand function, *f(z)/z*, that has exactly the same singularity of *f(z)* plus the additional *z=0* pole. Due to the fact that our paths do not pass through zero, *f(z)* and *f(z)/z* have the same singularities. Using this consideration, we do contour integration for the latter function using again the paths $C_1 + L_1$ and $C_2 + L_2$, namely

$$\frac{1}{2\pi i}\oint_{C_1+L_1} dz \frac{f(z)}{z} = \sum_{p_+} \frac{Res_{p_+}}{p_+} \tag{6.6}$$

while

$$\frac{1}{2\pi i}\oint_{C_2+L_2} dz \frac{f(z)}{z} = \sum_{p_+} \frac{Res_{p_+}}{p_+} - \frac{Res_a}{a}. \tag{6.7}$$

Subtracting the two contour integrations, one can write

$$J_a = \frac{Res_a}{a} = \frac{1}{2\pi i}\oint_{C_1+L_1} dz \frac{f(z)}{z} - \frac{1}{2\pi i}\oint_{C_2+L_2} dz \frac{f(z)}{z}. \tag{6.8}$$

At this point we can combine the two results of Eqs.(6.5,6.8) writing

$$a = \frac{I_a}{J_a}. \tag{6.9}$$

This last equation expresses the basis of our method. As can be seen from the right hand side of Eqs.(6.5,6.8), we have to consider contour integrations that cannot be handled numerically, so that we need to transform them into integrals over a real variable. For this purpose we divide the generic contour integration C+L in two different paths, the vertical straight line L which position on the real axis is indicated by b and the arc C (see Fig.(6.2)),

$$\begin{aligned} \frac{1}{2\pi i}\oint_{C+L} dz f(z) &= \frac{1}{2\pi i}\oint_{C} dz f(z) + \frac{1}{2\pi i}\oint_{L} dz f(z), \\ \frac{1}{2\pi i}\oint_{C+L} dz \frac{f(z)}{z} &= \frac{1}{2\pi i}\oint_{C} dz \frac{f(z)}{z} + \frac{1}{2\pi i}\oint_{L} dz \frac{f(z)}{z}. \end{aligned} \tag{6.10}$$

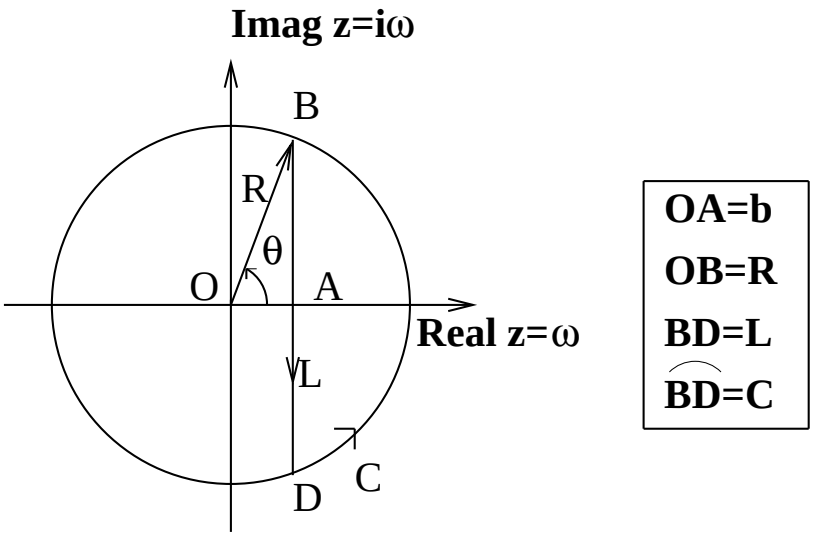

Figure 6.2: Definition of the contour C+L in terms of real variable

It is convenient to change variable in both of the above integrals and, in particular, we define $z = Re^{i\phi}$ with $\lim_{R\to\infty}$ for the arc-integration C and $z = iw + b$ for the line path L. In fact, any point on this line is a complex number with fixed real coordinate b and variable imaginary vertical coordinate $i\omega$. After these substitution we get

$$\frac{1}{2\pi i}\oint_{C+L} dz f(z) = \lim_{R\to\infty}\frac{1}{2\pi i}\int_{-\theta}^{\theta} d\phi i R e^{i\phi} f(Re^{i\phi}) - \lim_{R\to\infty}\frac{1}{2\pi i}\int_{D}^{B} d(i\omega) f(i\omega+b),$$

$$\frac{1}{2\pi i}\oint_{C+L} dz \frac{f(z)}{z} = \lim_{R\to\infty}\frac{1}{2\pi i}\int_{-\theta}^{\theta} d\phi i R e^{i\phi}\frac{f(Re^{i\phi})}{Re^{i\phi}} - \lim_{R\to\infty}\frac{1}{2\pi i}\int_{D}^{B} d(i\omega)\frac{f(i\omega+b)}{i\omega+b}, \tag{6.11}$$

where the minus signs in front of the vertical straight integrals come from the direction of the paths (see arrow in Fig.(6.2)) and the integration limits B and D are defined in Fig.(6.2). Actually, this finite integration becomes an infinite integral due to the $\lim_{R\to\infty}$ so that B can be substituted with $+\infty$ and D with -∞.

The arc-integration has a different behaviour depending on the integrand function but, as we will demonstrate below, its contribution can be neglected. This is simple to show when the integrand function is *f(z)/z* where *f(z)* goes to infinity like $1/z^n$ with $n \geq 1$, because

$$\lim_{R\to\infty}\frac{1}{2\pi i}\int_{-\theta}^{\theta} d\phi i R e^{i\phi}\frac{f(Re^{i\phi})}{Re^{i\phi}} \sim \frac{1}{2\pi i}\lim_{R\to\infty}\int_{-\theta}^{\theta} d\phi \frac{iRe^{i\phi}}{R^2 e^{2i\phi}} = \frac{1}{2\pi}\lim_{R\to\infty}\frac{1}{R}\int_{-\theta}^{\theta} d\phi e^{-i\phi} =$$
$$= \frac{1}{2\pi}\sin\theta \lim_{R\to\infty}\frac{1}{R} \to 0. \tag{6.12}$$

When the integrand function is *f(z)*, the situation is more involved because the arc-integration is different from zero. However, Eq.(6.5) tells us that we have to subtract two integrals $\frac{1}{2\pi i}\oint_{C_1} dz f(z) - \frac{1}{2\pi i}\oint_{C_2} dz f(z)$ and , as we will show below, this difference cancels out. For this purpose we have to take into account the definition of the angle θ (see Fig.(6.2), that is

$$\theta = \arctan\left(\frac{\bar{AB}}{\bar{OA}}\right) \sim \frac{\pi}{2}. \tag{6.13}$$

where the last relation comes from the fact that $R \to \infty$. In fact, in this limit $\bar{AB} \to \infty$ too while $\bar{OA}$ keeps a finite positive value b. As a consequence, the argument of the arctan is infinite and positive, a result which is independent on the choice of C_1 or C_2. This means that the two integrals give the same result and their difference is zero, namely

$$\lim_{R\to\infty}\frac{1}{2\pi i}\int_{-\theta_1}^{\theta_1}d\phi iRe^{i\phi}f(Re^{i\phi})-\lim_{R\to\infty}\frac{1}{2\pi i}\int_{-\theta_2}^{\theta_2}d\phi iRe^{i\phi}f(Re^{i\phi})$$
$$\approx \lim_{R\to\infty}\ \frac{1}{2\pi i}\int_{-\pi/2}^{\pi/2}d\phi iRe^{i\phi}f(Re^{i\phi})-\frac{1}{2\pi i}\int_{-\pi/2}^{\pi/2}d\phi iRe^{i\phi}f(Re^{i\phi})=0. \quad (6.14)$$

Combining these last results we can write down the building blocks of our method, that is

$$\begin{aligned} I_a &= Res_a=\frac{1}{2\pi}\int_{-\infty}^{+\infty}d\omega\left[f(i\omega+b_2)-f(i\omega+b_1)\right], \\ J_a &= \frac{Res_a}{a}=\frac{1}{2\pi}\int_{-\infty}^{+\infty}d\omega\left[\frac{f(i\omega+b_2)}{i\omega+b_2}-\frac{f(i\omega+b_1)}{i\omega+b_1}\right]. \end{aligned} \quad (6.15)$$

We summarise all steps of our technique in the following table

$$\begin{aligned} &\text{step}\quad 1\quad\longrightarrow\quad \text{evaluate}\quad I_a, \\ &\text{step}\quad 2\quad\longrightarrow\quad \text{evaluate}\quad J_a, \\ &\text{step}\quad 3\quad\longrightarrow\quad \text{evaluate}\quad a=\frac{I_a}{J_a}. \end{aligned} \quad (6.16)$$

As one can see from Eq.(6.15) and Fig. (6.1), the success of the method is based on the proper choice of the b value, that is connected with the position of the pole itself. This is not a difficult task in our calculations because the Nambu-Goldstone modes (our unknown poles) are completely isolated from the physical RPA solutions and lie very close to zero. We will show below in the case of ^{168}Yb how it is possible to fix the value of b with good accuracy.

6.3 Sum Rules in Integral Form

Before applying the technique (6.16) to the physical problem of removal of Nambu-Goldstone mode, we want to show that the contour integration is an alternative

method to calculate sum rules, which are useful yardsticks for measuring quantitatively the degree of collectiveness of a given excited state [1, 3, 4, 2].

Let us assume that $\widehat{F}$ is a generic one-body Hermitian operator. We define as sum rule the quantity

$$S_k \equiv \sum_\nu (E_\nu - E_0)^k |\langle \nu|\widehat{F}|0\rangle|^2, \tag{6.17}$$

which represents the k-th moment of the distribution of the excitation strength $|\langle \nu|\widehat{F}|0\rangle|^2$ produced by the operator $\widehat{F}$ and where ν indicates an excited state with energy E_ν. The expression above is straightforward but to evaluate it one needs to have a detailed knowledge of each of the excited states ν. This requirement can be circumvented using the RPA response function and contour integration.

The following description is based on the spectral representation of the linear response given in (2.42) which has the advantage of displaying explicitly the corresponding analytic properties, namely poles at $\pm\omega^\alpha_{\boldsymbol{q}}$ with residues $-\mathcal{Q}^*(\boldsymbol{q})\mathcal{Q}(\boldsymbol{q})$ and $\mathcal{Q}(\boldsymbol{q})\mathcal{Q}^*(\boldsymbol{q})$ respectively. The poles are in number of $\mathbf{q}$. At this point we can apply the Cauchy's integral using $\mathcal{R}^\alpha_{\rho\rho'}(z)$ a first time and $\mathcal{R}^\alpha_{\rho\rho'}(z)/z$ in the second case, that is

$$\begin{aligned}
\frac{1}{2\pi i}\oint_{C_1+L_1} dz \mathcal{R}^\alpha_{\rho\rho'}(z) &= -\sum_{\boldsymbol{q}} \mathcal{Q}^{\alpha\,*}_\rho(\boldsymbol{q})\mathcal{Q}^\alpha_{\rho'}(\boldsymbol{q}), \\
\frac{1}{2\pi i}\oint_{C_1+L_1} dz \frac{\mathcal{R}^\alpha_{\rho\rho'}(z)}{z} &= -\sum_{\boldsymbol{q}} \frac{\mathcal{Q}^{\alpha\,*}_\rho(\boldsymbol{q})\mathcal{Q}^\alpha_{\rho'}(\boldsymbol{q})}{\omega^\lambda_{\boldsymbol{q}}},
\end{aligned} \tag{6.18}$$

where the contour of integration C_1+L_1 should contain all the positive RPA solutions.

Comparing these results with Eq.(6.17) we see that the first integration gives us the $k=0$ moment, called, the *non energy weighted sum rule* (NEWSR), corresponding to the sum of all transition matrix elements between excited states and ground state, while the second one is the *inverse energy weighted sum rule* (IEWSR) corresponding to $k=-1$. This latter one is the sum of the ratio of transition matrix elements and

related excitation energy. To apply numerically this method one has to transform the above contour integrations on a real variable integration. As an example we give the result for the IEWSR, namely

$$\sum_{\boldsymbol{q}} \frac{\mathcal{Q}_{\rho}^{\alpha}{}^{*}(\boldsymbol{q})\mathcal{Q}_{\rho'}^{\alpha}(\boldsymbol{q})}{\omega_{\boldsymbol{q}}^{\lambda}} = \frac{1}{2\pi}\int_{-\infty}^{+\infty} d\omega \frac{\mathcal{R}_{\rho\rho'}^{\alpha}(i\omega + b_1)}{i\omega + b_1}, \tag{6.19}$$

where b_1 is chosen in such a way that all the positive real RPA solutions are encircled by the chosen path, that is $0 < b_1 < \omega_{\boldsymbol{q}}^{1,\alpha}$ where$\omega_{\boldsymbol{q}}^{1,\alpha}$ is the lowest RPA root.

6.4 Rotating Frame

As already explained in Chapter 5, in a rotating frame we are dealing with the problem of removal of Nambu-Goldstone mode from the RPA response function. In particular we have four different spurious states, two in the positive signature sector related to particle number conservation (neutron and proton case separately) and two connected with angular momentum conservation, $\widehat{J}_x$ in the positive part and $\widehat{J}_{\pm}$ in the negative sector of the RPA response. For this reason, we prefer to show how to remove the spurious states separately, starting from the negative signature case.

6.4.1 Negative Signature Sector

We are now dealing with only one Nambu-Goldstone mode so that the RPA response function can be written as

$$\mathcal{R}_{\rho\rho'}^{1\boldsymbol{TOT}}(\omega) = \mathcal{R}_{\rho\rho'}^{1}(\omega) + \mathcal{R}_{\rho\rho'}^{1\boldsymbol{NG}}(\omega), \tag{6.20}$$

where $\mathcal{R}_{\rho\rho'}^{1}(\omega)$ corresponds to physical excitations, as defined in Eq.(2.42), while $\mathcal{R}_{\rho\rho'}^{1\boldsymbol{NG}}(\omega)$ is the contribution of the Nambu-Goldstone mode. In the usual spectral representation, this term can be written as

$$\mathcal{R}_{\rho\rho'}^{1\boldsymbol{NG}}(\omega) = \frac{\mathcal{A}_{\rho\rho'}^{1}(\boldsymbol{NG})}{\omega_{\boldsymbol{NG}}^{(1)} - \omega} + \frac{\mathcal{B}_{\rho\rho'}^{1}(\boldsymbol{NG})}{\omega_{\boldsymbol{NG}}^{(1)} + \omega}, \tag{6.21}$$

where

$$\mathcal{A}_{\rho\rho'}^{1}(\boldsymbol{NG}) = \mathcal{Q}_{\rho}^{1}{}^{*}(\boldsymbol{q})\mathcal{Q}_{\rho'}^{1}(\boldsymbol{q}),$$

$$\mathcal{B}^1_{\rho\rho'}(\boldsymbol{NG}) = \mathcal{Q}^1_\rho(\boldsymbol{q})\mathcal{Q}^{1^*}_{\rho'}(\boldsymbol{q}),$$

(6.22)

are the transition matrix elements of the Nambu-Goldstone mode , that is $\mathbf{q} = \mathbf{NG}$ on the right hand side of the last equations. We have introduced this notation to simplify as much as possible the formulae.

We now apply the method given in Eq.(6.16) using $\mathcal{R}^{1\boldsymbol{TOT}}_{\rho\rho'}(z)$ instead of $f(z)$, that is we consider the following contour integrations

$$\frac{1}{2\pi i}\oint_{C+L} dz\mathcal{R}^{1\boldsymbol{TOT}}_{\rho\rho'}(z) \qquad \text{and} \qquad \frac{1}{2\pi i}\oint_{C+L} dz\frac{\mathcal{R}^{1\boldsymbol{TOT}}_{\rho\rho'}(z)}{z}, \tag{6.23}$$

taking into account that the unknown pole is the energy of the Nambu-Goldstone mode $\omega^{(1)}_{\boldsymbol{NG}}$ with residue $-\mathcal{A}^1_{\rho\rho'}(\boldsymbol{NG})(-\mathcal{A}^1_{\rho\rho'}(\boldsymbol{NG})/\omega^{(1)}_{\boldsymbol{NG}})$ for the function $\mathcal{R}^\alpha_{\rho\rho'}(z)(\mathcal{R}^\alpha_{\rho\rho'}(z)/z)$. Following step 1 and step 2 of (6.16) we obtain

$$\begin{aligned}
I^{1,\boldsymbol{NG}}_{\rho\rho'} &= -\mathcal{A}^1_{\rho\rho'}(\boldsymbol{NG}) = \frac{1}{2\pi i}\oint_{C_1+L_1} dz\mathcal{R}^{1\boldsymbol{TOT}}_{\rho\rho'}(z) - \frac{1}{2\pi i}\oint_{C_2+L_2} dz\mathcal{R}^{1\boldsymbol{TOT}}_{\rho\rho'}(z),\\
J^{1,\boldsymbol{NG}}_{\rho\rho'} &= -\frac{\mathcal{A}^1_{\rho\rho'}(\boldsymbol{NG})}{\omega^{(1)}_{\boldsymbol{NG}}} = \frac{1}{2\pi i}\oint_{C_1+L_1} dz\frac{\mathcal{R}^{1\boldsymbol{TOT}}_{\rho\rho'}(z)}{z} - \frac{1}{2\pi i}\oint_{C_2+L_2} dz\frac{\mathcal{R}^{1\boldsymbol{TOT}}_{\rho\rho'}(z)}{z}.
\end{aligned} \tag{6.24}$$

In real integration variable these relations become

$$\begin{aligned}
I^{1,\boldsymbol{NG}}_{\rho\rho'} &= -\mathcal{A}^1_{\rho\rho'}(\boldsymbol{NG}) = \int_{-\infty}^{+\infty} d\omega\left[\mathcal{R}^{1\boldsymbol{TOT}}_{\rho\rho'}(i\omega+b_2) - \mathcal{R}^{1\boldsymbol{TOT}}_{\rho\rho'}(i\omega+b_1)\right],\\
J^{1,\boldsymbol{NG}}_{\rho\rho'} &= -\frac{\mathcal{A}^1_{\rho\rho'}(\boldsymbol{NG})}{\omega^{(1)}_{\boldsymbol{NG}}} = \int_{-\infty}^{+\infty} d\omega\left[\frac{\mathcal{R}^{1\boldsymbol{TOT}}_{\rho\rho'}(i\omega+b_2)}{i\omega+b_2} - \frac{\mathcal{R}^{1\boldsymbol{TOT}}_{\rho\rho'}(i\omega+b_1)}{i\omega+b_1}\right],
\end{aligned} \tag{6.25}$$

where $0 < b_1 < \omega^{(1)}_{\boldsymbol{NG}} < b_2$. At this point we can evaluate the energy of the Nambu-Goldstone mode using step 3 of Eq.(6.16), namely

$$\omega^{(1)}_{\boldsymbol{NG}} = \frac{I^{1,\boldsymbol{NG}}_{\rho\rho'}}{J^{1,\boldsymbol{NG}}_{\rho\rho'}}, \tag{6.26}$$

From the knowledge of $\mathcal{A}^1_{\rho\rho'}(\boldsymbol{NG})$ we can evaluate $\mathcal{B}^1_{\rho\rho'}(\boldsymbol{NG})$ because they are simply their complex conjugate (see Eq.(6.22)) and, together with $\omega^{(1)}_{\boldsymbol{NG}}$ we can calculate the Nambu-Goldstone response using (6.21). The linear response of the physical solutions is obtained subtracting this contribution from the total one (see (6.20). We have only to remember the multidimensional character of our RPA response function (see Chapter 2) so that we have to repeat this procedure several times running over the index ρ and ρ'.

We want now to show that the above contour integrations correspond to retaining only the Nambu-Goldstone part of the response as integrand function. In fact, introducing Eq.(6.20) in the Cauchy's integrals, we obtain

$$\begin{aligned}
\mathcal{A}^1_{\rho\rho'}(\boldsymbol{NG}) &= \frac{1}{2\pi i}\oint_{C_2+L_2} dz \mathcal{R}^1_{\rho\rho'}(z) - \frac{1}{2\pi i}\oint_{C_1+L_1} dz \mathcal{R}^1_{\rho\rho'}(z) + \\
&+ \frac{1}{2\pi i}\oint_{C_2+L_2} dz \mathcal{R}^{1\,\boldsymbol{NG}}_{\rho\rho'}(z) - \frac{1}{2\pi i}\oint_{C_1+L_1} dz \mathcal{R}^{1\,\boldsymbol{NG}}_{\rho\rho'}(z),
\end{aligned} \tag{6.27}$$

for the first type and

$$\begin{aligned}
\frac{\mathcal{A}^1_{\rho\rho'}(\boldsymbol{NG})}{\omega^{(1)}_{\boldsymbol{NG}}} &= \frac{1}{2\pi i}\oint_{C_2+L_2} dz \frac{\mathcal{R}^1_{\rho\rho'}(z)}{z} - \frac{1}{2\pi i}\oint_{C_1+L_1} dz \frac{\mathcal{R}^1_{\rho\rho'}(z)}{z} + \\
&+ \frac{1}{2\pi i}\oint_{C_2+L_2} dz \frac{\mathcal{R}^{1\,\boldsymbol{NG}}_{\rho\rho'}(z)}{z} - \frac{1}{2\pi i}\oint_{C_1+L_1} dz \frac{\mathcal{R}^{1\,\boldsymbol{NG}}_{\rho\rho'}(z)}{z}.
\end{aligned} \tag{6.28}$$

for the second one. The integrals containing $\mathcal{R}^1_{\rho\rho'}(z)(\mathcal{R}^1_{\rho\rho'}(z)/z)$ give the same result independently on the paths $C_1 + L_1$ and $C_2 + L_2$ because the number of poles is the same in both contours. The integrals containing the Nambu-Goldstone part behave in a different way because the chosen paths may contain$(C_1 + L_1)$ or not$(C_2 + L_2)$ the Nambu-Goldstone modes. In particular, the path $C_2 + L_2$ does not contain the

Nambu-Goldstone mode so that the corresponding contour integrals are zero. We can finally write that

$$\begin{aligned} \mathcal{A}^1_{\rho\rho'}(\boldsymbol{NG}) &= -\frac{1}{2\pi i}\oint_{C_1+L_1} dz \mathcal{R}^{1\,\boldsymbol{NG}}_{\rho\rho'}(z), \\ \frac{\mathcal{A}^1_{\rho\rho'}(\boldsymbol{NG})}{\omega^{(1)}_{\boldsymbol{NG}}} &= -\frac{1}{2\pi i}\oint_{C_1+L_1} dz \frac{\mathcal{R}^{1\,\boldsymbol{NG}}_{\rho\rho'}(z)}{z}. \end{aligned} \tag{6.29}$$

This is not a surprising result if one remembers the analytic character of the response function. In the particular case of the Nambu-Goldstone response this function has only one pole $\omega^{(1)}_{\boldsymbol{NG}}$ that lies inside the path $C_1 + L_1$ so that the above result expresses simply the Cauchy's integral theorem applied directly to the spurious state response. The main problem is that, at the RPA level, we do not know this function but only the total one given in Eq.(6.20).

6.4.2 Positive Signature Sector

This case is numerically more involved because we have, as explained at the beginning of the section, three different Nambu-Goldstone modes. The complication will result only in a increased number of proper contour integrations, that is we have to find four different contours chosen in such a way that, moving the vertical straight line from left to right at each path, we loose one of the Nambu-Goldstone mode. To be precise we take the first path $C_1 + L_1$ including all poles, the second one is $C_2 + L_2$ that does not contain the first singularity, $C_3 + L_3$ excludes the second spurious state and, finally $C_4 + L_4$ contains only the real physical solutions (see fig.(6.4.2).

The total response function in this case can be written now has

$$\mathcal{R}^{0\,\boldsymbol{TOT}}_{\rho\rho'}(\omega) = \mathcal{R}^0_{\rho\rho'}(\omega) + \sum_j \mathcal{R}^{0\,\boldsymbol{NG},\boldsymbol{j}}_{\rho\rho'}(\omega), \tag{6.30}$$

with

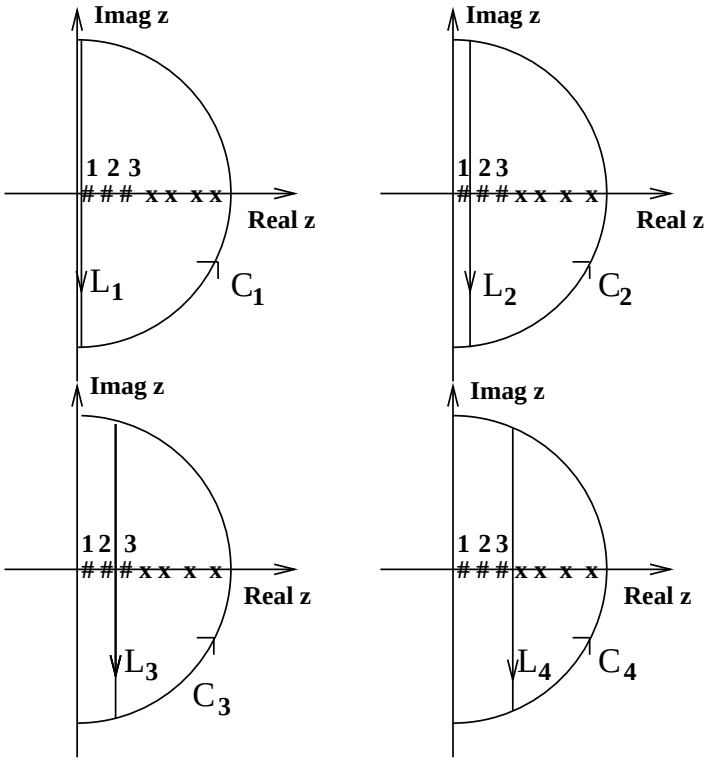

Figure 6.3: The four different contour integrations for the positive signature sector Nambu-Goldstone modes. The symbol # is used for the spurious states and X for the physical solutions

$$\mathcal{R}^{0\,\boldsymbol{NG},\boldsymbol{j}}_{\rho\rho'}(\omega) = \frac{\mathcal{A}^{0,j}_{\rho\rho'}(\boldsymbol{NG})}{\omega^{(0,j)}_{\boldsymbol{NG}} - \omega} + \frac{\mathcal{B}^{0,j}_{\rho\rho'}(\boldsymbol{NG})}{\omega^{(0,j)}_{\boldsymbol{NG}} + \omega}. \tag{6.31}$$

The index j runs over the three Nambu-Goldstone modes corresponding to breaking of gauge-symmtery (neutron and proton case) and rotational invariance. At this point we follow exactly the same method of Eq.(6.16), applied already in the negative signature sector, to look for the three energies corresponding to the spurious states, $\omega^{(j)}_{\boldsymbol{NG}}$, j=1,2,3, where we choose, for convenience, $\omega^{(0,1)}_{\boldsymbol{NG}} < \omega^{(0,2)}_{\boldsymbol{NG}} < \omega^{(0,3)}_{\boldsymbol{NG}}$. In this way $\omega^{(1)}_{\boldsymbol{NG}}$ is packed between the two straight lines L_1 and L_2, $\omega^{(2)}_{\boldsymbol{NG}}$ is inside L_2 and L_3 and so on. Before going on, we would like to comment on the above notation, that is the meaning of the the index j=1,2,3. This label simply enumerates our spurious states without identifying them, that is we do not know to which Nambu-Goldstone mode corresponds, for example, the index *j=1*. We only know that they are real, positive

and very close to zero. Using the four distinct paths, we can write that

$$\begin{aligned}
\mathcal{A}^{0,1}_{\rho\rho'}(\boldsymbol{NG}) &= \frac{1}{2\pi i}\oint_{C_2+L_2} dz \mathcal{R}^{0\boldsymbol{TOT}}_{\rho\rho'}(z) - \frac{1}{2\pi i}\oint_{C_1+L_1} dz \mathcal{R}^{0\boldsymbol{TOT}}_{\rho\rho'}(z), \\
\mathcal{A}^{0,2}_{\rho\rho'}(\boldsymbol{NG}) &= \frac{1}{2\pi i}\oint_{C_3+L_3} dz \mathcal{R}^{0\boldsymbol{TOT}}_{\rho\rho'}(z) - \frac{1}{2\pi i}\oint_{C_2+L_2} dz \mathcal{R}^{0\boldsymbol{TOT}}_{\rho\rho'}(z), \\
\mathcal{A}^{0,3}_{\rho\rho'}(\boldsymbol{NG}) &= \frac{1}{2\pi i}\oint_{C_4+L_4} dz \mathcal{R}^{0\boldsymbol{TOT}}_{\rho\rho'}(z) - \frac{1}{2\pi i}\oint_{C_3+L_3} dz \mathcal{R}^{0\boldsymbol{TOT}}_{\rho\rho'}(z),
\end{aligned} \tag{6.32}$$

for the transition matrix elements (that is the residues)and

$$\begin{aligned}
\frac{\mathcal{A}^{0,1}_{\rho\rho'}(\boldsymbol{NG})}{\omega^{(0,1)}_{\boldsymbol{NG}}} &= \frac{1}{2\pi i}\oint_{C_2+L_2} dz \frac{\mathcal{R}^{0\boldsymbol{TOT}}_{\rho\rho'}(z)}{z} - \frac{1}{2\pi i}\oint_{C_1+L_1} dz \frac{\mathcal{R}^{0\boldsymbol{TOT}}_{\rho\rho'}(z)}{z}, \\
\frac{\mathcal{A}^{0,2}_{\rho\rho'}(\boldsymbol{NG})}{\omega^{(0,2)}_{\boldsymbol{NG}}} &= \frac{1}{2\pi i}\oint_{C_3+L_3} dz \frac{\mathcal{R}^{0\boldsymbol{TOT}}_{\rho\rho'}(z)}{z} - \frac{1}{2\pi i}\oint_{C_2+L_2} dz \frac{\mathcal{R}^{0\boldsymbol{TOT}}_{\rho\rho'}(z)}{z}, \\
\frac{\mathcal{A}^{0,3}_{\rho\rho'}(\boldsymbol{NG})}{\omega^{(0,3)}_{\boldsymbol{NG}}} &= \frac{1}{2\pi i}\oint_{C_4+L_4} dz \frac{\mathcal{R}^{0\boldsymbol{TOT}}_{\rho\rho'}(z)}{z} - \frac{1}{2\pi i}\oint_{C_3+L_3} dz \frac{\mathcal{R}^{0\boldsymbol{TOT}}_{\rho\rho'}(z)}{z},
\end{aligned} \tag{6.33}$$

for the ratio of the transition matrix elements and energies (namely the contribution of the different Nambu Goldstone mode to the IEWSR sum rule). Even in this case we need to translate all the contour integrations in real integrals as

$$\begin{aligned}
\mathcal{A}^{0,1}_{\rho\rho'}(\boldsymbol{NG}) &= \frac{1}{2\pi}\int_{-\infty}^{+\infty} d\omega \left[\mathcal{R}^{0\boldsymbol{TOT}}_{\rho\rho'}(i\omega+b_1) - \mathcal{R}^{0\boldsymbol{TOT}}_{\rho\rho'}(i\omega+b_2)\right], \\
\mathcal{A}^{0,2}_{\rho\rho'}(\boldsymbol{NG}) &= \frac{1}{2\pi}\int_{-\infty}^{+\infty} d\omega \left[\mathcal{R}^{0\boldsymbol{TOT}}_{\rho\rho'}(i\omega+b_2) - \mathcal{R}^{0\boldsymbol{TOT}}_{\rho\rho'}(i\omega+b_3)\right], \\
\mathcal{A}^{0,3}_{\rho\rho'}(\boldsymbol{NG}) &= \frac{1}{2\pi}\int_{-\infty}^{+\infty} d\omega \left[\mathcal{R}^{0\boldsymbol{TOT}}_{\rho\rho'}(i\omega+b_3) - \mathcal{R}^{0\boldsymbol{TOT}}_{\rho\rho'}(i\omega+b_4)\right],
\end{aligned}$$

$$
\begin{aligned}
\frac{\mathcal{A}^{0,1}_{\rho\rho'}(\boldsymbol{NG})}{\omega^{(0,1)}_{\boldsymbol{NG}}} &= \frac{1}{2\pi}\int_{-\infty}^{+\infty} d\omega \left[\frac{\mathcal{R}^{0\boldsymbol{TOT}}_{\rho\rho'}(i\omega+b_1)}{i\omega+b_1} - \frac{\mathcal{R}^{0\boldsymbol{TOT}}_{\rho\rho'}(i\omega+b_2)}{i\omega+b_2}\right], \\
\frac{\mathcal{A}^{0,2}_{\rho\rho'}(\boldsymbol{NG})}{\omega^{(0,2)}_{\boldsymbol{NG}}} &= \frac{1}{2\pi}\int_{-\infty}^{+\infty} d\omega \left[\frac{\mathcal{R}^{0\boldsymbol{TOT}}_{\rho\rho'}(i\omega+b_2)}{i\omega+b_2} - \frac{\mathcal{R}^{0\boldsymbol{TOT}}_{\rho\rho'}(i\omega+b_3)}{i\omega+b_3}\right], \\
\frac{\mathcal{A}^{0,3}_{\rho\rho'}(\boldsymbol{NG})}{\omega^{(0,3)}_{\boldsymbol{NG}}} &= \frac{1}{2\pi}\int_{-\infty}^{+\infty} d\omega \left[\frac{\mathcal{R}^{0\boldsymbol{TOT}}_{\rho\rho'}(i\omega+b_3)}{i\omega+b_3} - \frac{\mathcal{R}^{0\boldsymbol{TOT}}_{\rho\rho'}(i\omega+b_4)}{i\omega+b_4}\right],
\end{aligned}
\tag{6.34}
$$

where $0 < b_1 < \omega^{(0,1)}_{\boldsymbol{NG}} < b_2 < \omega^{(0,2)}_{\boldsymbol{NG}} < b_3 < \omega^{(0,3)}_{\boldsymbol{NG}} < b_4$. As done before in the negative signature part, these integrals can be transformed in the Cauchy's integrals corresponding only to the Nambu- Goldstone part of the response function (see Appendix B).

6.5 Illustration

We are going to show how to apply the above mentioned method to a realistic case, that is the study of the broken symmetries in a deformed superfluid nucleus as ^{168}Yb where the deformation breaks the rotational invariance while the pairing wave function describes a non-conserving number state. We start showing the RPA response function in Fig.(6.4) for the components of the quadrupole operator describing the collective vibrations of a deformed nucleus, that is β- and γ- vibrations. The former one corresponds to an oscillation of the surface along the symmetry axis, that is an oscillation of the deformation parameter preserving cylindrical symmetry, while the latter describes the transverse vibrational motion of the surface to the symmetry axis. In this last case we have violation of the cylindrical symmetry. This means that the quantum numbers for these modes are $K = 0$ for the β- and $K = \pm 2$ for γ- vibration,respectively. The components $K = \pm 1$ correspond to a rotation around the symmetry axis leaving the intrinsic structure of the system unchanged. For this reason the β- and γ- vibration are called intrinsic states upon which rotational bands

can be built. If the intrinsic state has spin different from zero, the rotational band built on that state will have the sequence of spin $I, I+1, I+2, \cdots$.

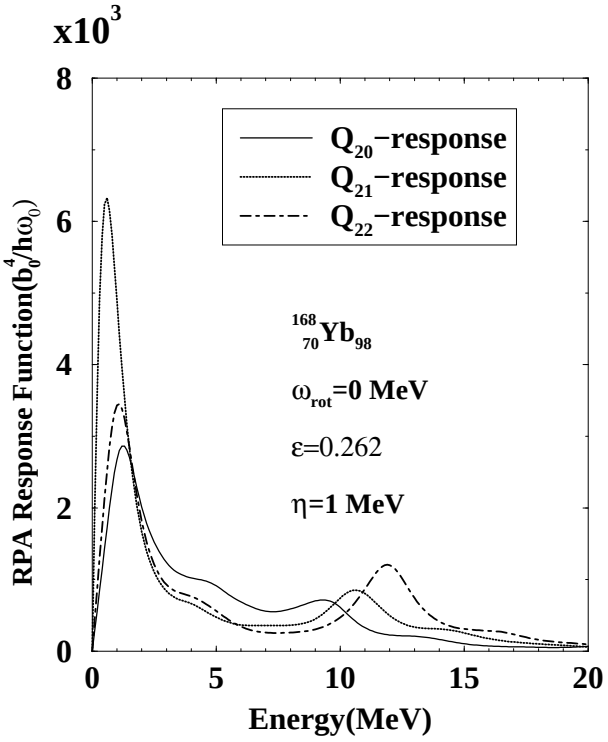

Figure 6.4: Quadrupole RPA response function for ^{168}Yb at $\omega_{\rm rot} = 0$ MeV with averaging parameter $\eta = 1$ MeV. $b_0^2 = \hbar/M\omega_0$ with $\hbar\omega_0$=41.0A^{-}1/3 MeV.

The low-lying peak in $\widetilde{Q}_{21}$ represents the spurious contribution to the linear response function of the Nambu-Goldstone mode. One can be tempted to subtract its contribution fitting the RPA response function in the low-lying region. This can be very wrong because the tail of the Nambu-Goldstone contribution can contain physical solutions. One can understand this looking at the Fig.(6.5) where the $\widetilde{Q}_{21}$ response is plotted for different values of the average parameters η.

Already at $\eta = 0.5$ MeV (case (b) of Fig.(6.5)) one is able to resolve one of the physical solutions in the low-lying region that it was completely hidden in case (a) of the same figure where η=1 MeV. Moreover the position of the peak moves towards zero with an increasing divergent value of the response function. This is connected

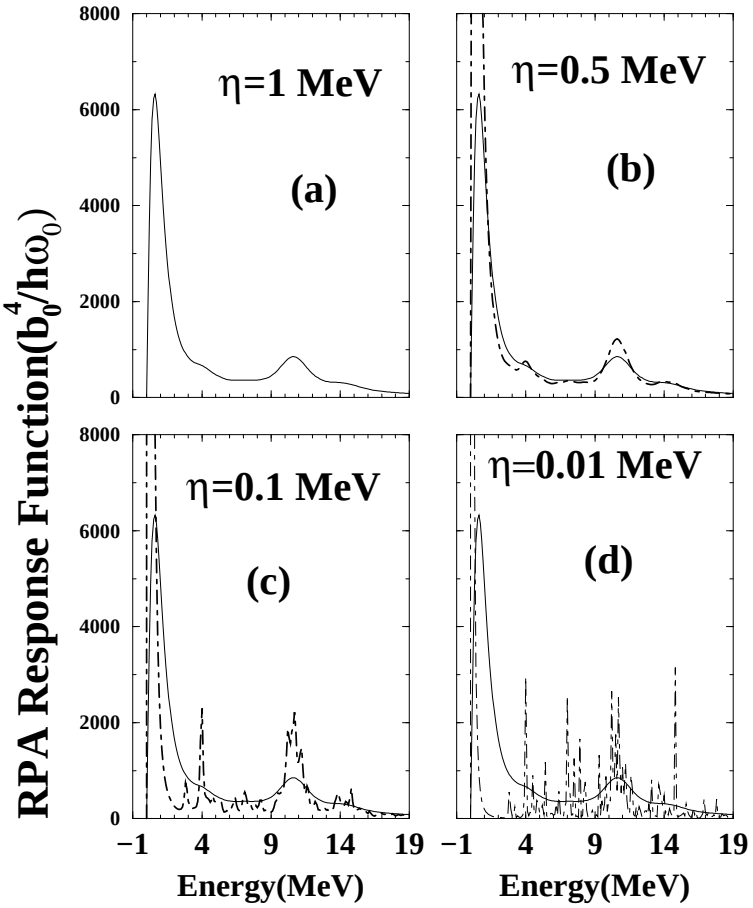

Figure 6.5: RPA response function at $\omega_{\rm rot} = 0$ MeV as a function of the average parameter η. Graph (a) corresponds to η=1 MeV, in (b) η=0.5 MeV was used while for case (c) and (d) η is 0.1 MeV and 0.01 MeV, respectively. See Caption of Fig.(6.4) for units definition.

with the fact that the transition matrix element between ground and excited states of the zero-energy solution has an infinite value. The situation becomes much more complicated decreasing furthermore the value of η (see case (d)) where an increased number of physical solutions are now visible in the low-energy region. This means that one should be aware to subtract or move toward higher energy region the Nambu-Goldstone response contribution without been completely sure that RPA solutions are not contained in it. First of all one has to localize with good precision the position of the spurious state and, as we have seen above, this depends on the averaging parameter chosen. One can plot the response function using a zero value for η because, in this limit, the RPA solutions and the Nambu-Goldstone energy are not $\eta-$depending. Moreover, due to the fact that each RPA solution is a pole for the RPA response function (see spectral representation given in Eq.(2)), one will have a

divergent singularity in the RPA response plot in correspondence of a pole. This is shown in Fig.(6.6), where we draw a small region around zero of the RPA response functions corresponding to rotational and gauge broken symmetries. The energy step used to evaluate these functions was 1 eV.

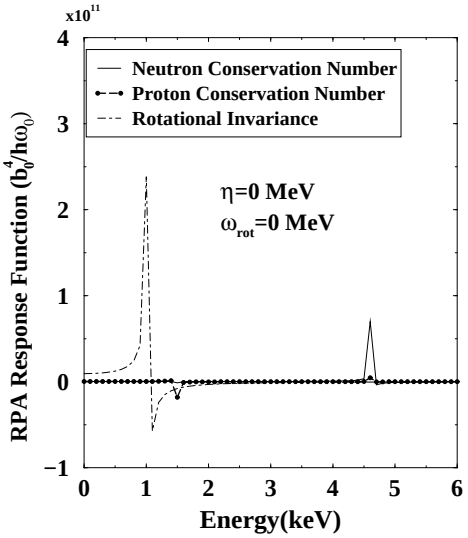

Figure 6.6: RPA response functions at $\omega_{\rm rot} = 0$ MeV with $\eta = 0$ MeV corresponding to rotational and gauge broken symmetries. See Caption of Fig.(6.4) for units definition.

We see from the Fig.(6.6) that, below 6 keV, there are three singularities well recognisable but it is not possible to extract graphically the exact value of their energy. We can only identify with absolute certainty the energy intervals in which they lie. For example, the Nambu-Goldstone mode associated with rotational broken symmetry is inside the interval $(0 - 1.3)$ keV while the neutron- and proton-gauge invariance are in the regions $(4 - 5)$ keV and $(1.3 - 2)$ keV respectively. This is enough to apply our method because these three different intervals allow us to choose the parameters b's used in the integration procedure, see Eqs.(6.34). As one can see, we have infinite possibilities for the choices of the b's values because any number contained, for example, in the interval $(0 - 1.3)$ keV can be selected to evaluate the first Nambu-Goldstone mode while we can pick up any value from $(4 - 5)$ keV for the second one and so on. The result does not depend on which specific value of b one decides to

use but, of course, on the interval in which is chosen because, as explained above, the b's values define the paths of integration. After evaluating the energies and matrix elements corresponding to the Nambu-Goldstone modes, one can subtract the RPA contribution to obtain the physical one. We give the result of this subtraction in Fig.(6.7).

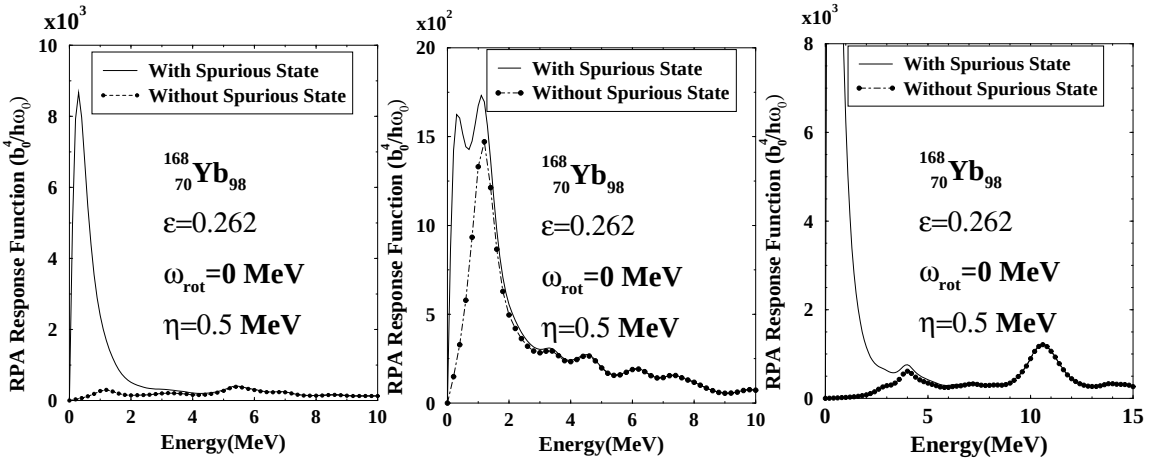

Figure 6.7: Removal of the Nambu-Goldstone modes from the RPA response function corresponding to broken neutron- and proton-gauge invariance (left and middle side, respectively), and rotational symmetry (right side). See Caption of Fig.(6.4) for units definition.

As one can notice in the proton case (middle case of the Fig.(6.7), the low-energy region still presents a quite consistent contribution to the RPA response function nevertheless we have performed the removal of the Nambu-Goldstone mode. This is due to the fact the some physical solutions of the RPA equations are concentrated in that region and cannot be removed from it. We shall now analyze the nature of these RPA roots contributing to the proton response function. For this purpose we compare the proton RPA response function after subtraction of the spurious state in the range $(0-5)$ MeV using $\eta = 0.5$ MeV (as in the middle graph of Fig.(6.7) and the β- and γ- responses evaluated using a very small value of the averaging parameter, that is $\eta = 0.001$ keV. The reason for this choice is that we can resolve graphically the RPA solutions and notice (see Fig.(6.8)) that the peak is nothing more that the

contribution of the β- and γ-vibration to the proton response.

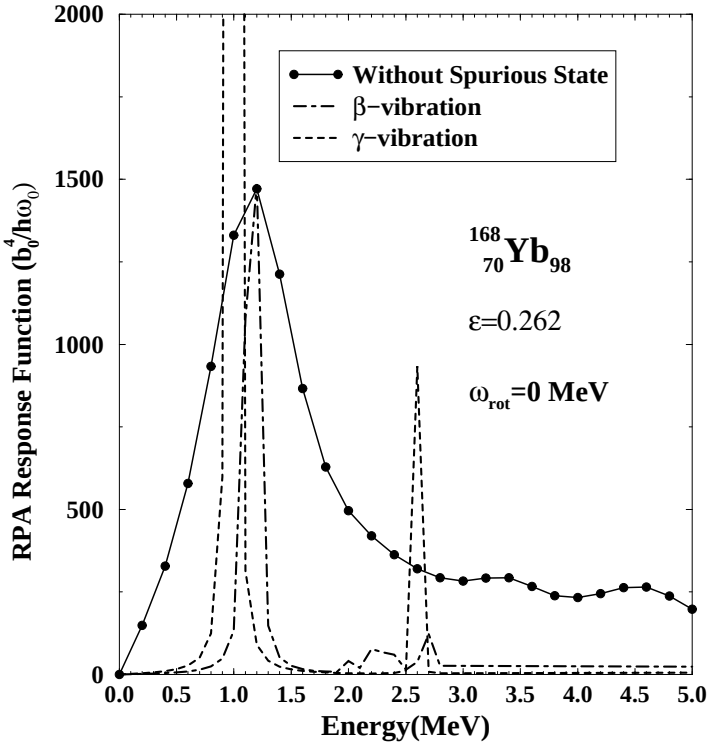

Figure 6.8: Nature of the low-lying region of the proton response function after removal of the Nambu-Goldstone modes. The RPA solutions greater that 3 MeV are not drawn for convenience to have a neat picture. See Caption of Fig.(6.4) for units definition.

Chapter 7

Imaginary Nambu-Goldstone Modes

7.1 Introduction

The scenario that we usually encounter in the treatment of the Nambu Goldstone modes is the one that we have depicted in the last Chapter, that is the spurious states corresponding to the restoration of the broken symmetries in the RPA framework are real and very close to zero. This is possible when $\omega_{\mathrm{rot}} = 0$ because we can choose the value of the coupling strengths $\chi^{\alpha}_{\rho\rho'}$(see Chapter 2) to reproduce this situation, that is we can fix them to have good agreement with the experimental values of the β- and γ- vibrations and to push the energies of the Nambu-Goldstone modes at zero energy. These coupling strengths are kept constant as a function of rotation so that when our system starts to rotate we don't have anymore control on the value of the Nambu Goldstone energies. This means that these modes not only can mix with the physical solutions, but they can become complex (because the RPA equations can have in general complex solutions). While the former case can be solved using the same method developed in Chapter 6 keeping more attention to the choice of the integration paths, the latter case needs a separate treatment that involves again contour integration.

7.2 Imaginary poles

As we have done before, we start with a generic function *f(z)* with two different kind of poles, real and purely imaginary (Fig.(7.1)).

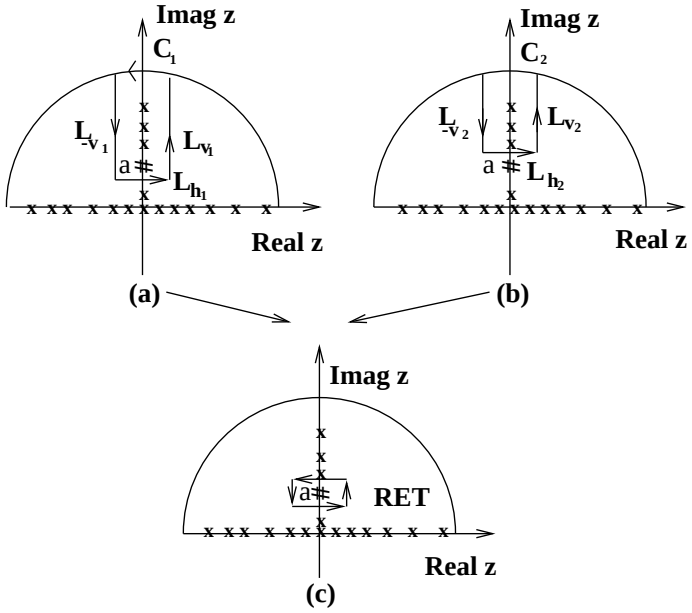

Figure 7.1: Imaginary poles of a generic function f.(a) The contour encircles the unknown pole a (b) The contour does not encircle the pole a (c) Difference between path a and b

Using Cauchy's theorem we can write

$$\frac{1}{2\pi i}\oint_{C_1+L_{v1}+L_{-v1}+L_{h1}} dzf(z) \rightarrow \sum_{i_+} Res_{i_+}, \tag{7.1}$$

where i_+ means positive imaginary poles contained in the contour path $C_1 + L_{v1} + L_{-v1} + L_{h1}$ (see Fig.(7.1)). If one wants to evaluate the pole marked with a needs to proceed exactly in the same way of Chapter 6 but choosing paths on the upper half part of the complex plane. Choosing a second path that does not contain the imaginary pole, we can write, analogously to the real case, that

$$I_a \quad = \quad Res_a = \frac{1}{2\pi i}\oint_{C_1+L_{v1}+L_{-v1}+L_{h1}} dzf(z) - \frac{1}{2\pi i}\oint_{C_2+L_{v2}+L_{-v2}+L_{h2}} dzf(z),$$

$$J_a = \frac{Res_a}{a} = \frac{1}{2\pi i}\oint_{C_1+L_{v1}+L_{-v1}+L_{h1}} dz\frac{f(z)}{z} - \frac{1}{2\pi i}\oint_{C_2+L_{v2}+L_{-v2}+L_{h2}} dz\frac{f(z)}{z}. \tag{7.2}$$

In this particular case, all the calculations can be greatly simplified if we move only the horizontal lines when choosing the contour paths. This implies that the two arcs C_1 and C_2 actually coincide and the difference between the contours transforms in a rectangular contour integration encircling the pole(see Fig.(7.2)).

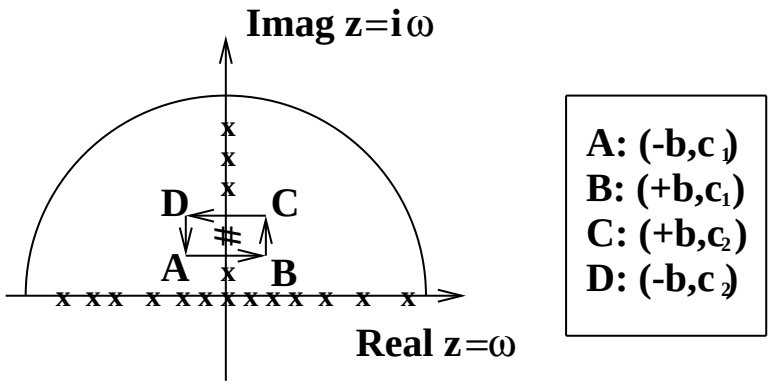

Figure 7.2: Contour integration for an imaginary pole in terms of real variable

Using the notation of this figure, we can write the final result in terms of real variable integrals, that is

$$I_a = Res_a = \frac{1}{2\pi}\int_{c_1}^{c_2} d\omega\,[f(i\omega+b) - f(i\omega-b)] + \frac{1}{2\pi i}\int_{-b}^{b} d\omega\,[f(\omega+ic_1) - f(\omega+ic_2]\,,$$

$$J_a = \frac{Res_a}{a} = \frac{1}{2\pi}\int_{c_1}^{c_2} d\omega\left[\frac{f(i\omega+b)}{i\omega+b} - \frac{f(i\omega-b)}{i\omega-b}\right] + \frac{1}{2\pi i}\int_{-b}^{b} d\omega\left[\frac{f(\omega+ic_1)}{\omega+ic_1} - \frac{f(\omega+ic_2)}{\omega+ic_2}\right], \tag{7.3}$$

where in performing the integrals along the vertical we have used the substitution $z \to i\omega + b$ while for that along the horizontal the variable becomes $z \to \omega + ic$.

7.3 Rotating Frame

We now discuss the two cases of positive and negative signature separately, taking into account the different number of Nambu-Goldstone modes present in each sector. The choice of paths follows exactly the same reasonings of the previous Chapter so we give directly the results without discussing them further. However, it is necessary to point out that in real situations, as we will see in next Chapters, there will be a coexistence of real and purely imaginary Nambu-Goldstone modes, so that one needs to use both methods.

7.3.1 Negative Signature Sector

Similarly to the case of real solutions (see Chapter 6), we can divide the linear response function in two terms corresponding, respectively, to the physical solutions and the purely imaginary Nambu-Goldstone mode, namely

$$\mathcal{R}^{1\,\mathbf{TOT}}_{\rho\rho'}(\omega) = \mathcal{R}^{1}_{\rho\rho'}(\omega) + \mathcal{R}^{1\,\mathbf{NG}}_{\rho\rho'}(\omega), \tag{7.4}$$

where

$$\mathcal{R}^{1\,\mathbf{NG}}_{\rho\rho'}(\omega) = \frac{\mathcal{A}^{1}_{\rho\rho'}(\boldsymbol{NG})}{i\omega^{(1)}_{\boldsymbol{NG}} - \omega} + \frac{\mathcal{B}^{1}_{\rho\rho'}(\boldsymbol{NG})}{i\omega^{(1)}_{\boldsymbol{NG}} + \omega}, \tag{7.5}$$

is the contribution of the spurious state $i\omega^{(1)}_{\boldsymbol{NG}}$. The notation is the same as the last Chapter so we refer to it for details. After choosing the two paths as in Fig.(7.1) and transforming the contour integrations in real one, we obtain

$$\begin{aligned} I^{1,\boldsymbol{NG}}_{\rho\rho'} &= -\mathcal{A}^{1}_{\rho\rho'}(\boldsymbol{NG}) = \frac{1}{2\pi}\int_{c_2}^{c_1} d\omega \left[\mathcal{R}^{1\,\mathbf{TOT}}_{\rho\rho'}(i\omega + b) - \mathcal{R}^{1\,\mathbf{TOT}}_{\rho\rho'}(i\omega - b)\right] + \\ &+ \frac{1}{2\pi i}\int_{-b}^{b} d\left[\mathcal{R}^{1\,\mathbf{TOT}}_{\rho\rho'}(\omega + ic_1) - \mathcal{R}^{1\,\mathbf{TOT}}_{\rho\rho'}(\omega + ic_2)\right], \end{aligned}$$

$$\begin{aligned} J^{1,\boldsymbol{NG}}_{\rho\rho'} &= -\frac{\mathcal{A}^{1}_{\rho\rho'}(\boldsymbol{NG})}{i\omega^{(1)}_{\boldsymbol{NG}}} = \frac{1}{2\pi}\int_{c_2}^{c_1} d\omega \left[\frac{\mathcal{R}^{1\,\mathbf{TOT}}_{\rho\rho'}(i\omega + b)}{i\omega + b} - \frac{\mathcal{R}^{1\,\mathbf{TOT}}_{\rho\rho'}(i\omega - b)}{i\omega - b}\right] + \\ &+ \frac{1}{2\pi i}\int_{-b}^{b} d\left[\frac{\mathcal{R}^{1\,\mathbf{TOT}}_{\rho\rho'}(\omega + ic_1)}{\omega + ic_1} - \frac{\mathcal{R}^{1\,\mathbf{TOT}}_{\rho\rho'}(\omega + ic_2)}{\omega + ic_2}\right], \end{aligned}$$

(7.6)

as the positive pole in this case is $i\omega^{(1)}_{\boldsymbol{NG}}$ with residue $-\mathcal{A}^1_{\rho\rho'}(\boldsymbol{NG})$. At this point we can evaluate the energy of the Nambu-Goldstone mode using step 3 of (6.16), namely

$$i\omega^{(1)}_{\boldsymbol{NG}} = \frac{I^{1,\boldsymbol{NG}}_{\rho\rho'}}{J^{1,\boldsymbol{NG}}_{\rho\rho'}}, \tag{7.7}$$

7.3.2 Positive Signature

In this sector there is the possibility to have three purely imaginary Nambu-Goldstone modes. The total response function looks like

$$\mathcal{R}^{0\,\mathbf{TOT}}_{\rho\rho'}(\omega) = \mathcal{R}^0_{\rho\rho'}(\omega) + \sum_j \mathcal{R}^{0\,\mathbf{NG,j}}_{\rho\rho'}(\omega), \tag{7.8}$$

with

$$\mathcal{R}^{0\,\mathbf{NG,j}}_{\rho\rho'}(\omega) = \frac{\mathcal{A}^{0,j}_{\rho\rho'}(\boldsymbol{NG})}{i\omega^{(0,j)}_{\boldsymbol{NG}} - \omega} + \frac{\mathcal{B}^{0,j}_{\rho\rho'}(\boldsymbol{NG})}{i\omega^{(0,j)}_{\boldsymbol{NG}} + \omega}. \tag{7.9}$$

To evaluate the three purely imaginary energies we need four different paths, as in the real case, chosen with the same criterion. For this reason we don't enter in details and we give immediately the conclusions

$$\begin{aligned}
\mathcal{A}^{0,1}_{\rho\rho'}(\boldsymbol{NG}) &= \frac{1}{2\pi}\int_{c_2}^{c_1} d\omega \left[\mathcal{R}^{0\,\mathbf{TOT}}_{\rho\rho'}(i\omega - b) - \mathcal{R}^{0\,\mathbf{TOT}}_{\rho\rho'}(i\omega + b)\right] + \\
&+ \frac{1}{2\pi i}\int_{-b}^{b} d\omega \left[\mathcal{R}^{0\,\mathbf{TOT}}_{\rho\rho'}(\omega + ic_2) - \mathcal{R}^{0\,\mathbf{TOT}}_{\rho\rho'}(\omega + ic_1)\right], \\
\mathcal{A}^{0,2}_{\rho\rho'}(\boldsymbol{NG}) &= \frac{1}{2\pi}\int_{c_2}^{c_1} d\omega \left[\mathcal{R}^{0\,\mathbf{TOT}}_{\rho\rho'}(i\omega - b) - \mathcal{R}^{0\,\mathbf{TOT}}_{\rho\rho'}(i\omega + b)\right] + \\
&+ \frac{1}{2\pi i}\int_{-b}^{b} d\omega \left[\mathcal{R}^{0\,\mathbf{TOT}}_{\rho\rho'}(\omega + ic_2) - \mathcal{R}^{0\,\mathbf{TOT}}_{\rho\rho'}(\omega + ic_1)\right], \\
\mathcal{A}^{0,3}_{\rho\rho'}(\boldsymbol{NG}) &= \frac{1}{2\pi}\int_{c_2}^{c_1} d\omega \left[\mathcal{R}^{0\,\mathbf{TOT}}_{\rho\rho'}(i\omega - b) - \mathcal{R}^{0\,\mathbf{TOT}}_{\rho\rho'}(i\omega + b)\right] +
\end{aligned}$$

$$
\begin{aligned}
&+ \quad \frac{1}{2\pi i}\int_{-b}^{b} d\left[\mathcal{R}^{0\,\mathbf{TOT}}_{\rho\rho'}(\omega+ic_2)-\mathcal{R}^{0\,\mathbf{TOT}}_{\rho\rho'}(\omega+ic_1)\right],\\
\frac{\mathcal{A}^{0,1}_{\rho\rho'}(\boldsymbol{NG})}{i\omega^{(0,1)}_{\boldsymbol{NG}}} &= \frac{1}{2\pi}\int_{c_2}^{c_1} d\omega\left[\frac{\mathcal{R}^{0\,\mathbf{TOT}}_{\rho\rho'}(i\omega-b)}{i\omega-b}-\frac{\mathcal{R}^{0\,\mathbf{TOT}}_{\rho\rho'}(i\omega+b)}{i\omega+b}\right]+\\
&+ \quad \frac{1}{2\pi i}\int_{-b}^{b} d\omega\left[\frac{\mathcal{R}^{0\,\mathbf{TOT}}_{\rho\rho'}(\omega+ic_2)}{\omega+ic_2}-\frac{\mathcal{R}^{0\,\mathbf{TOT}}_{\rho\rho'}(\omega+ic_1)}{\omega+ic_1}\right],\\
\frac{\mathcal{A}^{0,2}_{\rho\rho'}(\boldsymbol{NG})}{i\omega^{(0,2)}_{\boldsymbol{NG}}} &= \frac{1}{2\pi}\int_{c_2}^{c_1} d\omega\left[\frac{\mathcal{R}^{0\,\mathbf{TOT}}_{\rho\rho'}(i\omega-b)}{i\omega-b}-\frac{\mathcal{R}^{0\,\mathbf{TOT}}_{\rho\rho'}(i\omega+b)}{i\omega+b}\right]+\\
&+ \quad \frac{1}{2\pi i}\int_{-b}^{b} d\omega\left[\frac{\mathcal{R}^{0\,\mathbf{TOT}}_{\rho\rho'}(\omega+ic_2)}{\omega+ic_2}-\frac{\mathcal{R}^{0\,\mathbf{TOT}}_{\rho\rho'}(\omega+ic_1)}{\omega+ic_1}\right],\\
\frac{\mathcal{A}^{0,3}_{\rho\rho'}(\boldsymbol{NG})}{i\omega^{(0,3)}_{\boldsymbol{NG}}} &= \frac{1}{2\pi}\int_{c_2}^{c_1} d\omega\left[\frac{\mathcal{R}^{0\,\mathbf{TOT}}_{\rho\rho'}(i\omega-b)}{i\omega-b}-\frac{\mathcal{R}^{0\,\mathbf{TOT}}_{\rho\rho'}(i\omega+b)}{i\omega+b}\right]+\\
&+ \quad \frac{1}{2\pi i}\int_{-b}^{b} d\omega\left[\frac{\mathcal{R}^{0\,\mathbf{TOT}}_{\rho\rho'}(\omega+ic_2)}{\omega+ic_2}-\frac{\mathcal{R}^{0\,\mathbf{TOT}}_{\rho\rho'}(\omega+ic_1)}{\omega+ic_1}\right],
\end{aligned}
\tag{7.10}
$$

In this sector of signature there is the possibility that not all the Nambu Goldstone mode become purely imaginary but that there is a mixing. In this situation the RPA response function can be written as

$$
\mathcal{R}^{0\,\mathbf{TOT}}_{\rho\rho'}(\omega)=\mathcal{R}^{0}_{\rho\rho'}(\omega)+\sum_{r}\mathcal{R}^{0\,\mathbf{NG,r}}_{\rho\rho'}(\omega)+\sum_{i}\mathcal{R}^{0\,\mathbf{NG,i}}_{\rho\rho'}(\omega),
\tag{7.11}
$$

where

$$
\begin{aligned}
\mathcal{R}^{0\,\mathbf{NG,r}}_{\rho\rho'}(\omega) &= \frac{\mathcal{A}^{0,r}_{\rho\rho'}(\boldsymbol{NG})}{\omega^{(0,r)}_{\boldsymbol{NG}}-\omega}+\frac{\mathcal{B}^{0,r}_{\rho\rho'}(\boldsymbol{NG})}{\omega^{(0,r)}_{\boldsymbol{NG}}+\omega},\\
\mathcal{R}^{0\,\mathbf{NG,i}}_{\rho\rho'}(\omega) &= \frac{\mathcal{A}^{0,i}_{\rho\rho'}(\boldsymbol{NG})}{i\omega^{(0,i)}_{\boldsymbol{NG}}-\omega}+\frac{\mathcal{B}^{0,i}_{\rho\rho'}(\boldsymbol{NG})}{i\omega^{(0,i)}_{\boldsymbol{NG}}+\omega},
\end{aligned}
\tag{7.12}
$$

are the corresponding contributions to the RPA response for the real (r label) and imaginary (i index) Nambu-Goldstone modes. In this case we have to use both methods leading to a quite demanding computational effort due to the increased number of integrations.

7.4 Illustration

As we have done in Chapter 6 we show a realistic situation in ^{168}Yb in which the Nambu-Goldstone modes can become purely imaginary and this happens at finite rotational frequency. The coupling constants are considered constants as a function of rotation because we cannot fix their values with the experimental values of the β- and γ- vibration so that, in principle, all kind of solutions are possible in the RPA equation including complex one. A very direct way to check if a purely imaginary solution exists is to evaluate the RPA response function at zero energy with averaging parameter η=0 MeV. This will give us the IEWSR (see Chapter 6) and, in case of real solutions, this is a positive value. This means that every time the linear response at zero energy has a negative value we are in presence of a complex solution. The procedure to localize this purely imaginary solution is equivalent to the one for real poles (see Chapter 6,sect.6) but this time we need to plot our RPA response using an imaginary variable $i\omega$. The result of this plotting is given in Fig.(7.3) The value of the Nambu-Goldstone mode relating to neutron-gauge invariance case (graph (a)) is in an energy interval around 2 keV while the Nambu-Goldstone mode in (b), corresponding to rotational broken symmetry, is around 0.1 MeV.

The real Nambu-Goldstone mode corresponding to proton-gauge invariance can be localized with the same method explained in Chapter 6. From Fig.(7.4,case (a)) we see that the real pole is around 2.4 keV and its presence is also noticeable in the rotational response (case (b)) even if is not a big contribution.

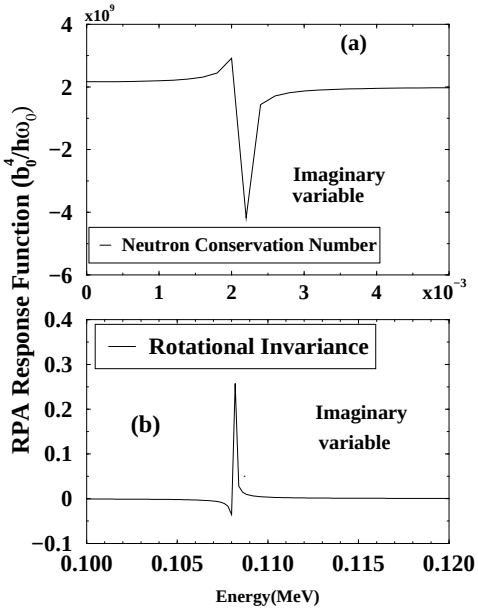

Figure 7.3: Imaginary Nambu-Goldstone modes corresponding to neutron-gauge invariance and of the rotational broken symmetry (case (b)) at $\omega_{\rm rot} = 0.4$ MeV. See caption of Fig.(6.4) for units deifnition.

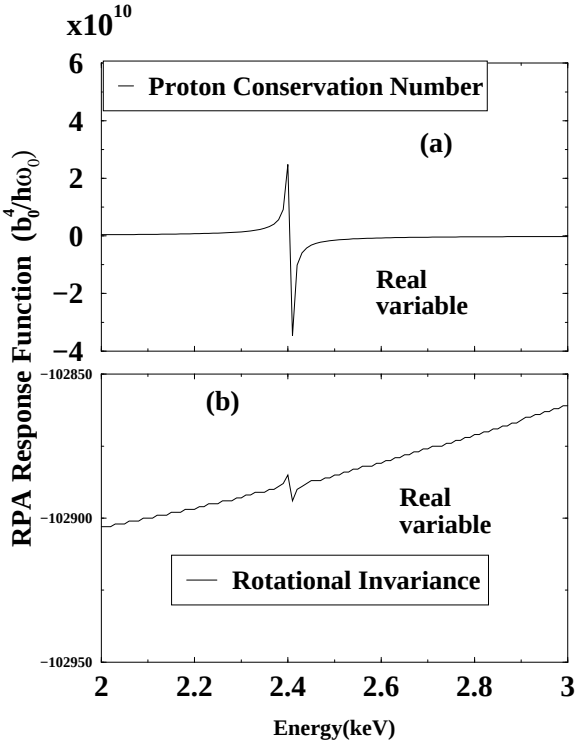

Figure 7.4: Real Nambu-Goldstone mode corresponding to proton-gauge invariance in the case of finite rotation, $\omega_{\rm rot} = 0.4$ MeV. See Caption of Fig.(6.4) for units definition.

Chapter 8

Effective Mass

8.1 Introduction

We now consider the effect of the energy and momentum dependence of the self-energy on the propagation of a elementary excitation of an interacting system. Whereas the analysis pertains to a variety of interesting physical systems, such as a ^{3}He atom in liquid ^{3}He or a low energy nucleon propagating in a nucleus (our case), we will illustrate the major points for the case of a nucleon in translationally invariant nuclear matter for simplicity.

The one-body Schrödinger equation can be easily solved taking into account that, due to the absence of space-limitations in the system, the eigenfunctions are plane wave of the form

$$\varphi(x,t) \sim \exp[i(kx - \omega t)]. \tag{8.1}$$

The dispersion relation that one obtains substituting the above definition of the plane wave inside the one-body equation reads as

$$\omega = \frac{k^2}{2m} + \mathcal{V}(k,\omega), \tag{8.2}$$

where $\mathcal{V}(k,\omega)$ is the Fourier transform of the one-body single particle potential. This term is called, equivalently, mass operator or self-energy correction because, as one can see from Eq.(8.2) it renormalizes the free particle energy $\frac{k^2}{2m}$ and it practically represents the effects of the medium on the propagation of a particle. The depen-

dence on the momentum k carries information on the non-locality in space of the effective interaction. This non-locality is already present in the Hartree-Fock (HFB) solutions and is due to the exchange term in the potential. Both direct and exchange contributions, which are instantaneous in time, are schematically shown in Fig.(8.1)

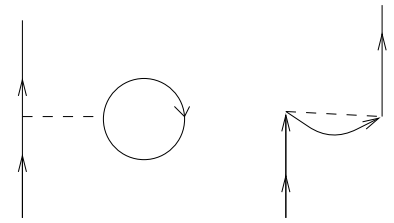

Figure 8.1: Schematic representation of the direct(a) and exchange (b) diagrams which are included in the Hartree-Fock mean field

The dependence on the variable ω is associated with contributions to the effective interaction which are non-local in time (for example particle-vibration coupling, electron-phonon coupling and so on). These contributions were already discussed in details in Chapters 3 (for a non-superconducting system) and Chapter 4 (for a condensate state). As suggested by the graphical perturbation expansion and shown in detailed in nuclear matter calculations [33] one can well use the following approximation

$$\mathcal{V}(k,\omega) = V_{\rm HF} + \Sigma(\omega), \tag{8.3}$$

where the two terms arise from the contributions of the graphs shown in Fig.(8.1) and Fig.(3.2) respectively.

It is convenient to describe the complicated effect of the medium on a particular process into a siutably defined effective mass. The definition is made so as to enforce a free-particle relationship between frequency and momentum, that is

$$\frac{{\rm d}\omega}{{\rm d}k} = \frac{k}{m^*}. \tag{8.4}$$

Making use of Eq.(8.3) one obtains

$$\begin{aligned}\frac{\mathrm{d}\omega}{\mathrm{d}k} &= \frac{k}{m}+\frac{\partial\mathcal{V}}{\partial k}+\frac{\partial\mathcal{V}}{\partial\omega}\frac{\mathrm{d}\omega}{\mathrm{d}k} \\ &+ \frac{k}{m}\left(1+\frac{m}{k}\frac{\partial\mathcal{V}}{\partial k}\right)\left(1-\frac{\partial\mathcal{V}}{\partial\omega}\right)^{-1},\end{aligned} \tag{8.5}$$

which can also be written as

$$m^* = m\left(1+\frac{m}{k}\frac{\partial\mathcal{V}}{\partial k}\right)^{-1}\left(1-\frac{\partial\mathcal{V}}{\partial\omega}\right). \tag{8.6}$$

Noting that m^* itself is the product of factors associated with the energy and momentum dependence of $\mathcal{V}(k,\omega)$, it is useful to define the additional effective masses m_ω and m_k as follow

$$\begin{aligned}\frac{m_\omega}{m} &\equiv \left(1-\frac{\partial\mathcal{V}}{\partial\omega}\right) \\ \frac{m_k}{m} &\equiv \left(1+\frac{m}{k}\frac{\partial\mathcal{V}}{\partial k}\right)^{-1} \\ \frac{m^*_\omega}{m} &= \frac{m_\omega}{m}\times\frac{m_k}{m},\end{aligned} \tag{8.7}$$

and to study them separately.

Although the product of m_ω and m_k appears in the density of states, other observable depend on these quantities. In fact, the effective masses display a quantitatively significant role in determining the mean free path of a nucleon in the nuclear medium and serve to resolve a long-standing discrepancy with experiment [34].

8.2 Ytterbium 168

In finite nuclei the energy-dependent effective mass m_ω is expected to arise from the coupling of the single-particle (or quasiparticles) states to the density oscillations (see Chapters 3 and 4). These are the needed building blocks to construct the self-energy correction so that we are going to analyze in details their behaviour as a function of rotation in a well-deformed rare-earth nucleus, ^{168}Yb.

8.2.1 Quasiparticle Spectrum

The potential energy surface in this nucleus has a stable minimum at prolate deformation up to spin $I \sim 60\hbar$. The deformation, together with the chemical potential λ, are fixed at $\omega_{\rm rot} = 0$ using a Nilsson-Strutinsky technique in order to obtain neutron and proton pairing gaps in agreement with the experimental values. The adopted input parameters are given in Table (8.1) (see caption for further information)

Input Parameters	
ε=0.262	γ=0°
Δ_n=1.039 MeV	**N_{osc} =3-8**
Δ_p=0.983 MeV	**N_{osc} =2-7**

Table 8.1: Input parameters used in the cranked Nilsson potential for ^{168}Yb. The shell-model space used is: $N_{\rm osc}$=3,4,5,6,7,8 for neutrons, $N_{\rm osc}$=2,3,4,5,6,7 for protons.

The obtained neutron quasiparticle spectrum is given in Fig.(8.2) where the routhians, that is the eigenvalues of the cranked Hamiltonian, are drawn as a function of the rotational frequency. This figure illustrates the complexity of the rotating framework because, due to the violation of time-reversal invariance caused by inertial forces, all degeneracies are removed. This means that each particle must occupy an identifiable state in the rotating deformed potential. Already at this level one can understand the challenge in calculating the self-energy correction of quasiparticle states. In fact, non only is increased the number of levels around the Fermi surface (see Fig.(8.2)) but, automatically, it is also increased the number of intermediate states generated by the quasiparticle-vibration coupling Hamiltonian. For example, in the case of the spherical nucleus ^{98}Mo the intermediate states are in number of 14 while in ^{168}Yb we have four different contributions to the self-energy correction (see Fig.(4.3)) each of them having 60 to 90 possible distinct coupled states (in the same chosen single-particle space). The wiggle in the graphs displayed by the routhians in the rotational frequency interval $(0.2 - 0.3)$ MeV, is due to a rather abrupt decrease of the neutron

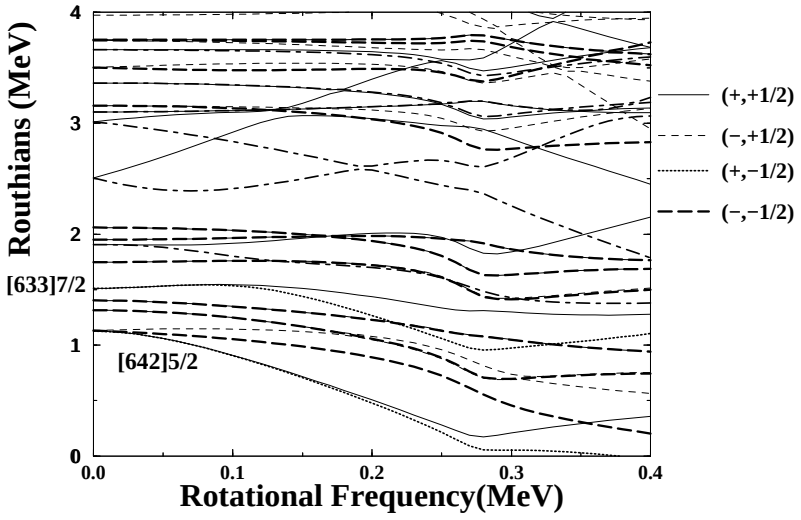

Figure 8.2: Neutron quasiparticle spectrum as a function of the rotational frequency for ^{168}Yb. The input parameters are shown in Table (8.1). Nilsson quantum numbers are used for labelling two of the routhians for reference. The used symbols are explained on the right hand side.

pairing gap in this interval (see Fig.(8.3)).

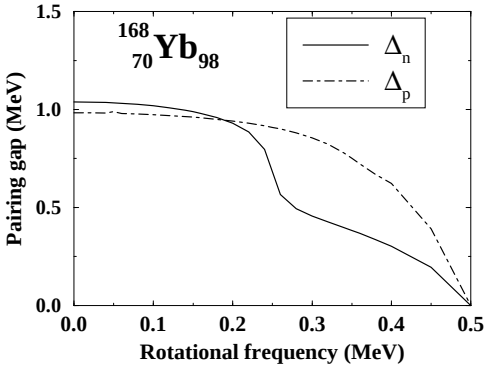

Figure 8.3: Neutron and proton pairing gap parameters as a function of $\omega_{\rm rot}$ for ^{168}Yb

8.2.2 Collective Modes

We now analyze the surface modes associated with the density oscillations of our nucleus, that is the $\beta-$ and $\gamma-$ vibrations. The experimental values of these excitations are, respectively, $E_\beta = 1.154$ MeV and $E_\gamma = 0.984$ MeV (see Fig.(8.4) taken from Nuclear Data Sheets Vol 53 (1988)).

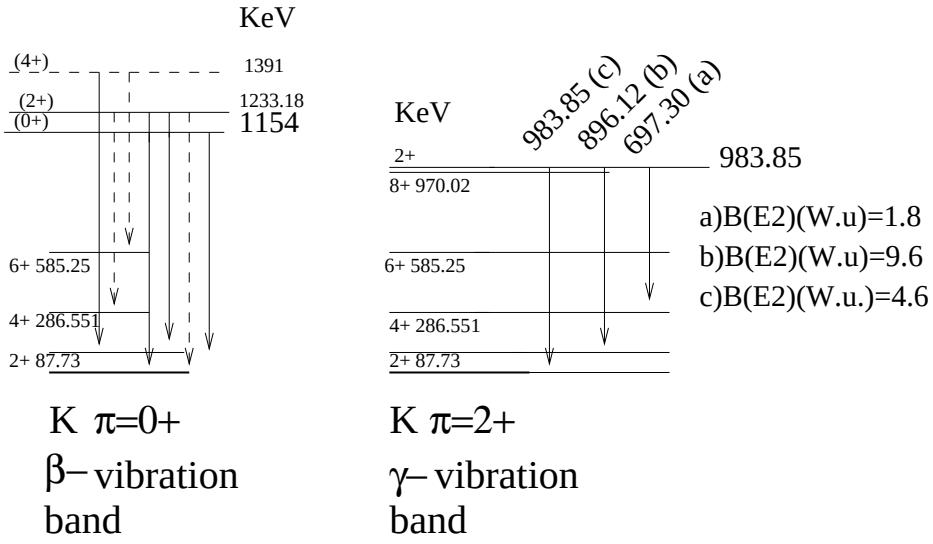

Figure 8.4: β- and γ- experimental vibrational bands for ^{168}Yb.

As explained in Chapter 2 we need to fix the coupling constant of the residual interaction in such a way that the calculated values are in good agreement with the experimental ones while the Nambu-Goldstone modes $K = 1$ should have zero-energy. The adopted values of the coupling constants are given in Table(8.2) We can

Adopted coupling constants	
χ^0_{20}= 137.47	G_n = 0.092 MeV
χ^0_{21}=χ^1_{21}=117.99	G_p =0.102 MeV
χ^0_{22}=χ^1_{22} =119.71	

Table 8.2: Coupling constants used in the calculations at equilibrium deformation $\varepsilon = 0.262$. Quadrupole strengths χ^{α}_{2K} are in units of $b_0^{-4}A^{-5/3}$ MeV fm^{-4}, where $b_0^2 = \hbar/M\omega_0$ with $\hbar\omega_0 = 41.0A^{-1/3}$ MeV=7.43 MeV. The values of the pairing coupling constants are in MeV. All these values are fixed at $\omega_{\rm rot} = 0$.

now study the behaviour of the quadrupole response as a function of the rotational frequency using the coupling constants defined in Table(8.2). The results are shown in Fig.(8.5) where the upper row contains the positive signature operators while the

$\alpha = 1$ negative components are in the lower sector. In this calculations was used $\eta = 0.5$ MeV as averaging parameter.

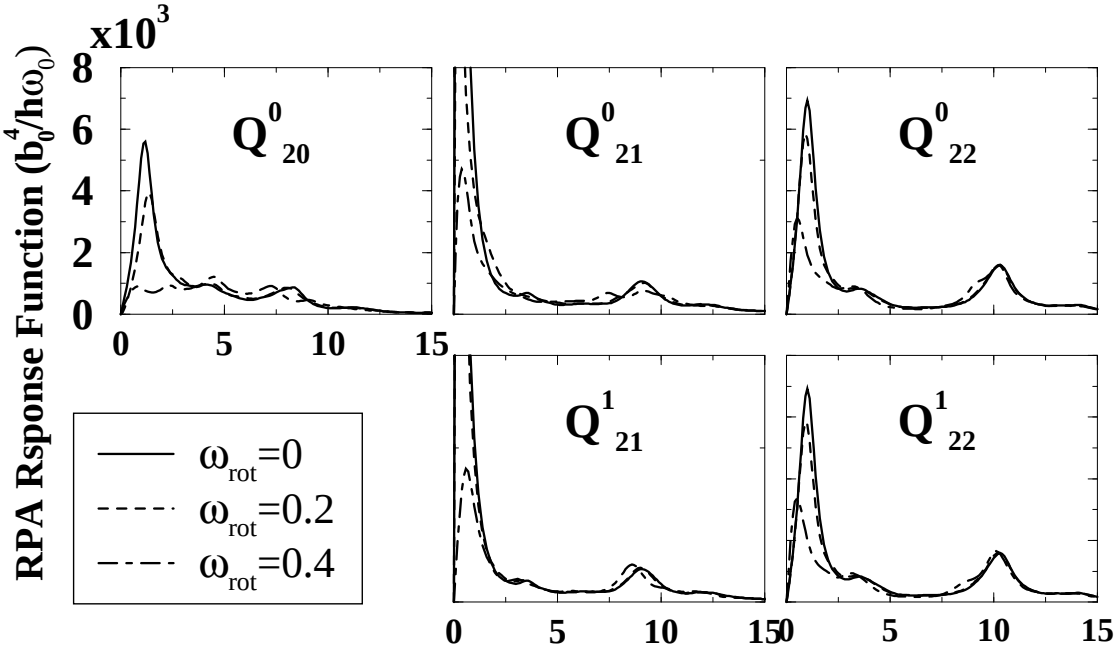

Figure 8.5: Quadrupole response in units of $b_0^4/\hbar\omega_0$ as a function of the rotational frequency. The adopted value for the averaging parameter is $\eta = 0.5$ MeV. The upper row contains signature positive components($\alpha = 0$) while the lower one the $\alpha = 1$ terms. Notice that Q_{20} lies entirely in the $\alpha = 0$ sector. The definition of b_0 is given in the Caption of table(8.2).

The excitation energies of the giant quadrupole resonances are reproduced about 10 MeV, quite in good agreement with the prediction of the harmonic oscillator potential, $\sqrt{2}\hbar\omega_0 = 10.5MeV$. The low-energy peaks around 1 MeV in the RPA strength function correspond to the low-lying $\beta(K = 0)$, $\gamma(K = 2)$ and the Nambu-Goldstone modes ($K = 1$). The effect of the spurious state is quite visible in the Q_{21} response that is an order of magnitude bigger than the others. To proceed further in the calculation of self-energy corrections we have to remove the contribution of these Nambu-Goldstone modes from the RPA strengths because they do not represent intrinsic states(see Chapters 5). We can apply the method outlined in Chapters 6 (real solutions) and 7(imaginary roots) at both zero and finite rotational frequency and see how the RPA strength will be modified after the subtraction of the spurious

states.

We have already given illustrations on how to localize the spurious states and determine contour paths (see examples in Chapters 6 and 7) so that we will not enter in details about this point but we give in Table(8.3) the final answer, that is all the calculated energy of the Nambu-Goldstone modes at different rotational frequencies. From the table one notice that at $\omega_{\rm rot} = 0$ the spurious states are real

$\omega_{\rm rot}$ (MeV)	Nambu-Goldstone Energies	
	α=0	α=1
0	2.52R, 3.4R, 4.5R	3.4R keV
0.2	2.65R, 4.07R, 250I	190I keV
0.4	2.4R, 1.38R, 26.4I	0 keV

Table 8.3: Nambu-Goldstone modes energies at different values of the rotational frequency separately for $\alpha = 0$ operators and $\alpha = 1$ sector. The label R means real solution while I purely imaginary root.

while at finite rotational frequency some of them becomes purely imaginary. This is at $\omega_{\rm rot} = 0$ we choose the coupling constants (8.2) so that the the calculated value of the β- and γ- vibration reproduce the experimental values of the β- and γ-vibration while the χ^{α}_{21} should give zero-energy solutions corresponding to the restoration of the broken symmetries. When the system is cranked the value of the two-quasiparticle-like excitations decreases because the single quasiparticle energies are also decreasing (see Fig.(8.2). This can result in a so low-value in the first two-quasiparticle transition energy that the coupled RPA equation can have numerically a complex solution. The knowledge of the energies of the Nambu-Goldstone modes and the corresponding matrix elements allows us to subtract their contribution from the total RPA response function, obtaining only the physical strength. We have already shown in Chapters 6 and 7 how to proceed in this sense and how these results look like so that we don't discuss this subject anymore. We concentrate here mainly on the intrinsic excitations as the β-and γ- vibration, that is we consider only a portion of Fig.(8.5) that represent only the vibrational modes. As one can see from the Fig.(8.6), the β-vibration is

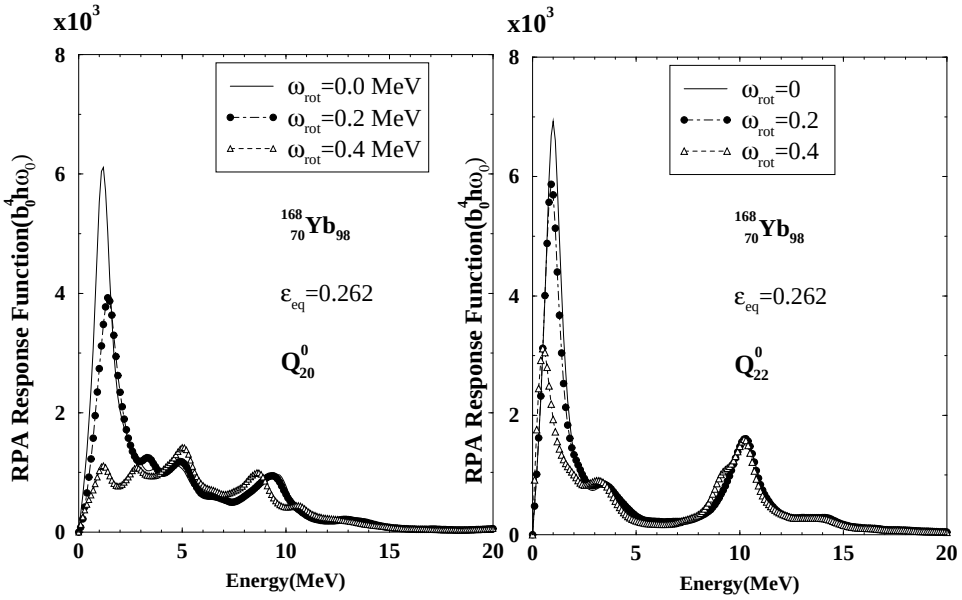

Figure 8.6: RPA Response functions in units of $b_0/\hbar\omega_0$ for the quadrupole components *K=0* (on the right hand side) and *K=2* (left hand side). The graphs are obtained at equilibrium deformation $\varepsilon = 0.262$ at three different rotational frequencies $\omega_{\rm rot} = 0., 0.2, 0.4$ MeV. The value $\eta = 0.5$ MeV was used for the averaging parameter.

very much influenced by the rotation giving a complete spread of its collectivity at $\omega_{\rm rot} = 0.4$ MeV while the γ-vibration is much more coherent. The difference comes from the fact that the pairing is dying out, especially in the neutron case in the range $(0.2 - 0.4)$MeV of the rotational frequency. This means that the β-vibration is influenced by this trend due to the fact it is coupled with pairing vibrations.

8.3 Self-Energy Correction

We are now in condition to evaluate the self-energy correction for quasiparticle states around the Fermi energy. Due to the complexity of the calculations, in particular the very high-time consuming search of the Nambu-Goldstone modes in association with integral formulation of the self-energy, we have limited the choice on only very few levels, 10 negative parity states and 5 positive. This means that we are considering an interval of 4 MeV in excitation energy. The first step is to evaluate the renormalized energy of the chosen quasiparticle states due to the coupling with respect to the

surface modes. The value of this energy is extracted from the solutions of the so called Dyson's equation, that is $E - \varepsilon_j = \Sigma(E)$. From the knowledge of this new energy it is possible to calculate the effective mass from the relation (8.7) where the derivative is taken in an interval around the mentioned calculated renormalized quasiparticle energy. We are going now to show how the energies of the routhians can be changed due to the particle-vibration interaction. Figure (8.7) represents the effect of the coupling on the original routhians energies (labelled Nilsson in the figure) at two different rotational frequency, $\omega_{\rm rot} = 0$ on the left and $\omega_{\rm rot} = 0.4MeV$ on the right. The extreme left and right part of the graph show the corrected energies due to the coupling at the mentioned two different rotational frequencies.

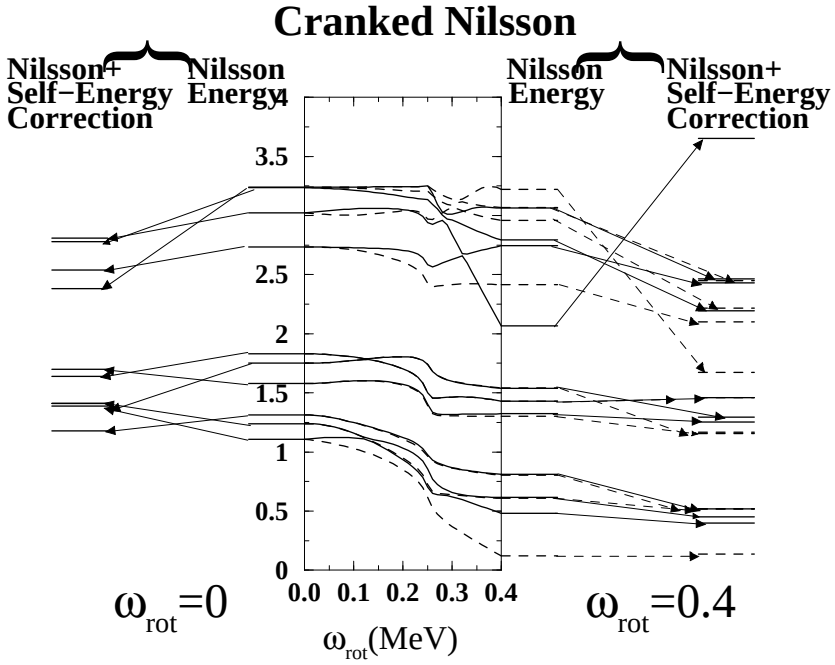

Figure 8.7: Renormalized neutron quasiparticle spectrum due the particle-vibration coupling interaction. Only negative parity states are drawn. The solid line corresponds to signature positive states ($\alpha = 1/2$) while the dashed one to negative signature case ($\alpha = -1/2$). On the left the renormalized levels at zero-rotation are represented while the right hand side shows the results at $\omega_{\rm rot} = 0.4$ MeV. These new energies are compared with the original routhians.

It is quite clear that the coupling term gives rises to a specific change in the energies of these levels. The behaviour shown in Fig.(8.7) reminds us that in a system without pairing correlations, due to the self-energy correction, hole states have positive correction bringing them close to the Fermi energy while particle states are moved towards the Fermi energy from above because of a negative contribution [36]. In the superfluid case one has to remember that a quasiparticle is a linear combination of particle and hole with finite probability to be in a hole-state or in a particle state. In this case the pairing gap is the reference energy so that the shift of the energy is towards the pairing gap value. One can study the effect of the coupling around the equilibrium deformation, in particular at the values $\varepsilon = 0.2$ and $\varepsilon = 0.3$ of the deformation parameter. We summarize the results showing the trend of the m_ω at different deformations and rotations (see Fig. (8.8))

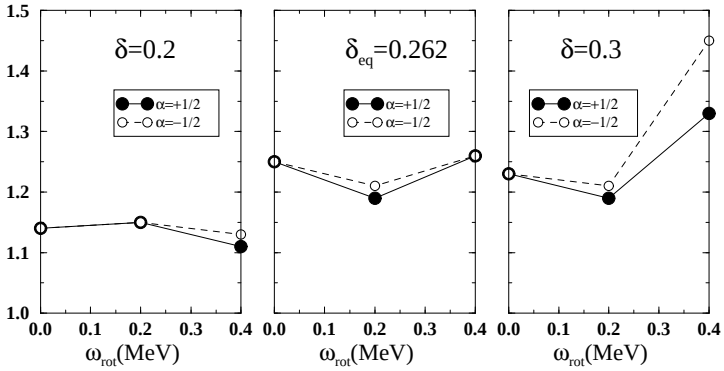

Figure 8.8: m_ω evaluated at three different deformation and rotation. The central case is the equilibrium solution. The results include both positive and negative parity states where the filled circle indicates positive signature states while the open one the negative signature case.

The main observation that comes out from Fig.(8.8) is that the m_ω has values quite small compared to the spherical case [14]. This is not very surprising because the collectivity of the surface modes in a deformed case is used mainly to build up the deformation. The most surprising result of Fig.(8.8) is the increase with rotation of m_ω because we were expecting that, due to the loss of the collectivity of the low-lying energy region in the RPA response function due to rotation (see Fig.(8.6)), there shouldn't be important contribution to the self-energy correction. In practice we

were looking for an equivalent situation of the spherical case where the temperature reduced the coherence of the collective mode in a very drastic way [14]. Studying in more details the results, especially in the case of deformation $\varepsilon = 0.3$ where the increase is more sensitive, we found out that the two-quasiparticle transition energies presents a very low-lying energy, practically at zero-energy at $\omega_{\rm rot} = 0.4$ (see the inset of Fig.(8.9)). This means that we are in regime of instability because the RPA equation can have an imaginary solution.

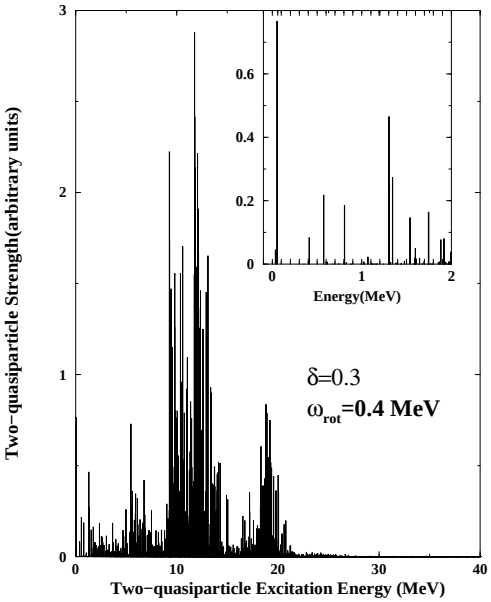

Figure 8.9: Two quasiparticle-like excitation strength for Q^0_{20} at $\varepsilon = 0.3$. The inset represents an enlargement of the graph in the range $(-0.1 - 2)$MeV where it appears the low-energy two-quasiparticle excitation energy bringing instability in the system.

Using the same method developed for the removal of the imaginary Nambu-Goldstone mode we can evaluate this instability to remove it from the physical solutions so that the we can proceed to calculate the corrected effective mass (see Fig.(8.10). We have also checked the case $\varepsilon = 0.262$ but we didn't find any instability in the RPA solutions.

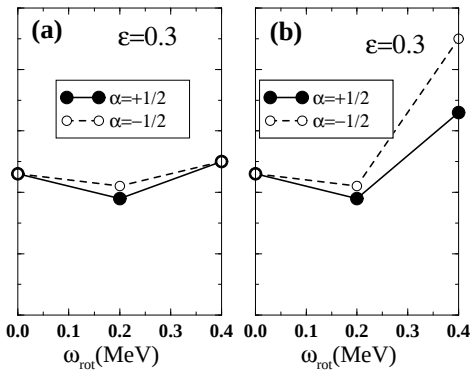

Figure 8.10: m_ω after subtraction of the instability in the case of deformation $\varepsilon = 0.3$. Case (a) without instability, case (b) with instability. Only negative parity states are depicted. The filled circle indicates signature positive states while signature negative states are drawn by open circle.

8.3.1 Octupole Correlations

In these last years a lot of theoretical and experimental studies of low-lying octupole correlations have been developed showing that the octupole vibrations are very important more than the quadrupole one in the superdeformed case[26]. It could then be interesting analyze the effect of a quasiparticle-octupole coupling interaction on the quasiparticle spectrum. Tee procedure is exactly the same as in the quadrupole case so that we give directly the results. First of all, the renormalized neutron quasiparticle spectrum gives a much smaller effect compared to the quadrupole case. The fact that the octupole correlations are not important and effective in a normal deformed nucleus is much more evident looking at the results of the effective mass as a function of rotation and deformation. As one can see in Fig.(8.11) the results do not depend on rotation and deformation and, moreover, the value of the effective mass is practically 1. This can be explained with the fact that the low-lying octupole vibration is too high in energy compared with the quadrupole case so that quasiparticle-vibration coupling is less effective.

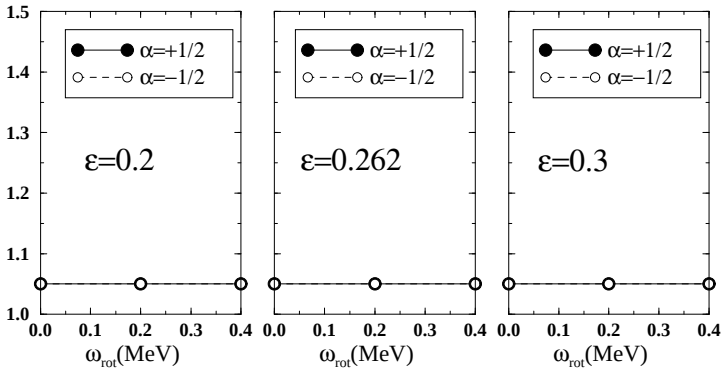

Figure 8.11: m_ω as a function of rotation and deformation due to octupole coupling

We show in Fig.(8.12) the renormalized neutron quasiparticle spectrum due to octupole coupling for comparison with the case of quadrupole results (Fig.(8.7)).

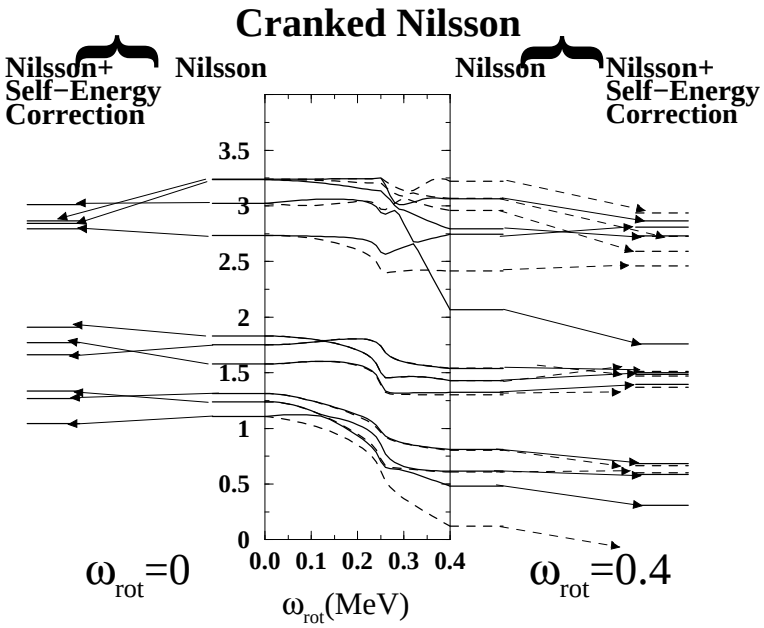

Figure 8.12: Neutron quasiparticle spectrum (central part) renormalized due to the coupling with octupole vibration (left at $\omega_{\rm rot} = 0$ and right at $\omega_{\rm rot} = 0.4$). See caption of Fig.(8.7) for details.

8.3.2 Signature Splitting

It can be interesting to analyze the consequence of the particle-vibration coupling for the states that are signature partners, that is they have opposite value of α but they are almost degenerate in energy. We are going to show below that the phonon coupling produces a splitting of these pairs in a specific way depending on the particular state chosen. The results are shown in Fig.(8.13) for the quadrupole correlation case and Fig.(8.14) when considering octupole vibration. Even in this case we can anticipate that the octupole coupling is much less important than the quadrupole one. In the quadrupole case (Fig.(8.13)) the particle-vibration coupling produces a very evident splitting in some of the paired states (for example a splitting of 20 keV becomes 128 keV) while in the case indicated by the white box the pair remains degenerate. The

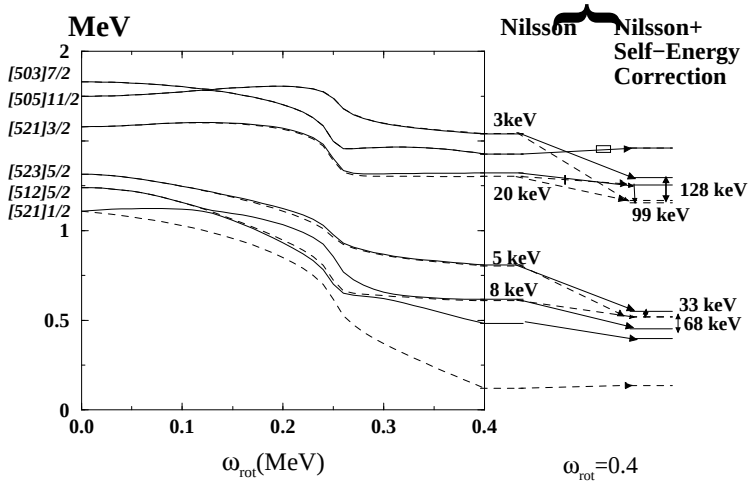

Figure 8.13: Signature splitting produced by the quadrupole coupling. Only negative parity states are shown. The solid line indicates positive signature states while the negative signature states are drawn with dashed line.

paired states $\alpha = \pm 1/2$ couple with the surface modes generated by different residual interactions with different signature (see Chapter 2). The intermediate states of the four distinct contributions to the self-energy correction (Fig.(4.3)) are different for $\alpha = 1/2$ and $\alpha = -1/2$, respectively, due to the selection rule on signature quantum number. For example, in the case of diagram (a) of Fig.(4.3) where initial state has signature positive , the intermediate state has also signature positive if the surface

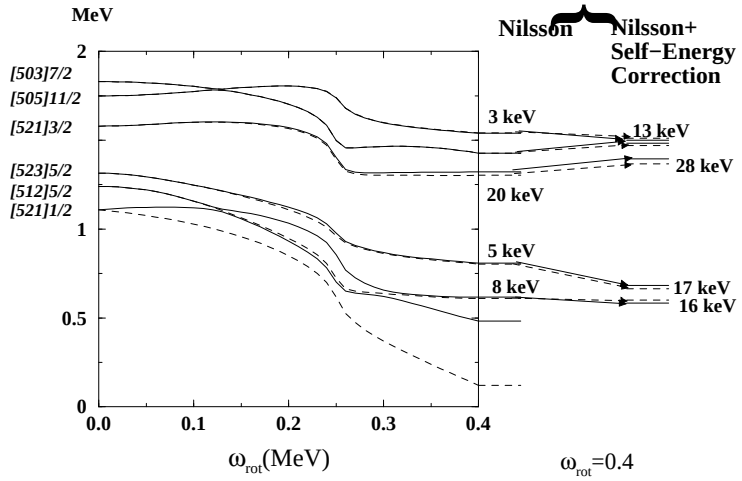

Figure 8.14: Signature splitting due to octupole vibration coupling. See caption of Fig.(8.13) for details.

mode has $\alpha = 0$. If the initial state has $\alpha = -1/2$ and the collective mode is generated by an $\alpha = 0$ operator, due to conservation of the signature quantum number, the intermediate state will be a signature negative orbital, that is $\alpha = -1/2$. This means that the paired initial states, by coupling to surface modes with $\alpha = 0$, reach different intermediate states (the same is true if the signature of the collective mode is $\alpha = 1$). This means that the paired states will have different self-energy corrections. It is then interesting to understand why the states labelled with the white box in Fig.(8.13) do no split but keep their degeneracy in energy. The reason is that these states have a very high projection of the angular momentum on the symmetry axis, that is 11/2. This means that the quasiparticle-vibration coupling is effective only for intermediate states which wavefunctions have maximum overlap with the initial ones, that is with states at high projection too. But these obitals are usually paired signature states, that is the intermediate states, although different in signature, have same energy so that the self-energy correction is the same.

8.3.3 k-mass=0.85

In all the calculations discussed until now we have never referred to the so-called k-mass. This is because, in the Nilsson potential, there is no momentum dependence so that this quantity is 1. One can then argue that in our calculations we take into account a double-counting due to the fact that the Nilsson potential and corresponding

parameters, are defined in such a way to reproduce the experimental values. These last quantities already contain all the correlations that we have considered throughout this work. It is important, as a consequence, to scale the Nilsson potential so that it can be considered as a momentum-dependent with an effective k-mass different from 1. At this purpose we have performed the following substitution

$$\hbar\omega_0 \longrightarrow \hbar\omega_0 \times (\frac{m_k}{m})^{-1}. \tag{8.8}$$

The adopted value of this effective mass is $\frac{m_k}{m} = 0.85$. We have repeated all the calculations and have found out that the ω-mass, at the equilibrium deformation $\varepsilon = 0.262$, has increased from 1.26 to 1.43 while, as a function of rotation is value is practically constant(see Fig.(8.15)

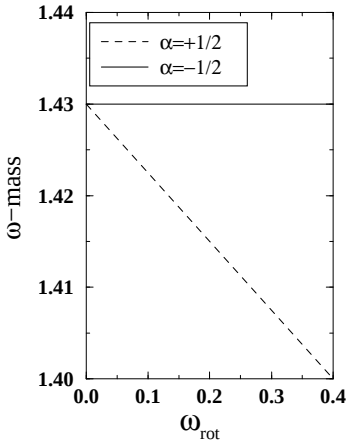

Figure 8.15: m_ω at equilibrium deformation as a function of rotation with $m_k = 0.85$. Negative and positive parity states are included. As usual solid line represents positive signature states and dashed line negative signature case.

We have also checked the signature splitting considering the $m_k = 0.85$ and we have found out that the effect is much larger (see Table(8.4) for some values of the splitting)

For completeness we give the usual renormalized neutron quasiparticle spectrum for this last case while, as in the former case, the octupole correlations are absolutely negligible.

Signature Splitting (keV)				
State	$m_k/m=1$		$m_k/m=0.85$	
[512]5/2	$\Delta E=8$	$\Delta E=68$	$\Delta E=9$	$\Delta E=268$
[523]5/2	$\Delta E=5$	$\Delta E=33$	$\Delta E=1$	$\Delta E=82$
[505]11/2	$\Delta E=0$	$\Delta E=0$	$\Delta E=0$	$\Delta E=0$
[503]7/2	$\Delta E=3$	$\Delta E=128$	$\Delta E=1$	$\Delta E=170$

Table 8.4: Comparison of the signature splitting in case of quadrupole coupling with $m_k = 0.85$ and $m_k = 1$.

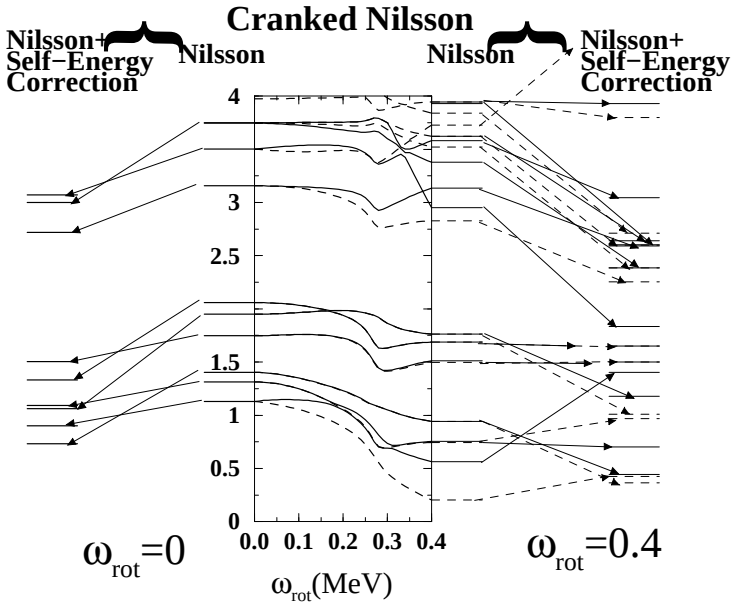

Figure 8.16: Renormalized neutron quasiparticle spectrum due to quadrupole coupling with $m_k = 0.85$. See caption of Fig.(8.7) for details.

Chapter 9

Conclusions

The particle-vibration coupling formalism have been generalized to deal with hot, strongly rotating nuclei. In this way we have developed the basis to carry out microscopic desription of the structure of compound nuclei, in particular of the effective mass of nucleons close to the Fermi energy. In this way it will be possible to provide a quantitative description of the level density as a function of rotational frequency and temperature, and then of the evolution of the cooling of the compound nuclei through nucleon and $\gamma-$deacy. The lack of such a description has been the single, most important factor hampering the analyzis of experiments designed at studying evolution of the nuclear spectrum as a function of rotation and temperature.

We have been able to check numerically, the soundeness of the method employed to eliminate the Nambu-Goldstone modes in deformed strongly rotating nuclei and which constitutes the central, most difficult technical step in the whole project. We do not expect finite temperature to jeopardize the validity of our approach.

In any case, from the present work one can conclude: (a) The effective mass of nucleons moving close to the Fermi energy displays a modest increase of the value of ω-mass and reminds of the corresponding quantity calculated in the case of the spherical nuclei [14]. The apparent rigidity of the deformed nuclei is associated with the fact that most of the collectivity in the quadrupole channel has been absorbed into the static deformation of the mean field. (b)It is expected that the level density in deformed nuclei displays a similar value to the corresponding quantity in closed shell nuclei. Furthermore, one expects it to be rather insensitive to rotational frequency.

Making use of the result previuosly obtained in the studies carried out at finite temperature in spherical nuclei [14], one would expect that there is not a well defined, critical temperature T_0 where the coupling effects on the effective nucleon mass are essentially quenched. In keeping with the moderate collectivity of β- and γ-vibrations, and the almost negligible contribution to m_ω arising from the coupling to octupole vibration, one rather expects a smooth decrease of m_ω as a function of T.

We are aware that this result seems to be in contradiction with particle-evaporation data in medium heavy nuclei [40]). We feel however that this difficult, but central subject of nuclear structure is still quite open, in particular in view of the results obtained in studying the particle evaporation data of Ca-isotopes [41], where no variation of the level density parameter was found up to temperature of the order of 3 MeV.

The application of the present formalism to finite temperature, which would be forthcoming, is expected to contribute to a better understanding of the experimental findings and hopefully of trigger the set up of new, more exclusive experimental research.

As an unexpected finding of this work, one can mention the state dependent, signature splitting arising from the coupling of the single-particle motions, to vibrations of the nuclear surface, in particular to β- and γ- vibrations.

Acknowledgements

I would like to thank all staff of the Niels Bohr Institute, in particular Ulla Holm, Hanne Christensen, Agnethe Elsving and Lisa Frieding for their competence and attention. A special thank goes to Björn Nilsson for his infinite patience in helping me with computer problems (especially in the last period). I have benefited a lot from discussions with Yoshifumi R. Shimizu and PierFrancesco Bortignon. I would like also to thank my supervisor, Thomas Døssing and Ricardo A. Broglia for their interest in this work. Last but not least, I would like to remember all the person that I met in that wonderful place that is the Ke-floor. Here it is the list: Michael Stampe, Rasmus Dahl, Ove Scavenius, Jesper Borg(Bond), Ander Andersen, Jørn Jensen, Martin Drews, Raju Venugopalan, Greg Carter, Igor Mishustin, Jacob Bondorf, Alberto Polleri,Morten Hjorth-Jensen, Raffaele Mattiello, Andy Jackson and Maged ElHajal. A special thanks goes to my room-mate Henrik Pedersen because he was so understanding in let me use the only computer of the office every days. A special mention goes to Anna that has supported me in all these years.

Appendix A

A.1 Boson factor

We want to express some properties of the boson factor as a function of its argument in the limit of zero temperature. We start with its definition in terms of Poisson sum, that is

$$n_B(x+iy) = -\frac{1}{2} - \frac{1}{\beta}\sum_{i\omega_n} \frac{1}{i\omega_n - x - iy}. \tag{A.1}$$

In the limit of zero temperature, $\beta \to \infty$, we substitute the sum with an integral over continuous variable, so that

$$n_B(x+iy) = -\frac{1}{2} - \frac{1}{2\pi}\int_{-\infty}^{+\infty} d\omega \frac{1}{i\omega - x - iy}. \tag{A.2}$$

This is a very easy integration because

$$n_B(x+iy) = -\frac{1}{2} - \frac{1}{2\pi}\int_{-\infty}^{+\infty} d\omega \left[\frac{-x}{x^2+(\omega-y)^2} - i\frac{\omega-y}{x^2+(\omega-y)^2}\right]. \tag{A.3}$$

The imaginary integral cancels out because the integrand function is odd, while the real one is different from zero if $x \neq 0$, so that

$$\begin{aligned} n_B(x+iy) &= -\frac{1}{2} - \frac{1}{2\pi}\arctan\left(\frac{\omega-y}{x}\right)\Big|_{-\infty}^{+\infty} = \\ &= \frac{1}{2}(\mathrm{sign}(x)-1) = \begin{cases} 0 & x>0 \\ -\frac{1}{2} & x=0 \\ -1 & x<0 \end{cases} \end{aligned} \tag{A.4}$$

A.2 Integrals I_1 and I_2

We evaluate the integrals defined in (3.66) in Chapter 3. We start with the first one separating the real and imaginary part of the integrand, that is

$$\begin{aligned} I_1 &= \int_{-\infty}^{+\infty} d\omega \frac{1}{\omega_{\boldsymbol{q}}^{\lambda} - i\omega} \\ &= \int_{-\infty}^{+\infty} d\omega \frac{\omega_{\boldsymbol{q}}^{\lambda}}{{\omega_{\boldsymbol{q}}^{\lambda}}^2 + \omega^2} + i \int_{-\infty}^{+\infty} d\omega \frac{\omega}{{\omega_{\boldsymbol{q}}^{\lambda}}^2 + \omega^2} = \\ &= \arctan\left(\frac{\omega}{\omega_{\boldsymbol{q}}^{\lambda}}\right)\Bigg|_{-\infty}^{+\infty} + \quad i \times 0 = \pi. \end{aligned} \tag{A.5}$$

The imaginary part of the integrand is an odd function respect with the integration variable ω so that the corresponding integral is zero. This is the reason why only the result of integation is a real function.

We can proceed exactly in the same way for the second integral, that is

$$\begin{aligned} I_2 &= \int_{-\infty}^{+\infty} d\omega \frac{1}{\omega_{\boldsymbol{q}}^{\lambda} + i\omega} \\ &= \int_{-\infty}^{+\infty} d\omega \frac{\omega_{\boldsymbol{q}}^{\lambda}}{{\omega_{\boldsymbol{q}}^{\lambda}}^2 + \omega^2} - i \int_{-\infty}^{+\infty} d\omega \frac{\omega}{{\omega_{\boldsymbol{q}}^{\lambda}}^2 + \omega^2} = \\ &= \arctan\left(\frac{\omega}{\omega_{\boldsymbol{q}}^{\lambda}}\right)\Bigg|_{-\infty}^{+\infty} - \quad i \times 0 = \pi. \end{aligned} \tag{A.6}$$

The last integral requires some algebraic steps. Even in this case we can divide the integrand in real and imaginary part so taht

$$\begin{aligned} I_3 &= \int_{-\infty}^{+\infty} d\omega \frac{1}{E + i\eta - i\omega} = \\ &= \int_{-\infty}^{+\infty} d\omega \frac{E}{E^2 + (\omega - \eta)^2} + i \int_{-\infty}^{+\infty} d\omega \frac{\omega - \eta}{E^2 + (\omega - \eta)^2}. \end{aligned}$$

The second integral gives zero contribution because the integrand term is an odd function, as one can see changing integration variable

$$\int_{-\infty}^{+\infty} d\omega \frac{\omega - \eta}{E^2 + (\omega - \eta)^2} = \int_{-\infty}^{+\infty} dy \frac{y}{E^2 + y^2} = 0 \tag{A.7}$$

The final result for the integral I_3 is

$$I_3 = \arctan\left(\frac{\omega - \eta}{E}\right)\Big|_{-\infty}^{+\infty} = \begin{cases} \pi & E > 0 \\ -\pi & E < 0 \end{cases} \tag{A.8}$$

Appendix B

In this appendix we want to show that the method of removal of the Nambu Goldstone modes in the positive signature sector is equivalent to apply the residues theorem to the Nambu Goldstone RPA response , as it was done for signature negative in chapter 6.

We summarize here the results of signature positive (see Chapter 6 for details), that is

$$\begin{aligned}
\mathcal{A}^{0,1}_{\rho\rho'}(\boldsymbol{NG}) &= \frac{1}{2\pi i}\oint_{C_2+L_2} dz \mathcal{R}^{0\boldsymbol{TOT}}_{\rho\rho'}(z) - \frac{1}{2\pi i}\oint_{C_1+L_1} dz \mathcal{R}^{0\boldsymbol{TOT}}_{\rho\rho'}(z), \\
\mathcal{A}^{0,2}_{\rho\rho'}(\boldsymbol{NG}) &= \frac{1}{2\pi i}\oint_{C_3+L_3} dz \mathcal{R}^{0\boldsymbol{TOT}}_{\rho\rho'}(z) - \frac{1}{2\pi i}\oint_{C_2+L_2} dz \mathcal{R}^{0\boldsymbol{TOT}}_{\rho\rho'}(z), \\
\mathcal{A}^{0,3}_{\rho\rho'}(\boldsymbol{NG}) &= \frac{1}{2\pi i}\oint_{C_4+L_4} dz \mathcal{R}^{0\boldsymbol{TOT}}_{\rho\rho'}(z) - \frac{1}{2\pi i}\oint_{C_3+L_3} dz \mathcal{R}^{0\boldsymbol{TOT}}_{\rho\rho'}(z), \\
\frac{\mathcal{A}^{0,1}_{\rho\rho'}(\boldsymbol{NG})}{\omega^{(0,1)}_{\boldsymbol{NG}}} &= \frac{1}{2\pi i}\oint_{C_2+L_2} dz \frac{\mathcal{R}^{0\boldsymbol{TOT}}_{\rho\rho'}(z)}{z} - \frac{1}{2\pi i}\oint_{C_1+L_1} dz \frac{\mathcal{R}^{0\boldsymbol{TOT}}_{\rho\rho'}(z)}{z}, \\
\frac{\mathcal{A}^{0,2}_{\rho\rho'}(\boldsymbol{NG})}{\omega^{(0,2)}_{\boldsymbol{NG}}} &= \frac{1}{2\pi i}\oint_{C_3+L_3} dz \frac{\mathcal{R}^{0\boldsymbol{TOT}}_{\rho\rho'}(z)}{z} - \frac{1}{2\pi i}\oint_{C_2+L_2} dz \frac{\mathcal{R}^{0\boldsymbol{TOT}}_{\rho\rho'}(z)}{z}, \\
\frac{\mathcal{A}^{0,3}_{\rho\rho'}(\boldsymbol{NG})}{\omega^{(0,3)}_{\boldsymbol{NG}}} &= \frac{1}{2\pi i}\oint_{C_4+L_4} dz \frac{\mathcal{R}^{0\boldsymbol{TOT}}_{\rho\rho'}(z)}{z} - \frac{1}{2\pi i}\oint_{C_3+L_3} dz \frac{\mathcal{R}^{0\boldsymbol{TOT}}_{\rho\rho'}(z)}{z},
\end{aligned} \tag{B.1}$$

In the following we will use the quantities

$$
\begin{aligned}
\mathcal{A}^{0,j}_{\rho\rho'}(\boldsymbol{NG}) &= \frac{1}{2\pi i}\oint_{C_b+L_b} dz \mathcal{R}^{0\,\boldsymbol{TOT}}_{\rho\rho'}(z) - \frac{1}{2\pi i}\oint_{C_a+L_a} dz \mathcal{R}^{0\,\boldsymbol{TOT}}_{\rho\rho'}(z), \\
\frac{\mathcal{A}^{0,j}_{\rho\rho'}(\boldsymbol{NG})}{\omega^{(0,1)}_{\boldsymbol{NG}}} &= \frac{1}{2\pi i}\oint_{C_b+L_b} dz \frac{\mathcal{R}^{0\,\boldsymbol{TOT}}_{\rho\rho'}(z)}{z} - \frac{1}{2\pi i}\oint_{C_a+L_a} dz \frac{\mathcal{R}^{0\,\boldsymbol{TOT}}_{\rho\rho'}(z)}{z},
\end{aligned}
\tag{B.2}
$$

where j=1,2,3 and $C_a + L_a, C_b + L_b$ can be two of the four contours defined in 6.4.2.

It is convenient in the above integrals to use the spectral representation of the response function (2.42) separating the physical solutions from the Nambu-Golstone modes (6.30,6.31), that is

$$
\begin{aligned}
\mathcal{A}^{0,j}_{\rho\rho'}(\boldsymbol{NG}) &= \frac{1}{2\pi i}\oint_{C_b+L_b} dz \mathcal{R}^{0}_{\rho\rho'}(z) - \frac{1}{2\pi i}\oint_{C_a+L_a} dz \mathcal{R}^{0}_{\rho\rho'}(z) + \\
&+ \frac{1}{2\pi i}\oint_{C_b+L_b} dz \mathcal{R}^{0\,\boldsymbol{NG,1}}_{\rho\rho'}(z) - \frac{1}{2\pi i}\oint_{C_a+L_a} dz \mathcal{R}^{0\,\boldsymbol{NG,1}}_{\rho\rho'}(z) + \\
&+ \frac{1}{2\pi i}\oint_{C_b+L_b} dz \mathcal{R}^{0\,\boldsymbol{NG,2}}_{\rho\rho'}(z) - \frac{1}{2\pi i}\oint_{C_a+L_a} dz \mathcal{R}^{0\,\boldsymbol{NG,2}}_{\rho\rho'}(z) + \\
&+ \frac{1}{2\pi i}\oint_{C_b+L_b} dz \mathcal{R}^{0\,\boldsymbol{NG,3}}_{\rho\rho'}(z) - \frac{1}{2\pi i}\oint_{C_a+L_a} dz \mathcal{R}^{0\,\boldsymbol{NG,3}}_{\rho\rho'}(z) \\
\frac{\mathcal{A}^{0,j}_{\rho\rho'}(\boldsymbol{NG})}{\omega^{(0,j)}_{\boldsymbol{NG}}} &= \frac{1}{2\pi i}\oint_{C_b+L_b} dz \frac{\mathcal{R}^{0}_{\rho\rho'}(z)}{z} - \frac{1}{2\pi i}\oint_{C_a+L_a} dz \frac{\mathcal{R}^{0}_{\rho\rho'}(z)}{z} + \\
&+ \frac{1}{2\pi i}\oint_{C_b+L_b} dz \frac{\mathcal{R}^{0\,\boldsymbol{NG,1}}_{\rho\rho'}(z)}{z} - \frac{1}{2\pi i}\oint_{C_a+L_a} dz \frac{\mathcal{R}^{0\,\boldsymbol{NG,1}}_{\rho\rho'}(z)}{z} + \\
&+ \frac{1}{2\pi i}\oint_{C_b+L_b} dz \frac{\mathcal{R}^{0\,\boldsymbol{NG,2}}_{\rho\rho'}(z)}{z} - \frac{1}{2\pi i}\oint_{C_a+L_a} dz \frac{\mathcal{R}^{0\,\boldsymbol{NG,2}}_{\rho\rho'}(z)}{z} + \\
&+ \frac{1}{2\pi i}\oint_{C_b+L_b} dz \frac{\mathcal{R}^{0\,\boldsymbol{NG,3}}_{\rho\rho'}(z)}{z} - \frac{1}{2\pi i}\oint_{C_a+L_a} dz \frac{\mathcal{R}^{0\,\boldsymbol{NG,3}}_{\rho\rho'}(z)}{z}.
\end{aligned}
\tag{B.3}
$$

The integrals involving the physical response cancel out in all cases because the number of real poles in C_a+L_a and C_b+L_b is the same. We can use the analytical prop-

erties of the response function to simplify the above integrals, that is $\mathcal{R}^{0\,\boldsymbol{NG,1}}_{\rho\rho'}(z)$ has only one pole $\omega^{(0,1)}_{\boldsymbol{NG}}$ so that the only contour integral involving $\mathcal{R}^{0\,\boldsymbol{NG,1}}_{\rho\rho'}(z)$ different from zero is the one with C_1+L_1. For the same reason we can use C_1+L_1, C_2+L_2 for $\mathcal{R}^{0\,\boldsymbol{NG,1}}_{\rho\rho'}(z)$ and $C_1+L_1, C_2+L_2, C_3+L_3$ for $\mathcal{R}^{0\,\boldsymbol{NG,1}}_{\rho\rho'}(z)$. At this point we can write that

$$
\begin{aligned}
\mathcal{A}^{0,1}_{\rho\rho'}(\boldsymbol{NG}) &= -\frac{1}{2\pi i}\oint_{C_1+L_1} dz\mathcal{R}^0_{\rho\rho'}(z) + \\
&+ \frac{1}{2\pi i}\oint_{C_2+L_2} dz\mathcal{R}^{0\,\boldsymbol{NG,1}}_{\rho\rho'}(z) - \frac{1}{2\pi i}\oint_{C_1+L_1} dz\mathcal{R}^{0\,\boldsymbol{NG,1}}_{\rho\rho'}(z) + \\
&+ \frac{1}{2\pi i}\oint_{C_2+L_2} dz\mathcal{R}^{0\,\boldsymbol{NG,2}}_{\rho\rho'}(z) - \frac{1}{2\pi i}\oint_{C_1+L_1} dz\mathcal{R}^{0\,\boldsymbol{NG,2}}_{\rho\rho'}(z) + \\
&+ \frac{1}{2\pi i}\oint_{C_2+L_2} dz\mathcal{R}^{0\,\boldsymbol{NG,3}}_{\rho\rho'}(z) - \frac{1}{2\pi i}\oint_{C_1+L_1} dz\mathcal{R}^{0\,\boldsymbol{NG,3}}_{\rho\rho'}(z) \\
\frac{\mathcal{A}^{0,1}_{\rho\rho'}(\boldsymbol{NG})}{\omega^{(0,1)}_{\boldsymbol{NG}}} &= -\frac{1}{2\pi i}\oint_{C_2+L_2} dz\frac{\mathcal{R}^0_{\rho\rho'}(z)}{z} + \\
&+ \frac{1}{2\pi i}\oint_{C_2+L_2} dz\frac{\mathcal{R}^{0\,\boldsymbol{NG,1}}_{\rho\rho'}(z)}{z} - \frac{1}{2\pi i}\oint_{C_1+L_1} dz\frac{\mathcal{R}^{0\,\boldsymbol{NG,1}}_{\rho\rho'}(z)}{z} + \\
&+ \frac{1}{2\pi i}\oint_{C_2+L_2} dz\frac{\mathcal{R}^{0\,\boldsymbol{NG,2}}_{\rho\rho'}(z)}{z} - \frac{1}{2\pi i}\oint_{C_1+L_1} dz\frac{\mathcal{R}^{0\,\boldsymbol{NG,2}}_{\rho\rho'}(z)}{z} + \\
&+ \frac{1}{2\pi i}\oint_{C_2+L_2} dz\frac{\mathcal{R}^{0\,\boldsymbol{NG,3}}_{\rho\rho'}(z)}{z} - \frac{1}{2\pi i}\oint_{C_1+L_1} dz\frac{\mathcal{R}^{0\,\boldsymbol{NG,3}}_{\rho\rho'}(z)}{z}.
\end{aligned}
\tag{B.4}
$$

The integral differences involving $\mathcal{R}^{0\,\boldsymbol{NG,2}}_{\rho\rho'}(z)$ and $\mathcal{R}^{0\,\boldsymbol{NG,3}}_{\rho\rho'}(z)$ cancel out because the integrand functions have the same number of poles inside C_1+L_1 and C_2+L_2 so that we obtain

$$
\begin{aligned}
\mathcal{A}^{0,1}_{\rho\rho'}(\boldsymbol{NG}) &= -\frac{1}{2\pi i}\oint_{C_1+L_1} dz\mathcal{R}^0_{\rho\rho'}(z) \\
\frac{\mathcal{A}^{0,1}_{\rho\rho'}(\boldsymbol{NG})}{\omega^{(0,1)}_{\boldsymbol{NG}}} &= -\frac{1}{2\pi i}\oint_{C_1+L_1} dz\frac{\mathcal{R}^0_{\rho\rho'}(z)}{z}
\end{aligned}
\tag{B.5}
$$

This is the solution for the first spurious state. In the second case we have

$$
\begin{aligned}
\mathcal{A}^{0,2}_{\rho\rho'}(\boldsymbol{NG}) &= -\frac{1}{2\pi i}\oint_{C_2+L_2} dz \mathcal{R}^{0\,\boldsymbol{NG,2}}_{\rho\rho'}(z) + \\
&+ \frac{1}{2\pi i}\oint_{C_3+L_3} dz \mathcal{R}^{0\,\boldsymbol{NG,3}}_{\rho\rho'}(z) - \frac{1}{2\pi i}\oint_{C_2+L_2} dz \mathcal{R}^{0\,\boldsymbol{NG,3}}_{\rho\rho'}(z) \\
\frac{\mathcal{A}^{0,2}_{\rho\rho'}(\boldsymbol{NG})}{\omega^{(0,2)}_{\boldsymbol{NG}}} &= -\frac{1}{2\pi i}\oint_{C_2+L_2} dz \frac{\mathcal{R}^{0\,\boldsymbol{NG,2}}_{\rho\rho'}(z)}{z} + \\
&+ \frac{1}{2\pi i}\oint_{C_3+L_3} dz \frac{\mathcal{R}^{0\,\boldsymbol{NG,3}}_{\rho\rho'}(z)}{z} - \frac{1}{2\pi i}\oint_{C_2+L_2} dz \frac{\mathcal{R}^{0\,\boldsymbol{NG,3}}_{\rho\rho'}(z)}{z},
\end{aligned}
\tag{B.6}
$$

where, for the same reasons explained above, the integral differences with the Nambu Goldtsone response corresponding to the third solutions give zero contributions. The result for the second spurious state is

$$
\begin{aligned}
\mathcal{A}^{0,2}_{\rho\rho'}(\boldsymbol{NG}) &= -\frac{1}{2\pi i}\oint_{C_2+L_2} dz \mathcal{R}^{0\,\boldsymbol{NG,2}}_{\rho\rho'}(z) \\
\frac{\mathcal{A}^{0,2}_{\rho\rho'}(\boldsymbol{NG})}{\omega^{(0,2)}_{\boldsymbol{NG}}} &= -\frac{1}{2\pi i}\oint_{C_2+L_2} dz \frac{\mathcal{R}^{0\,\boldsymbol{NG,2}}_{\rho\rho'}(z)}{z}.
\end{aligned}
\tag{B.7}
$$

Finally the last Nambu Goldstone mode have the following non-zero integrals as solutions

$$
\begin{aligned}
\mathcal{A}^{0,3}_{\rho\rho'}(\boldsymbol{NG}) &= -\frac{1}{2\pi i}\oint_{C_3+L_3} dz \mathcal{R}^{0\,\boldsymbol{NG,3}}_{\rho\rho'}(z) \\
\frac{\mathcal{A}^{0,3}_{\rho\rho'}(\boldsymbol{NG})}{\omega^{(0,3)}_{\boldsymbol{NG}}} &= -\frac{1}{2\pi i}\oint_{C_3+L_3} dz \frac{\mathcal{R}^{0\,\boldsymbol{NG,3}}_{\rho\rho'}(z)}{z}.
\end{aligned}
\tag{B.8}
$$

Appendix C

This appendix contains all numerics used in chapter 4 to find the retarded self-energy expression in the rotating frame.

C.1 Integral $I^{\alpha}_{\rho\rho'}(\varepsilon + i\eta)$

We have defined in chapter 4 the following integral

$$I^{\alpha}_{\rho\rho'}(\varepsilon + i\eta) = \int_{-\infty}^{+\infty} d\omega \frac{\mathcal{R}^{\alpha}_{\rho\rho'}(i\omega)}{\varepsilon + i\eta - i\omega}. \tag{C.1}$$

It is convenient express the RPA response in its spectral decomposition (2.42), that is

$$\begin{aligned} I^{\alpha}_{\rho\rho'}(\varepsilon + i\eta) &= \sum_{\boldsymbol{q}} \int_{-\infty}^{+\infty} d\omega \frac{1}{\varepsilon + i\eta - i\omega} \left[\frac{\mathcal{Q}^{\alpha}_{\rho}{}^{*}(\boldsymbol{q}) \mathcal{Q}^{\alpha}_{\rho'}(\boldsymbol{q})}{\omega^{\alpha}_{\boldsymbol{q}} - i\omega} + \frac{\mathcal{Q}^{\alpha}_{\rho}(\boldsymbol{q}) \mathcal{Q}^{\alpha}_{\rho'}{}^{*}(\boldsymbol{q})}{\omega^{\alpha}_{\boldsymbol{q}} + i\omega} \right] = \\ &= \sum_{\boldsymbol{q}} \frac{\mathcal{Q}^{\alpha}_{\rho}{}^{*}(\boldsymbol{q}) \mathcal{Q}^{\alpha}_{\rho'}(\boldsymbol{q})}{\varepsilon + i\eta - \omega^{\alpha}_{\boldsymbol{q}}} \int_{-\infty}^{+\infty} d\omega \left[\frac{1}{\omega^{\alpha}_{\boldsymbol{q}} - i\omega} - \frac{1}{\varepsilon + i\eta - i\omega} \right] + \\ &+ \sum_{\boldsymbol{q}} \frac{\mathcal{Q}^{\alpha}_{\rho}(\boldsymbol{q}) \mathcal{Q}^{\alpha}_{\rho'}{}^{*}(\boldsymbol{q})}{\varepsilon + i\eta + \omega^{\alpha}_{\boldsymbol{q}}} \int_{-\infty}^{+\infty} d\omega \left[\frac{1}{\omega^{\alpha}_{\boldsymbol{q}} + i\omega} - \frac{1}{\varepsilon + i\eta - i\omega} \right] = \\ &= \sum_{\boldsymbol{q}} \frac{\mathcal{Q}^{\alpha}_{\rho}{}^{*}(\boldsymbol{q}) \mathcal{Q}^{\alpha}_{\rho'}(\boldsymbol{q})}{\varepsilon + i\eta - \omega^{\alpha}_{\boldsymbol{q}}} [I_1 - I_3] + \sum_{\boldsymbol{q}} \frac{\mathcal{Q}^{\alpha}_{\rho}(\boldsymbol{q}) \mathcal{Q}^{\alpha}_{\rho'}{}^{*}(\boldsymbol{q})}{\varepsilon + i\eta + \omega^{\alpha}_{\boldsymbol{q}}} [I_2 - I_3], \end{aligned} \tag{C.2}$$

where the integrals I_i with i=1,2,3 were introduce in Chapter 3 and solved in appendix A. After substituting their solution, one can write that

$$
\begin{aligned}
I^{\alpha}_{\rho\rho'}(\varepsilon+i\eta) &= \sum_{\boldsymbol{q}} \frac{\mathcal{Q}^{\alpha}_{\rho}{}^{*}(\boldsymbol{q})\mathcal{Q}^{\alpha}_{\rho'}(\boldsymbol{q})}{\varepsilon+i\eta-\omega^{\alpha}_{\boldsymbol{q}}}\left[\pi-\pi\mathrm{sign}(\varepsilon)\right]+ \\
&+ \sum_{\boldsymbol{q}} \frac{\mathcal{Q}^{\alpha}_{\rho}(\boldsymbol{q})\mathcal{Q}^{\alpha}_{\rho'}{}^{*}(\boldsymbol{q})}{\varepsilon+i\eta+\omega^{\alpha}_{\boldsymbol{q}}}\left[\pi+\pi\mathrm{sign}(\varepsilon)\right].
\end{aligned}
\tag{C.3}
$$

This means that

$$
\begin{aligned}
\sum_{\boldsymbol{q}} \frac{\mathcal{Q}^{\alpha}_{\rho}{}^{*}(\boldsymbol{q})\mathcal{Q}^{\alpha}_{\rho'}(\boldsymbol{q})}{\varepsilon+i\eta-\omega^{\alpha}_{\boldsymbol{q}}} &= \frac{1}{2\pi}\int_{-\infty}^{+\infty} d\omega \frac{\mathcal{R}^{\alpha}_{\rho\rho'}(i\omega)}{\varepsilon+i\eta-i\omega}, \qquad \varepsilon<0 \\
\sum_{\boldsymbol{q}} \frac{\mathcal{Q}^{\alpha}_{\rho}(\boldsymbol{q})\mathcal{Q}^{\alpha}_{\rho'}{}^{*}(\boldsymbol{q})}{\varepsilon+i\eta+\omega^{\alpha}_{\boldsymbol{q}}} &= \frac{1}{2\pi}\int_{-\infty}^{+\infty} d\omega \frac{\mathcal{R}^{\alpha}_{\rho\rho'}(i\omega)}{\varepsilon+i\eta-i\omega}. \qquad \varepsilon>0
\end{aligned}
\tag{C.4}
$$

This is only a partial answer because one should be able to evaluate the sums on the left hand side of last equation for all value of ε and not only in one region of the real axis. For this purpose, we use again the RPA response function to find a relation between the two sums, namely

$$
\sum_{\boldsymbol{q}} \frac{\mathcal{Q}^{\alpha}_{\rho}{}^{*}(\boldsymbol{q})\mathcal{Q}^{\alpha}_{\rho'}(\boldsymbol{q})}{\varepsilon+i\eta-\omega^{\alpha}_{\boldsymbol{q}}} = \sum_{\boldsymbol{q}} \frac{\mathcal{Q}^{\alpha}_{\rho}(\boldsymbol{q})\mathcal{Q}^{\alpha}_{\rho'}{}^{*}(\boldsymbol{q})}{\varepsilon+i\eta+\omega^{\alpha}_{\boldsymbol{q}}} - \mathcal{R}^{\alpha}_{\rho}(\rho'). \tag{C.5}
$$

At this point one can write that

$$
\sum_{\boldsymbol{q}} \frac{\mathcal{Q}^{\alpha}_{\rho}{}^{*}(\boldsymbol{q})\mathcal{Q}^{\alpha}_{\rho'}(\boldsymbol{q})}{\varepsilon+i\eta-\omega^{\lambda}_{\boldsymbol{q}}} = \begin{cases} \frac{1}{2\pi}\int_{-\infty}^{+\infty} d\omega \frac{\mathcal{R}^{\alpha}_{\rho\rho'}(i\omega)}{\varepsilon+i\eta-i\omega} & \varepsilon<0 \\ \frac{1}{2\pi}\int_{-\infty}^{+\infty} d\omega \frac{\mathcal{R}^{\alpha}_{\rho\rho'}(i\omega)}{\varepsilon+i\eta-i\omega} - \mathcal{R}^{\alpha}_{\rho\rho'}(\varepsilon+i\eta) & \varepsilon>0 \end{cases} \tag{C.6}
$$

while

$$
\sum_{\boldsymbol{q}} \frac{\mathcal{Q}^{\alpha}_{\rho}(\boldsymbol{q})\mathcal{Q}^{\alpha}_{\rho'}{}^{*}(\boldsymbol{q})}{\varepsilon+i\eta+\omega^{\lambda}_{\boldsymbol{q}}} = \begin{cases} \frac{1}{2\pi}\int_{-\infty}^{+\infty} d\omega \frac{\mathcal{R}^{\alpha}_{\rho\rho'}(i\omega)}{\varepsilon+i\eta-i\omega} & \varepsilon>0 \\ \frac{1}{2\pi}\int_{-\infty}^{+\infty} d\omega \frac{\mathcal{R}^{\alpha}_{\rho\rho'}(i\omega)}{\varepsilon+i\eta-i\omega} + \mathcal{R}^{\alpha}_{\rho\rho'}(\varepsilon+i\eta) & \varepsilon<0 \end{cases} \tag{C.7}
$$

C.2 Integral $J^{\alpha}_{\rho\rho'}(i\omega_n)$

This integrals is defined as

$$J^{\alpha}_{\rho\rho'}(i\omega_n) = \int_{-\infty}^{+\infty} d\omega \frac{\mathcal{R}^{\alpha}_{\rho\rho'}(i\omega)}{i\omega_n - i\omega}. \tag{C.8}$$

We proceed exactly in the same way as in section above so that

$$\begin{aligned} J^{\alpha}_{\rho\rho'}(i\omega_n) &= \sum_{\boldsymbol{q}} \int_{-\infty}^{+\infty} d\omega \frac{1}{i\omega_n - i\omega} \left[\frac{\mathcal{Q}^{\alpha}_{\rho}{}^{*}(\boldsymbol{q}) \mathcal{Q}^{\alpha}_{\rho'}(\boldsymbol{q})}{\omega^{\alpha}_{\boldsymbol{q}} - i\omega} + \frac{\mathcal{Q}^{\alpha}_{\rho}(\boldsymbol{q}) \mathcal{Q}^{\alpha}_{\rho'}{}^{*}(\boldsymbol{q})}{\omega^{\alpha}_{\boldsymbol{q}} + i\omega} \right] = \\ &= \sum_{\boldsymbol{q}} \frac{\mathcal{Q}^{\alpha}_{\rho}{}^{*}(\boldsymbol{q}) \mathcal{Q}^{\alpha}_{\rho'}(\boldsymbol{q})}{i\omega_n - \omega^{\alpha}_{\boldsymbol{q}}} \int_{-\infty}^{+\infty} d\omega \left[\frac{1}{\omega^{\alpha}_{\boldsymbol{q}} - i\omega} - \frac{1}{i\omega_n - i\omega} \right] + \\ &+ \sum_{\boldsymbol{q}} \frac{\mathcal{Q}^{\alpha}_{\rho}(\boldsymbol{q}) \mathcal{Q}^{\alpha}_{\rho'}{}^{*}(\boldsymbol{q})}{E + i\eta + \omega^{\alpha}_{\boldsymbol{q}}} \int_{-\infty}^{+\infty} d\omega \left[\frac{1}{\omega^{\alpha}_{\boldsymbol{q}} + i\omega} - \frac{1}{i\omega_n + i\omega} \right] = \\ &= \sum_{\boldsymbol{q}} \frac{\mathcal{Q}^{\alpha}_{\rho}{}^{*}(\boldsymbol{q}) \mathcal{Q}^{\alpha}_{\rho'}(\boldsymbol{q})}{i\omega_n - \omega^{\alpha}_{\boldsymbol{q}}} \left[I_3 - I_4 \right] + \sum_{\boldsymbol{q}} \frac{\mathcal{Q}^{\alpha}_{\rho}(\boldsymbol{q}) \mathcal{Q}^{\alpha}_{\rho'}{}^{*}(\boldsymbol{q})}{i\omega_n + \omega^{\alpha}_{\boldsymbol{q}}} \left[I_3 - I_5 \right], \end{aligned} \tag{C.9}$$

where we have introduced two other different integrals I_4 and I_5 defined as

$$\begin{aligned} I_4 &= \int_{-\infty}^{+\infty} d\omega \frac{1}{i\omega_n - i\omega}, \\ I_5 &= \int_{-\infty}^{+\infty} d\omega \frac{1}{i\omega_n + i\omega}. \end{aligned} \tag{C.10}$$

These integrals cancel out because

$$\begin{aligned} I_4 &= i \int_{-\infty}^{+\infty} d\omega \frac{1}{\omega - \omega_n} = i \int_{-\infty}^{+\infty} dy \frac{1}{y} = 0, \\ I_5 &= -i \int_{-\infty}^{+\infty} d\omega \frac{1}{\omega + \omega_n} = -i \int_{-\infty}^{+\infty} dy \frac{1}{y} = 0. \end{aligned} \tag{C.11}$$

This allows us to write

$$J^{\alpha}_{\rho\rho'}(i\omega_n) \quad = \quad \pi \mathrm{sign}(\varepsilon) \left\{ -\sum_{\boldsymbol{q}} \frac{\mathcal{Q}^{\alpha}_{\rho}{}^{*}(\boldsymbol{q})\mathcal{Q}^{\alpha}_{\rho'}(\boldsymbol{q})}{\omega^{\alpha}_{\boldsymbol{q}} - i\omega_n} + \sum_{\boldsymbol{q}} \frac{\mathcal{Q}^{\alpha}_{\rho}(\boldsymbol{q})\mathcal{Q}^{\alpha}_{\rho'}{}^{*}(\boldsymbol{q})}{\omega^{\alpha}_{\boldsymbol{q}} + i\omega_n} \right\}, \tag{C.12}$$

that is

$$\frac{1}{\pi}\int_{-\infty}^{+\infty} d\omega \frac{\mathcal{R}^{\alpha}_{\rho\rho'}(i\omega)}{i\omega_n - i\omega} = \sum_{\boldsymbol{q}} \left[-\frac{\mathcal{Q}^{\alpha}_{\rho}{}^{*}(\boldsymbol{q})\mathcal{Q}^{\alpha}_{\rho'}(\boldsymbol{q})}{\omega^{\alpha}_{\boldsymbol{q}} - i\omega_n} + \frac{\mathcal{Q}^{\alpha}_{\rho}(\boldsymbol{q})\mathcal{Q}^{\alpha}_{\rho'}{}^{*}(\boldsymbol{q})}{\omega^{\alpha}_{\boldsymbol{q}} + i\omega_n} \right] \tag{C.13}$$

The right hand side of this equation looks like the linear RPA response function (2.42) except for the minus sign in front of the first term. This helps us to calculate the two sums included in the spectral representation of the RPA response separately. In fact, combining this last result with the definition of the response function, we can write that

$$\sum_{\boldsymbol{q}} \frac{\mathcal{Q}^{\alpha}_{\rho}{}^{*}(\boldsymbol{q})\mathcal{Q}^{\alpha}_{\rho'}(\boldsymbol{q})}{\omega^{\alpha}_{\boldsymbol{q}} - i\omega_n} = \frac{1}{2}\left\{ \mathcal{R}^{\alpha}_{\rho\rho'}(i\omega_n) - \frac{1}{\pi}\int_{-\infty}^{+\infty} d\omega \frac{\mathcal{R}^{\alpha}_{\rho\rho'}(i\omega)}{i\omega_n - i\omega} \right\}, \tag{C.14}$$

while

$$\sum_{\boldsymbol{q}} \frac{\mathcal{Q}^{\alpha}_{\rho}(\boldsymbol{q})\mathcal{Q}^{\alpha}_{\rho'}{}^{*}(\boldsymbol{q})}{\omega^{\alpha}_{\boldsymbol{q}} + i\omega_n} = \frac{1}{2}\left\{ \mathcal{R}^{\alpha}_{\rho\rho'}(i\omega_n) + \frac{1}{\pi}\int_{-\infty}^{+\infty} d\omega \frac{\mathcal{R}^{\alpha}_{\rho\rho'}(i\omega)}{i\omega_n - i\omega} \right\}. \tag{C.15}$$

C.3 Function $G^{\alpha}_{\rho\rho'}(i\omega)$

This term is defined as

$$G^{\alpha}_{\rho\rho'}(i\omega) = \frac{1}{\beta}\sum_{i\omega_n} \frac{1}{E + i\eta - E_{\gamma} - i\omega_n} \frac{1}{2\pi}\int_{-\infty}^{+\infty} d\omega \frac{\mathcal{R}^{\alpha}_{\rho'\rho}(i\omega) - \mathcal{R}^{\alpha}_{\rho\rho'}(i\omega)}{i\omega_n - i\omega}. \tag{C.16}$$

We are going to rewrite this term in such a way that we can use the definition of the boson factor in terms of Poisson sum [5], that is

$$n_B(x) = -\frac{1}{2} - \frac{1}{\beta}\sum_{i\omega_n} \frac{1}{i\omega_n - x}. \tag{C.17}$$

For this purpose we rewrite $G^{\alpha}_{\rho\rho'} i\omega$ in a more convenient way, that is

$$G^{\alpha}_{\rho\rho'}(i\omega) = \frac{1}{2\pi}\int_{-\infty}^{+\infty} d\omega \left[\mathcal{R}^{\alpha}_{\rho\rho'}(i\omega) - \mathcal{R}^{\alpha}_{\rho\rho'}(i\omega)\right] \times g^{\alpha}_{\rho\rho'} i\omega, \tag{C.18}$$

where

$$g^{\alpha}_{\rho\rho'}(i\omega) = \frac{1}{\beta}\sum_{i\omega_n} \frac{1}{E + i\eta - E_\gamma - i\omega_n}\frac{1}{i\omega_n - i\omega}. \tag{C.19}$$

This function can be separated in the sum of two different denominators, that is

$$g^{\alpha}_{\rho\rho'}(i\omega) = \frac{1}{\beta}\sum_{i\omega_n} \frac{1}{E + i\eta - E_\gamma - i\omega}\left[\frac{1}{E + i\eta - E_\gamma - i\omega_n} + \frac{1}{i\omega_n - i\omega}\right], \tag{C.20}$$

where we can use the definition (C.17) of the boson factor to eliminate the sum over discrete frequencies, namely

$$\begin{aligned} g^{\alpha}_{\rho\rho'}(i\omega) &= \frac{1}{E + i\eta - E_\gamma - i\omega}\left[n_B(E + i\eta - E_\gamma) + \frac{1}{2} - \frac{1}{2} - n_B(i\omega)\right] = \\ &= \frac{1}{E + i\eta - E_\gamma - i\omega}\left[n_B(E + i\eta - E_\gamma) - n_B(i\omega)\right]. \end{aligned} \tag{C.21}$$

We insert this result in the definition (C.18)

$$G^{\alpha}_{\rho\rho'}(i\omega) = \frac{1}{2\pi}\int_{-\infty}^{+\infty} d\omega \frac{\mathcal{R}^{\alpha}_{\rho\rho'}(i\omega) - \mathcal{R}^{\alpha}_{\rho\rho'}(i\omega)}{E + i\eta - E_\gamma - i\omega}\left[n_B(E + i\eta - E_\gamma) - n_B(i\omega)\right]. \tag{C.22}$$

C.4 Final sum

In this section we perform all steps that bring from (4.20) to (4.28) after inserting (C.22) and the expression of the extra terms. We start with the expression (4.20)

$$\sum_{\text{ret}}(\boldsymbol{\mu}, E + i\eta) = \sum_{\lambda,\rho\rho'}\sum_{\alpha=0}^{1}\sum_{\gamma=1}^{2} \times$$

$$
\begin{aligned}
\times \quad & \left\{ \frac{1}{\beta} \sum_{i\omega_n} \frac{\mathcal{R}^{\alpha}_{\rho\rho'}(i\omega_n) q^{\alpha}_{\rho\rho'}(\gamma)}{E + i\eta - E_\gamma - i\omega_n} + \right. \\
- \quad & q^{\alpha}_{\rho\rho'}(\gamma) \left[1 + n_B(E + i\eta - E_\gamma) - n_F(E_\gamma) \right] \mathcal{R}^{\alpha}_{\rho\rho'}(E + i\eta - E_\gamma) + \\
+ \quad & \frac{1}{\beta} \sum_{i\omega_n} \sum_{\boldsymbol{q}} \frac{q^{\alpha}_{\rho\rho'}(\gamma)}{E + i\eta - E_\gamma - i\omega_n} \frac{\mathcal{Q}^{\alpha}_{\rho}{}^{*}(\boldsymbol{q}) \mathcal{Q}^{\alpha}_{\rho'}(\boldsymbol{q}) - \mathcal{Q}^{\alpha}_{\rho}(\boldsymbol{q}) \mathcal{Q}^{\alpha}_{\rho'}{}^{*}(\boldsymbol{q})}{\omega^{\alpha}_{\boldsymbol{q}} + i\omega_n} + \\
- \quad & \sum_{\boldsymbol{q}} q^{\alpha}_{\rho\rho'}(\gamma) \left[1 + n_B(E + i\eta - E_\gamma) - n_F(E_\gamma) \right] \times \\
\times \quad & \left. \left[\frac{\mathcal{Q}^{\alpha}_{\rho}{}^{*}(\boldsymbol{q}) \mathcal{Q}^{\alpha}_{\rho'}(\boldsymbol{q}) - \mathcal{Q}^{\alpha}_{\rho}(\boldsymbol{q}) \mathcal{Q}^{\alpha}_{\rho'}{}^{*}(\boldsymbol{q})}{\omega^{\alpha}_{\boldsymbol{q}} + E + i\eta - E_\gamma} \right] \right\},
\end{aligned}
\tag{C.23}
$$

and we substitute the extra terms as a function of the RPA response, namely

$$
\begin{aligned}
\sum_{\text{ret}} (\boldsymbol{\mu}, E + i\eta) \quad = \quad & \sum_{\lambda,\rho\rho'} \sum_{\alpha=0}^{1} \sum_{\gamma=1}^{2} \times \left\{ \frac{1}{\beta} \sum_{i\omega_n} \frac{\mathcal{R}^{\alpha}_{\rho\rho'}(i\omega_n) q^{\alpha}_{\rho\rho'}(\gamma)}{E + i\eta - E_\gamma - i\omega_n} + \right. \\
- \quad & \sum_{\lambda,\rho\rho',\alpha} \sum_{\gamma=1}^{2} q^{\alpha}_{\rho\rho'}(\gamma) \left[1 + n_B(E + i\eta - E_\gamma) - n_F(E_\gamma) \right] \mathcal{R}^{\alpha}_{\rho\rho'}(E + i\eta - E_\gamma) + \\
+ \quad & \frac{1}{2\beta} \sum_{i\omega_n} \frac{\left[\left[\mathcal{R}^{\alpha}_{\rho'\rho}(i\omega_n) - \mathcal{R}^{\alpha}_{\rho\rho'}(i\omega_n) \right] q^{\alpha}_{\rho\rho'}(\gamma) \right]}{E + i\eta - E_\gamma - i\omega_n} + \\
+ \quad & \frac{1}{\beta} \sum_{i\omega_n} \frac{q^{\alpha}_{\rho\rho'}(\gamma)}{E + i\eta - E_\gamma - i\omega_n} \frac{1}{2\pi} \int_{-\infty}^{+\infty} d\omega \frac{\left[\mathcal{R}^{\alpha}_{\rho'\rho}(i\omega_n) - \mathcal{R}^{\alpha}_{\rho\rho'}(i\omega_n) \right]}{i\omega_n - i\omega} + \\
- \quad & q^{\alpha}_{\rho\rho'}(\gamma) \left[1 + n_B(E + i\eta - E_\gamma) - n_F(E_\gamma) \right] \times \\
\times \quad & \left\{ \begin{array}{ll}
\dfrac{1}{2\pi} \displaystyle\int_{-\infty}^{+\infty} d\omega \frac{\mathcal{R}^{\alpha}_{\rho'\rho}(i\omega) - \mathcal{R}^{\alpha}_{\rho\rho'}(i\omega)}{E + i\eta - E_\gamma - i\omega} & \mathrm{E} - \mathrm{E}_\gamma > 0 \\
\dfrac{1}{2\pi} \displaystyle\int_{-\infty}^{+\infty} d\omega \frac{\mathcal{R}^{\alpha}_{\rho'\rho}(i\omega) - \mathcal{R}^{\alpha}_{\rho\rho'}(i\omega)}{E + i\eta - E_\gamma - i\omega} + & \\
+ \mathcal{R}^{\alpha}_{\rho'\rho}(E + i\eta - E_\gamma) - \mathcal{R}^{\alpha}_{\rho\rho'}(E + i\eta - E_\gamma) & \mathrm{E} - \mathrm{E}_\gamma < 0
\end{array} \right\}
\end{aligned}
\tag{C.24}
$$

We now sum up the first and the third term while in the fourth we substitute (C.22)

$$
\begin{aligned}
\sum_{\text{ret}}(\boldsymbol{\mu}, E+i\eta) &= \sum_{\lambda,\rho\rho'}\sum_{\alpha=0}^{1}\sum_{\gamma=1}^{2}\times \\
&\times \left\{ \frac{1}{2\beta}\sum_{i\omega_n}\frac{[\mathcal{R}^{\alpha}_{\rho\rho'}(i\omega_n)+\mathcal{R}^{\alpha}_{\rho\rho'}(i\omega_n)]q^{\alpha}_{\rho\rho'}(\gamma)}{E+i\eta-E_\gamma-i\omega_n} + \right. \\
&- \left. q^{\alpha}_{\rho\rho'}(\gamma)\left[1+n_B(E+i\eta-E_\gamma)-n_F(E_\gamma)\right]\mathcal{R}^{\alpha}_{\rho\rho'}(E+i\eta-E_\gamma) + \right. \\
&+ \left. \frac{1}{2\pi}\int_{-\infty}^{+\infty}d\omega\frac{q^{\alpha}_{\rho\rho'}(\gamma)[\mathcal{R}^{\alpha}_{\rho'\rho}(i\omega)-\mathcal{R}^{\alpha}_{\rho\rho'}(i\omega)]}{E+i\eta-E_\gamma-i\omega}\left[n_B(E+i\eta-E_\gamma)-n_B(i\omega)\right] + \right. \\
&- \left. q^{\alpha}_{\rho\rho'}(\mu\gamma)\left[1+n_B(E+i\eta-E_\gamma)-n_F(E_\gamma)\right]\times \right. \\
&\times \left. \left[\begin{array}{ll} \frac{1}{2\pi}\int_{-\infty}^{+\infty}d\omega\frac{\mathcal{R}^{\alpha}_{\rho'\rho}(i\omega)-\mathcal{R}^{\alpha}_{\rho\rho'}(i\omega)}{E+i\eta-E_\gamma-i\omega} & \mathrm{E}-\mathrm{E}_\gamma>0 \\ \frac{1}{2\pi}\int_{-\infty}^{+\infty}d\omega\frac{\mathcal{R}^{\alpha}_{\rho'\rho}(i\omega)-\mathcal{R}^{\alpha}_{\rho\rho'}(i\omega)}{E+i\eta-E_\gamma-i\omega}+ & \\ +\mathcal{R}^{\alpha}_{\rho'\rho}(E+i\eta-E_\gamma)-\mathcal{R}^{\alpha}_{\rho\rho'}(E+i\eta-E_\gamma) & \mathrm{E}-\mathrm{E}_\gamma<0 \end{array} \right. \right\}
\end{aligned}
\tag{C.25}
$$

We can now sum the integrals, namely

$$
\begin{aligned}
\sum_{\text{ret}}(\boldsymbol{\mu}, E+i\eta) &= \sum_{\lambda,\rho\rho'}\sum_{\alpha=0}^{1}\sum_{\gamma=1}^{2}\times \\
&\times \left\{ \frac{1}{2\beta}\sum_{i\omega_n}\frac{[\mathcal{R}^{\alpha}_{\rho\rho'}(i\omega_n)+\mathcal{R}^{\alpha}_{\rho\rho'}(i\omega_n)]q^{\alpha}_{\rho\rho'}(\gamma)}{E+i\eta-E_\gamma-i\omega_n} + \right. \\
&+ \left. \frac{1}{2\pi}\int_{-\infty}^{+\infty}d\omega\frac{q^{\alpha}_{\rho\rho'}(\gamma)[\mathcal{R}^{\alpha}_{\rho'\rho}(i\omega)-\mathcal{R}^{\alpha}_{\rho\rho'}(i\omega)]}{E+i\eta-E_\gamma-i\omega}\times \right. \\
&\times \left. [n_B(E+i\eta-E_\gamma)-n_B(i\omega)-1-n_B(E+i\eta-E_\gamma)+n_F(E_\gamma)] + \right. \\
&- \left. q^{\alpha}_{\rho\rho'}(\gamma)\left[1+n_B(E+i\eta-E_\gamma)-n_F(E_\gamma)\right]\mathcal{R}^{\alpha}_{\rho\rho'}(E+i\eta-E_\gamma) + \right. \\
&- \left. q^{\alpha}_{\rho\rho'}(\gamma)\left[1+n_B(E+i\eta-E_\gamma)-n_F(E_\gamma)\right]\times \right. \\
&\times \left. \left[\begin{array}{ll} 0 & \mathrm{E}-\mathrm{E}_\gamma>0 \\ \mathcal{R}^{\alpha}_{\rho'\rho}(E+i\eta-E_\gamma)-\mathcal{R}^{\alpha}_{\rho\rho'}(E+i\eta-E_\gamma) & \mathrm{E}-\mathrm{E}_\gamma<0 \end{array} \right. \right\}
\end{aligned}
\tag{C.26}
$$

Combining together the last two terms , we finally obtain

$$
\begin{aligned}
\sum_{\text{ret}}(\boldsymbol{\mu}, E+i\eta) &= \sum_{\lambda,\rho\rho'}\sum_{\alpha=0}^{1}\sum_{\gamma=1}^{2}\times \\
&\times \left\{\frac{1}{2\beta}\sum_{i\omega_n}\frac{[\mathcal{R}^{\alpha}_{\rho\rho'}(i\omega_n)+\mathcal{R}^{\alpha}_{\rho\rho'}(i\omega_n)]q^{\alpha}_{\rho\rho'}(\gamma)}{E+i\eta-E_\gamma-i\omega_n}+\right. \\
&- \frac{1}{2\pi}\int_{-\infty}^{+\infty}d\omega\frac{q^{\alpha}_{\rho\rho'}(\gamma)[\mathcal{R}^{\alpha}_{\rho'\rho}(i\omega)-\mathcal{R}^{\alpha}_{\rho\rho'}(i\omega)]}{E+i\eta-E_\gamma-i\omega}\left[1+n_B(i\omega)-n_F(E_\gamma)\right]+ \\
&- q^{\alpha}_{\rho\rho'}(\gamma)\left[1+n_B(E+i\eta-E_\gamma)-n_F(E_\gamma)\right]\begin{cases}\mathcal{R}^{\alpha}_{\rho\rho'}(E+i\eta-E_\gamma) & \mathrm{E}-\mathrm{E}_\gamma>0 \\ \mathcal{R}^{\alpha}_{\rho'\rho}(E+i\eta-E_\gamma) & \mathrm{E}-\mathrm{E}_\gamma<0\end{cases}
\end{aligned}
$$

(C.27

Bibliography

[1] A. Bohr and B. Mottelson, "*Nuclear structure*", vols I and II, (Benjamin, New York, 1969 and 1975).

[2] J. P. Blaizot and G. Ripka, " *Quantum Theory of Finite Systems*", (MIT Press, 1986).

[3] P. Ring and P. Schuck, " *The Nuclear Many-Body Problem*", (Springer-Verlag New York Inc., 1980).

[4] D. J. Rowe, "*Nuclear Collective Motion*", (Butler & Tanner Ltd, 1970).

[5] G. Mahan, "*Many Particle Physics*", (Plenum,1981).

[6] P. Nozières, "*Theory of interacting Fermi systems*", (W. A. Benjamin, Inc., 1964).

[7] A. Fetter and J. Walecka, "*Quantum theory of many-particle systems*", (McGraw Hill,1971).

[8] A. A. Abrikosov, L. P. Gorkov, I. E. Dzyaloshinski, "*Quantum field theory in statistical physics*", (Prentice Hall, 1963).

[9] M. Baranger and K. Kumar, *Nucl.Phys.* **62** (1965) 113, M. Baranger and K. Kumar, *Nucl.Phys.* **A110** (1968) 490, M. Baranger and K. Kumar, *Nucl.Phys.* **A122** (1968) 241.

[10] T. Bengtsson and I. Ragnarsson, *Nucl.Phys.* **A436** (1985) 14.

[11] N. Bogoliubov, *Soviet Physics JETP* **7** (1958) 41.

[12] D. Bohm and D. Pines, *Phys. Rev.* **92** (1953) 609;626.

[13] P. F. Bortignon, R. A. Broglia, G. F. Bertsch and J. Pacheco, *Nucl. Phys.***A460** (1986) 149.

[14] P. Donati, P. M. Pizzochero, P. F. Bortignon and R. A. Broglia, *Phys.Rev.Lett* **72** (1994) 2835.

[15] P. Donati, "*Temperature Dependence of the Nucleon Effective Mass*", Master Thesis, 1993.

[16] A. L. Goodman, *Nucl.Phys.* **A230** (1974) 466,
A. L. Goodman, "*Advances in Nuclear Physics*", ed. J. W. Negele and E. Vogt, Vol 11, pag 263,(Plenum Press,Newy York).

[17] C. Gustafsson, I. L. Lamm, B. Nilsson and S. G. Nilsson, *Arkiv før Fysik* **36** (1967) 693.

[18] T. Kishimoto et al., *Phys.Rev.Lett.* **35** (1975) 552.

[19] D. Inglis, *Phys.Rev.* **96** (1954) 1059, D. Inglis, *Phys.Rev.* **103** (1956) 1786.

[20] E. R. Marshalek, *Phys.Rev. C* **11** (1975) 1426, E. R. Marshalek, *Nucl.Phys.* **A266** (1976) 317.

[21] E. R. Marshalek and J. Weneser, *Annals of Physics* **53** (1969) 569, E. R. Marshalek, *Nucl.Phys.* **A275** (1977) 416.

[22] J. L. Egido and H. A. Weidenmüller, *Phys. Rev.***C39** (1989) 39.

[23] Y. R. Shimizu,J. D. Garrett and R. A. Broglia, *Rev.Mod.Phys.* **61** (1989), 131.

[24] P. Ring, L. M. Robledo, J. L. Egido and M. Faber, *Nucl.Phys.***A419** (1984) 261.

[25] J. L. Egido, H. J. Mang and P. Ring, *Nucl.Phys.* **A339** (1980) 390, Y. R. Shimizu and K. Matsuyanagi, *Prog.Theor.Phys.* **70** (1983) 144, Y. R. Shimizu and K. Matsuyanagi, *Prog.Theor.Phys.* **72** (1984) 799, Y. R. Shimizu and K. Matsuzaki, *Nucl.Phys.* **A588** (1995) 559,

[26] J. M. Robledo, J. L. Egido and P. Ring, *Nucl.Phys* **A449** (1986) 201, S. Mizutori, Y. R. Shimizu and K. Matsuyanagi, *Prog.Theor.Phys* **83** (1990) 666, S. Mizutori, Y. R. Shimizu and K. Matsuyanagi, *Prog.Theor.Phys* **85** (1991) 559, S. Mizutori, Y. R. Shimizu and K. Matsuyanagi, *Prog.Theor.Phys* **86** (1991) 131, T. Nakatsukasa, S. Mizutori and K. Matusyanagi, *Prog.Theor.Phys.* **87** (1992) 607 T. Nakatsukasa, S. Mizutori and K. Matusyanagi, *Prog.Theor.Phys.* **89** (1993) 847 S. Mizutori,T. Nakatsukasa, K.Arita, Y. R. Shimizu and K. Matusyanagi, *Nucl.Phys.* **A557** (1993) 125c T. Nakatsukasa, K. Matusyanagi, S. Mizutori and W. Nazarewicz, *Phys.Lett. B* **343** (1995) 19.

[27] S. G. Nilsson, *Mat.Fys.Medd.,Dan.Vid.Selsk.* **29** (1955) No. 16.

[28] R. Arvieu, *Ann.Phys.* **8** (1963) 407, V. G.Soloviev and O. Vogel, *Phys.Lett.* **47B** (1973) 193.

[29] H. Sakamoto and T. Kishimoto, *Nucl.Phys.* **A501** (1989) 205.

[30] V. G. Soloviev, "*Theory of Complex Nuclei* (Nauka, Moscow,1971).

[31] V. M. Strutinsky, *Nucl.Phys.* **A95** (1967) 420, V. M. Strutinsky, *Nucl.Phys.* **A122** (1968) 1.

[32] K. E. Löbner, M. Vetter and V. Hønig, *Nuclear Data Tables*, **A7** (1970), 495

[33] C. Mahaux, P. F. Bortignon, R. A. Broglia and C. H. Dasso, *Phys. Rep.***120** (1985) 1.

[34] J. W. Negele and K. Yazaki, *Phys. Rev. Lett.* **47** (1981) 71.

[35] J. P. Jeukenne, A. Lejeune and C. Mahaux, *Phys. Rep.* **C25** (1976) 83.

[36] G. F. Bertsch and T. T. S. Kuo, *Nucl. Phys.***A112** (1968) 204.

[37] P. Quentin and H. Flocard, *Ann. Rev. Nucl. Sci.* **28** (1978) 523.

[38] G. E. Brown, J. H. Gunn and P. Gould, *Nucl. Phys.***45** (1963) 164

[39] I. Hamamoto and P. Siemens, *Nucl. Phys.* **A269** (1976) 199.

[40] Gonin et al., *Nucl.Phys.* **A495** (1989) 139c.

[41] B. Fornal et al., *Phys. Rev.***C44** (1991) 2588.